AUTOCRINE PROLIFERATION INHIBITION PATHWAYS IN *DICTYOSTELIUM DISCOIDEUM*

A Dissertation

by

YU TANG

Submitted to the Office of Graduate and Professional Studies of
Texas A&M University
in partial fulfillment of the requirements for the degree of

DOCTOR OF PHILOSOPHY

Chair of Committee,	Richard H. Gomer
Committee Members,	Bruce B. Riley
	Steve W. Lockless
	Kevin Burgess
Head of Department,	Thomas D. McKnight

August 2020

Major Subject: Biology

ABSTRACT

Very little is known about how tissues can regulate their size. In one possible mechanism, cells in a tissue secrete a factor that inhibits their proliferation, and as the tissue gets bigger, the concentration of the factor increases. If the factor reached the concentration that inhibits proliferation, the resulting negative feedback loop will limit tissue size. Despite evidence for such factors, very few have been identified and their signal transduction pathways are poorly understood. Our lab previously found that *Dictyostelium discoideum* accumulates such factors, autocrine proliferation repressor protein A (AprA) and inorganic polyphosphate, to slow or inhibit its proliferation. Previous work showed that AprA slows the proliferation via an unknown G protein coupled receptor (GPCR), and polyphosphate inhibits the proliferation using the G protein coupled receptor GrlD and the Ras GTPase RasC. In this dissertation, I showed that the GPCR GrlH is required for AprA to slow cell proliferation; I found several signaling components in the polyphosphate pathway through genetic screens, and showed that polyphosphate inhibits the proliferation of *D. discoideum* through an IP3/Ca^{2+} pathway.

DEDICATION

I would like to dedicate this dissertation to my family who have always been supportive and encouraged me.

ACKNOWLEDGEMENTS

I would like to thank my committee chair, Dr. Gomer, and my committee members, Dr. Riley, Dr. Lockless and Dr. Burgess, for their guidance and support throughout this research.

I would also like to thank all my former and current lab mates for their support, suggestions and kindness throughout my PhD training.

Thanks also go to my friends and colleagues and the department faculty and staff for making my time at Texas A&M University a great experience.

Finally, thanks to my parents for their concern, support and encouragement.

CONTRIBUTORS AND FUNDING SOURCES

This work was supervised by a dissertation committee consisting of Professor Gomer, Professor Riley and Professor Lockless of the Department of Biology and Professor Burgess of the Department of Chemistry.

The GPCR-KO strains in Chapter 2 were made by Dr. Yuantai Wu when he was a graduate student in Professor Janetopoulos' lab in the Department of Biological Sciences, University of the Sciences in Philadelphia. Dr. Sarah Herlihy, Francisco J. Brito-Aleman and Jose H. Ting contributed to the data for Figures 1 - 6 in Chapter 2.

The undergraduates David E. Zimmerhanzel, Jacquelyn R. McCullough and Louis Cadena contributed to part of the data for Figure 18 in chapter 4.

Dr. Sarah Herlihy and Dr. Jonathan E. Phillips contributed to the data for Figures 22, 26, and 27 and part of the data for Figures 23, 24, and 25 in appendix A.

All other work conducted for the dissertation was completed by the student independently.

Funding Sources

Graduate study was supported by the National Institutes of Health (grant R21 NS102600, grant R01 GM102280, and grant R01 GM118355).

TABLE OF CONTENTS

Page

LIST OF FIGURES

Page

LIST OF TABLES

Page

1. INTRODUCTION AND LITERATURE REVIEW

1.1. Tissue size regulation and chalones

A longstanding question in developmental biology is how a tissue or a group of cells, can regulate its own size or the spatial density of a specific cell type. In one possible mechanism, the tissue size or the spatial density of a specific cell type could be limited by an autocrine proliferation inhibitor, named 'chalone', where the concentration of the chalone increases as the size of the tissue, or density of cells, increases [1-3]. The resulting negative feedback loop will limit the tissue size, or density of cells.

Although a considerable amount is known about signals and pathways that promote cell proliferation, relatively little is known about the identities of chalones and their signal transduction pathways. Understand the mechanism of these chalones may help to treat abnormal-proliferation related diseases like cancer. For instance, melanocyte proliferation can be inhibited by an unknown secreted chalone, and when the crude chalone is injected under a melanoma, the melanoma cell proliferation ceases (3, 4). Despite their intrinsic interest and potential utility in controlling tumor growth, in most cases where chalone activity has been observed, the identity of the chalone and the identity of the associated signal transduction pathway are unknown. For example, there is evidence for the existence of chalones in mammalian tissues, such as liver, muscle and spleen [4-7], however, only the muscle chalone myostatin was identified [6]. Whether the chalones are proteins, peptides or inorganic molecules is unclear.

Our lab has found that the social amoeba, *Dictyostelium discoideum*, secretes an autocrine proliferation repressor protein A (AprA) to slow proliferation [8], and inorganic polyphosphate to stop proliferation [9]. In this dissertation, I report my contribution to understanding the mechanism of these chalones in *Dictyostelium discoideum*. An intriguing possibility is that similar mechanisms may be used in other eukaryotes for autocrine proliferation inhibition and group and tissue size regulation.

1.2. *Dictyostelium Discoideum*

Dictyostelium discoideum is a eukaryotic social amoeba. It lives in a unicellular form when there is enough food. When cells overgrow their food supply and starve, they will aggregate to form multicellular fruiting bodies, two types of cells: spore cells and stalk cells [10].

Dictyostelium discoideum serves as an excellent model organism for studying molecular and cellular processes. It has a sequenced, assembled and annotated 34 Mb genome [11], containing many genes that are homologous to those in mammals and are missing in fungi [12, 13]. There are numerous molecular genetic tools available. For example, random mutants can be easily generated by restriction enzyme mediated insertion [14] or shotgun antisense [15]. Lab strains of *Dictyostelium discoideum* can be cultured in liquid medium or on a bacterial (*E. coli*) lawn on an agar plate at room temperature.

Because of these advantages, *Dictyostelium discoideum* has been used for a wide variety of biological studies, including cell division, phagocytosis, chemotaxis, signal transduction, cell-cell communication and cell differentiation [16].

1.3. Autocrine proliferation repressor protein A

Autocrine proliferation repressor protein A (AprA) is a secreted *Dictyostelium discoideum* protein that inhibits the proliferation of *D. discoideum* cells [8, 17]. AprA functions in conjunction with another secreted protein called CfaD (counting factor-associated D), which also inhibits the proliferation of *D. discoideum* cells [18]. The addition of recombinant AprA (rAprA) or CfaD (rCfaD) to wild type cells causes a significant reduction in proliferation [18, 19]. Cells lacking either AprA or CfaD show abnormally fast proliferation, and this phenotype can be rescued either by expressing AprA in *aprA*$^{-}$ cells or CfaD in *cfaD*$^{-}$ cells or by adding recombinant AprA or CfaD to the respective mutant strains [8, 18, 19]. Both AprA and CfaD are necessary for proliferation inhibition, as rAprA cannot rescue the *cfaD*$^{-}$ phenotype and rCfaD cannot rescue the *aprA*$^{-}$ phenotype [18, 19]. Additionally, AprA but not CfaD, functions to chemorepel *D. discoideum* cells, causing cells to move in a biased direction away from a source of AprA [17]. Cells at the edge of wild type colonies move away from the dense colony center while cells at the edge of an *aprA*$^{-}$ colony form a tight edge with little movement outward [20]. Both wild type and *aprA*$^{-}$ cells move away from a source of rAprA [17].

Several components of the AprA-induced proliferation inhibition signaling pathway have been identified, including the ROCO kinase QkgA, the p21-activated kinase (PAK) family member PakD, the PTEN-like phosphatase CnrN, and the tumor suppressor RblA [20-24]. Additionally, QkgA, PakD, CnrN, and RblA are also involved in the AprA- induced chemorepulsion signaling pathway [17, 20-24]. Both AprA inhibition of proliferation and AprA induction of chemorepulsion require the G proteins Gβ and Gα subunit Gα8, and the binding of AprA to cell membrane is inhibited by GTPγS, suggesting that AprA functions through binding to a G protein-coupled receptor (GPCR) [17, 25].

1.4. Polyphosphate

Polyphosphate is a linear polymer of phosphate residues and is present in all kingdoms of life [26-29]. In bacteria, polyphosphate functions as energy and phosphate storage [26, 29], potentiates survival in some high stress conditions [29, 30], and potentiates biofilm formation [31, 32]. In mammals, polyphosphate inhibits bone calcification [33], potentiates pro-inflammatory responses [34], potentiates mTOR activation of plasma cells [35], inhibits the proliferation of leukemia cells [36], induces apoptosis [37], and accelerates blood coagulation [38].

Dictyostelium accumulates extracellular polyphosphate as cells grow and proliferate [9]. At very high cell densities, when the cells are about to starve, the accumulated extracellular polyphosphate reaches ~150 μM (monomer concentration),

and this concentration of polyphosphate inhibits cytokinesis (and thus cell proliferation), possibly to prevent the formation of small cells, and thus just before starvation increases the percentage of large cells with relatively large reserves of stored nutrients [9].

Polyphosphate inhibits *Dictyostelium* proliferation, and in low nutrient conditions, this requires the GPCR GrlD, a metabotropic Glutamate Receptor-Like receptor, and the small GTPase RasC in a low nutrient condition [39]. The downstream signaling of polyphosphate pathway is unclear.

2. AN AUTOCRINE PROLIFERATION REPRESSOR REGULATES *DICTYOSTELIUM DISCOIDEUM* PROLIFERATION AND CHEMOREPULSION USING THE G PROTEIN-COUPLED RECEPTOR GRLH*

2.1. Summary

In eukaryotic microbes, little is known about signals that inhibit the proliferation of the cells that secrete the signal, and little is known about signals (chemorepellents) that cause cells to move away from the source of the signal. Autocrine proliferation repressor protein A (AprA) is a protein secreted by the eukaryotic microbe *Dictyostelium discoideum*. AprA is a chemorepellent for and inhibits the proliferation of *D. discoideum*. We previously found that cells sense AprA using G proteins, suggesting the existence of a G protein-coupled AprA receptor. To identify the AprA receptor, we screened mutants lacking putative G protein-coupled receptors. We found that, compared to the wild-type strain, cells lacking putative receptor GrlH (*grlH*$^{-}$ cells) show rapid proliferation, do not have large numbers of cells moving away from the edges of colonies, are insensitive to AprA-induced proliferation inhibition and chemorepulsion, and have decreased AprA binding. Expression of GrlH in *grlH* cells (*grlH*$^{-}$*/grlH*^{OE}) rescues the phenotypes described above. These data indicate that AprA signaling may be mediated by GrlH in *D. discoideum*.

* Reprinted with permission. Tang, Y., Wu, Y., Herlihy, S. E., Brito-Aleman, F. J., Ting, J. H., Janetopoulos, C., & Gomer, R. H. (2018). An Autocrine Proliferation Repressor Regulates Dictyostelium discoideum Proliferation and Chemorepulsion Using the G Protein-Coupled Receptor GrlH. *mBio*, 9(1), e02443-17. Copyright © 2018, Tang et al.

2.2. Introduction

Chalones are secreted factors that inhibit the proliferation of the cells that secrete them [40, 41]. For instance, melanocyte proliferation can be inhibited by an unknown secreted chalone, and when the crude chalone is injected under a melanoma, the melanoma cell proliferation ceases [42, 43]. Despite their intrinsic interest and potential utility in controlling tumor growth, in most cases where chalone activity has been observed, the identity of the chalone and the identity of the associated signal transduction pathway are unknown.

We previously identified two *Dictyostelium discoideum* chalones, AprA and CfaD. Both are secreted proteins that inhibit *D. discoideum* cell proliferation [8, 18]. Cells lacking either AprA or CfaD show abnormally fast proliferation, and this phenotype can be rescued either by expressing AprA in *aprA*$^{-}$ cells or CfaD in *cfaD*$^{-}$ cells or by adding recombinant AprA or CfaD to the respective mutant strains [8, 18, 19]. Both AprA and CfaD are necessary for proliferation inhibition, as recombinant AprA (rAprA) cannot rescue the *cfaD*$^{-}$ phenotype and recombinant CfaD (rCfaD) cannot rescue the *aprA*$^{-}$ phenotype [19, 25]. Several components of the AprA-induced and/or CfaD-induced proliferation inhibition signaling pathway have been identified, including the ROCO kinase QkgA, the p21-activated kinase (PAK) family member PakD, the PTEN-like phosphatase CnrN, and the tumor suppressor RblA [20-24]. Additionally, AprA functions to chemorepel *D. discoideum* cells, causing cells to move in a biased direction away from a source of AprA [17]. QkgA, PakD, CnrN, and RblA

are also involved in the AprA- induced-chemorepulsion signaling pathway [17, 20-24]. Both AprA inhibition of proliferation and AprA induction of chemorepulsion require the G proteins Gβ and Gα subunit Gα8, and the binding of AprA to cell membrane is inhibited by GTPγS, suggesting that AprA functions through binding to a G protein-coupled receptor (GPCR) [17, 25].

D. discoideum has 61 genes encoding predicted proteins with sequence similarity to GPCRs [11, 44]. At least 35 of the 61 genes are expressed in growing and proliferating (vegetative) cells [45]. One GPCR mutant, the *crlA*$^{-}$ strain, proliferates faster than the wild type and is insensitive to rAprA-induced proliferation inhibition [46]. However, *crlA*$^{-}$ cells bind AprA with kinetics similar to those of wild-type cells, suggesting that CrlA is not the AprA receptor [19].

GPCR mutant screening done by previous lab members suggests several AprA receptor candidates. An available set of mutants with insertions of a blasticidin resistance cassette in the coding region for a putative G protein-coupled receptor were tested for phenotypes similar to those of cells lacking AprA. Cells lacking AprA, Gα8, Gβ, or the AprA signal transduction components PakD, RblA, and QkgA exhibit faster proliferation and proliferate to a higher maximal density than wild-type cells [8, 20, 21, 23, 25]. Examining the proliferation in a shaking culture of cells lacking putative G

protein-coupled receptors, they observed that *grlH* cells showed significantly faster proliferation than wild-type cells, while *grlD*$^{-}$ and *fscE*$^{-}$ cells were slower to proliferate (Figure 1) (Table 1). *grlH*$^{-}$ cells also died faster after the stationary phase than wild-type cells (Figure 1). None of the mutants proliferated to a higher density than the wild type, and some mutants proliferated to a lower maximal density (Figure 1) (Table 1). Together, these results indicate that *grlH*$^{-}$ cells, like *aprA*$^{-}$ cells [8], have fast proliferation and die quickly after the stationary phase but do not have the *aprA*$^{-}$ phenotype of proliferation to an abnormally high cell density.

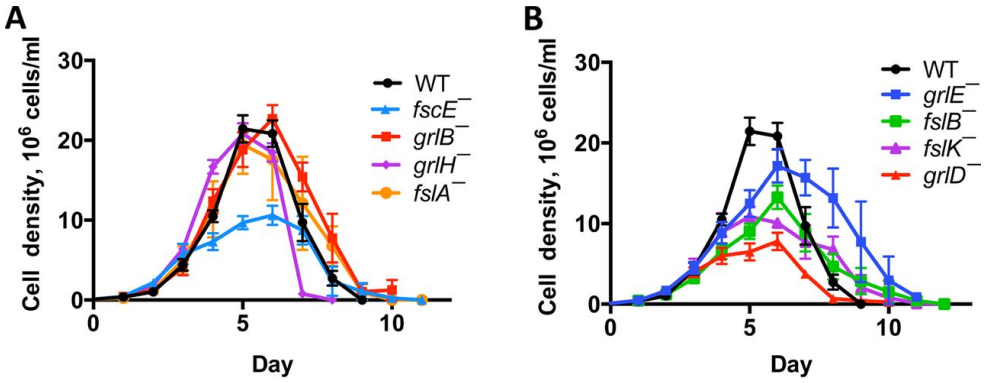

Figure 1. The effect of GPCR disruptions on proliferation.
Log-phase cells were grown in liquid shaking culture starting at 1×10^5 cells/ml and counted daily. WT, Ax2 wild type. For clarity, data from (A) fast-proliferation mutants and (B) normal-proliferation or slow-proliferation mutants were plotted separately. Values are means ± standard errors of the means (SEM); $n \geq 3$ independent experiments.

Table 1. The effect of GPCRs on doubling time and stationary density.
Doubling times and maximum cell densities were calculated using the data in Figure 1A and B. Values are mean ± SEM, n ≥ 4. Statistical significance compared to wild type is shown as * ($p < 0.05$) and ** ($p < 0.01$) (t test).

Cell Type	Doubling time, hours	Maximum observed cell density, 10^6 cells/ml
WT	14.3 ± 0.2	21.9 ± 1.7
grlB$^-$	14.0 ± 0.4	23.4 ± 1.5
grlD$^-$	16.9 ± 0.8*	9.0 ± 0.6**
grlE$^-$	15.2 ± 0.5	18.8 ± 1.7
grlH$^-$	13.0 ± 0.1**	20.8 ± 1.3
fslA$^-$	14.8 ± 1.2	22.1 ± 4.2
fslB$^-$	16.7 ± 1.1	13.6 ± 1.3**
fslK$^-$	16.1 ± 1.3	13.7 ± 1.2**
fscE$^-$	15.8 ± 0.5*	12.0 ± 0.8**

One possible reason that a mutant *Dictyostelium* strain would exhibit abnormal proliferation is an abnormal accumulation of AprA or CfaD. To test this possibility, conditioned media from the putative G protein-coupled receptor mutants were assayed for AprA and CfaD. None of the mutants accumulated significantly less AprA or CfaD than wild-type cells (Figure 2). Four mutants, including the *grlH* mutant, accumulated abnormally high levels of extracellular AprA. *grlH* cells accumulated normal levels of extracellular CfaD, and 3 other mutants accumulated abnormally high levels of extracellular CfaD. Together, these data indicate that the fast proliferation of *grlH* cells is not due to abnormally low extracellular levels of AprA or CfaD.

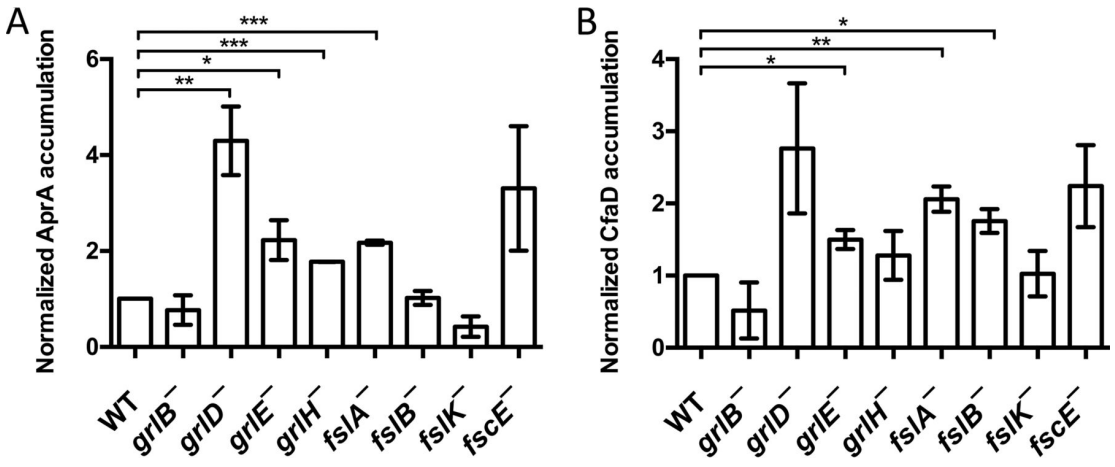

Figure 2. Accumulation of AprA and CfaD in GPCR mutants.
Conditioned media from log-phase cells were analyzed for accumulated (A) AprA and (B) CfaD using anti-AprA and anti-CfaD antibodies. Quantifications (n = 3 independent experiments, means ± SEM) of Western blot bands, normalized to the band intensity for the Ax2 wild type (WT), are shown. *, $P < 0.05$; **, $P < 0.01$; ***, $P < 0.001$ (compared to the wild type [t test]).

Possibly due to a decreased ability to cause cells at the edge of a colony to be repelled from the colony, *aprA*$^{-}$, *pakD*$^{-}$, *rblA*$^{-}$, and *qkgA*$^{-}$ cells form abnormally small colonies starting from single cells on bacterial lawns [8, 20, 21, 23](5, 10, 11, 18). The *grlB*$^{-}$, *grlH*$^{-}$, *fslA*$^{-}$, *fslB*$^{-}$, and *fslK*$^{-}$ cells also formed abnormally small colonies on bacterial lawns (Figure 3). Whereas wild-type cells form colonies in submerged liquid culture with cells dispersed from the colony edges, *aprA*$^{-}$, *rblA*$^{-}$, and *qkgA*$^{-}$ cells form colonies with well-defined edges and few dispersed cells [8, 20, 21]. They found that *grlB*$^{-}$, *grlH*$^{-}$, and *fslK*$^{-}$ cells also formed colonies with well-defined edges (Figure 4). Together, these results indicate that *grlB*$^{-}$, *grlH*$^{-}$, and *fslK*$^{-}$ cells all have the small

colony on bacterial lawns and that the abnormally few cells dispersing from a colony in submerged liquid culture show phenotypes characteristic of cells lacking AprA or some of the AprA signal transduction pathway components.

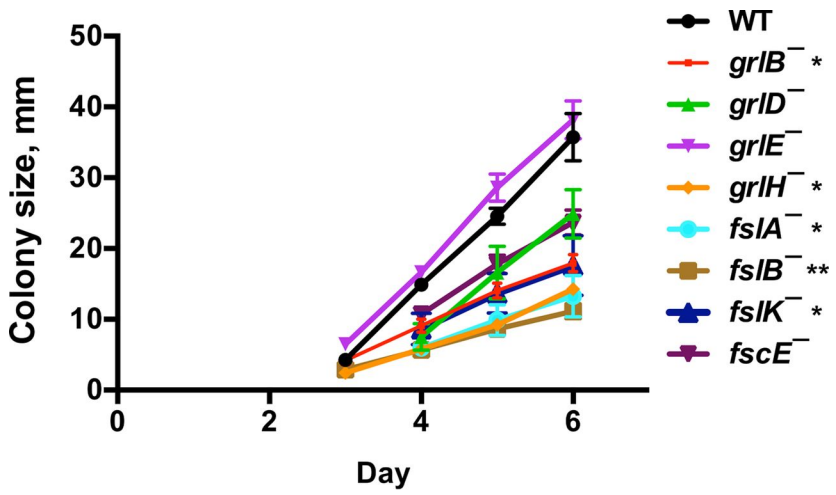

Figure 3. GPCR mutant colony expansion.
Approximately 10 cells were plated onto agar plates spread with *K. aerogenes* bacteria. At least 3 colonies were measured daily per plate. After 6 days, individual wild-type colonies were indistinguishable from each other. Values are means ± SEM; $n \geq 3$ independent experiments. The absence of error bars indicates that the SEM was less than the size of the marker. *, $P < 0.05$; **, $P < 0.01$ (for the change in colony size from day 4 to day 6 compared to the wild type [*t* test]).

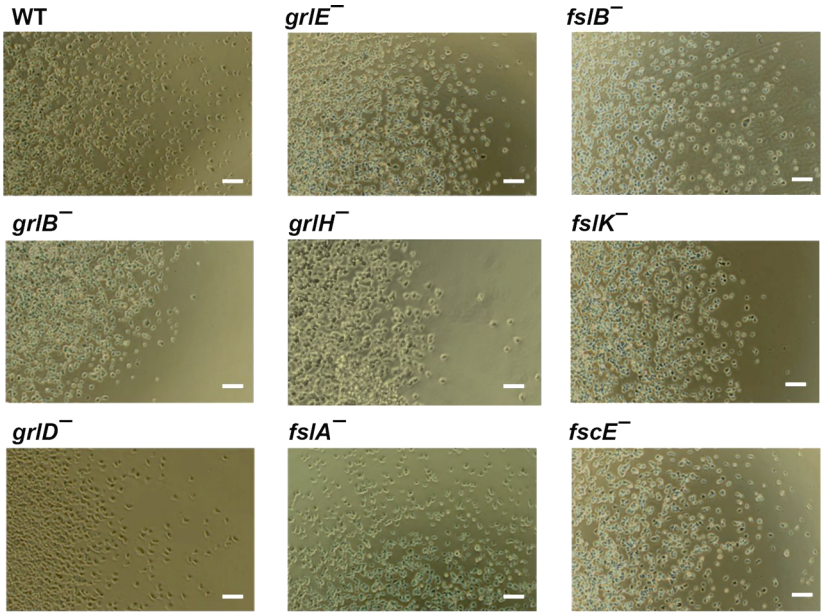

Figure 4. Colony edges of GPCR mutants.
Colonies of cells were allowed to adhere to glass well slides. Fresh media was added to the wells and cells were left overnight to spread. The edges of colonies were imaged with a 10x phase contrast objective. The right colony edge is shown for all strains except *fslA*$^{-}$, where the top colony edge is shown. Images are representative of at least three independent experiments. Bars are 50 μm.

Another characteristic of *aprA*$^{-}$ cells is that they tend to be multinucleate; a population of *aprA*$^{-}$ cells has fewer mononucleate cells and more cells with 2 nuclei or 3 or more nuclei than a population of wild-type cells [8]. Cells lacking the AprA signal transduction pathway component Gα8, Gβ, or QkgA have similar multinucleate phenotypes [20, 25]. They found that *grlD*$^{-}$, *fslA*$^{-}$, *fslB*$^{-}$, *fslK*$^{-}$, and *fscE*$^{-}$ cells had fewer cells with a single nucleus, and more cells with two nuclei, than wild-type cells (Table 2). *fslB*$^{-}$ and *fslK*$^{-}$ cells also had more cells with three or more nuclei. These data indicate that, like cells lacking AprA, Gα8, Gβ, or QkgA, cells of several mutants

lacking putative G protein-coupled receptors, but not *grlH* cells, tend to have more nuclei per cell than wild-type cells.

Table 2. The effect of GPCR on nuclei per cell.
Cells were stained with DAPI (4', 6-diamidino-2-phenylindole), the number of nuclei in cells was counted, and then the number of nuclei per 100 cells was calculated. Values are means ± SEM; n ≥ 3 independent experiments. *, P < 0.05; **, P < 0.01; ***, P < 0.001 (compared to the wild type [t test]).

Cell type	Percent of cells with n nuclei			Nuclei/100 cells
	1	2	3+	
WT	86 ± 2	14 ± 3	0.5 ± 0.2	116 ± 2
grlB$^-$	76 ± 3	22 ± 2	1.8 ± 0.6	126 ± 3*
grlD$^-$	62 ± 3***	34 ± 2**	3.7 ± 1.9	143 ± 5*
grlE$^-$	79 ± 4	20 ± 4	0.8 ± 0.6	122 ± 5
grlH$^-$	90 ± 2	9 ± 1	0.8 ± 0.2	109 ± 1
fslA$^-$	69 ± 4**	27 ± 3*	4.1 ± 2.2	136 ± 6*
fslB$^-$	71 ± 2**	27 ± 2*	2.4 ± 0.6*	132 ± 3*
fslK$^-$	49 ± 4***	41 ± 3***	9.4 ± 1.6**	167 ± 9**
fscE$^-$	71 ± 1***	29 ± 1**	0.9 ± 0.3	131 ± 2**

Both AprA and CfaD inhibit the proliferation of *D. discoideum* cells [8, 18]. To test the possibility that the fast proliferation of *grlH* cells may be due to reduced sensitivity either to AprA or to CfaD, the ability of recombinant AprA (rAprA) and recombinant CfaD (rCfaD) to inhibit proliferation were examined. Both proteins

inhibited the proliferation of wild-type cells as previously observed [8, 18] (Figure 5). As seen with the wild-type cells, AprA inhibited the proliferation of *fslA*$^{-}$, *fslB*$^{-}$, *and* *fscE*$^{-}$ cells, and CfaD inhibited the proliferation of *grlH*$^{-}$ cells. Cells lacking GrlB, GrlD, GrlE, or GrlH were insensitive to rAprA, and cells lacking GrlB, GrlD, GrlE, FslB, or FscE were insensitive to rCfaD (Figure 5). Together, these results suggest that, surprisingly, multiple receptors are required for the ability of rAprA or rCfaD to inhibit proliferation.

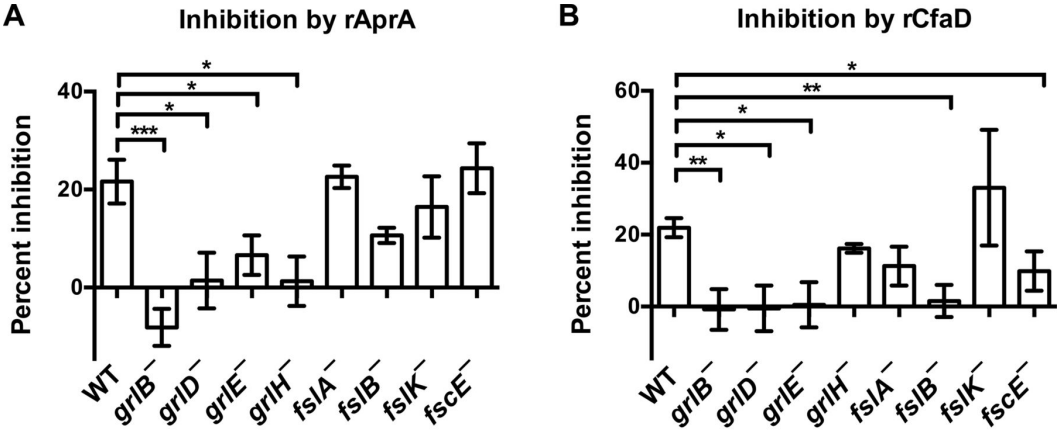

C

against 0	WT	*grlB*$^{-}$	*grlD*$^{-}$	*grlE*$^{-}$	*grlH*$^{-}$	*fslA*$^{-}$	*fslB*$^{-}$	*fslK*$^{-}$	*fscE*$^{-}$
AprA	**					*	*		*
CfaD	***				***				

Figure 5. Sensitivities of GPCR mutants to inhibition of proliferation by rAprA or rCfaD.
A 300-ng/ml volume of rAprA or rCfaD, or an equivalent volume of buffer, was added to cells in liquid shaking culture. After 16 h, cell densities were counted. (A and B) The

percentage of inhibition of proliferation caused by rAprA (A) or by rCfaD (B) compared to the buffer control was calculated. (C) The significance of the difference between the effect represented by a value of 0 (no effect of AprA or CfaD) and the observed effect was calculated. Values are means ± SEM; $n \geq 3$ independent experiments. *, $P < 0.05$; **, $P < 0.01$; ***, $P < 0.001$ (compared to the wild type [*t* test]).

AprA, but not CfaD, is a chemorepellent for *D. discoideum* cells [17]. An Insall chamber assay [17, 47] was used to determine if any of the putative G protein-coupled receptor mutants are insensitive to rAprA-induced chemorepulsion. As previously observed, wild-type cells moved in a biased direction away from rAprA [17] (Figure 6). *grlE*$^{-}$, *fslA*$^{-}$, and *fslK*$^{-}$ cells also moved away from rAprA (Figure 6). For unknown reasons, *grlD*$^{-}$, *grlH*$^{-}$, and *fscE*$^{-}$ cells moved toward the source of rAprA. *grlB*$^{-}$ and *fslB*$^{-}$ cells were insensitive to AprA-induced chemorepulsion (Figure 6). These data suggest that, with respect to chemorepulsion from a source of rAprA, several GPCR mutants are insensitive to AprA.

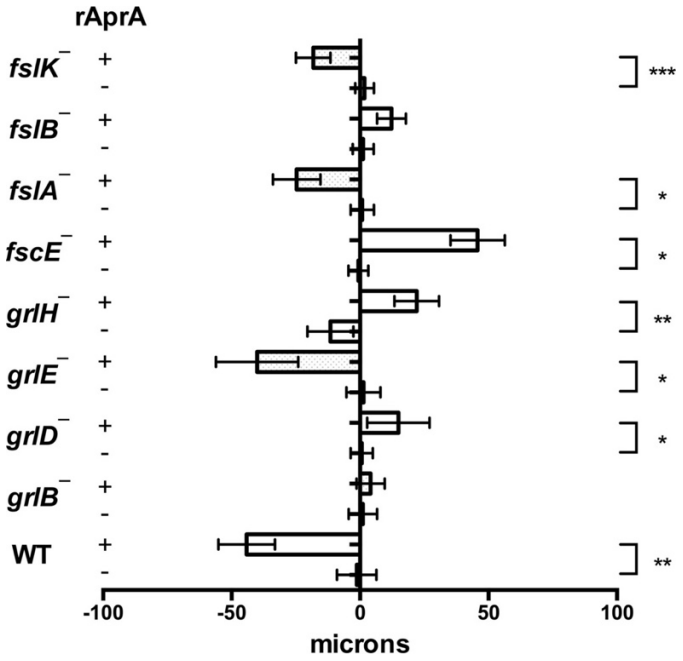

Figure 6. The effect of rAprA on chemorepulsion in GPCR mutants.
rAprA or an equivalent volume of buffer was added to one side of an Insall chamber. Videomicroscopy was used to visualize the movement of cells, which were then manually tracked. The migration distance along the gradient over the course of 60 min was measured. Values are means ± SEM; $n \geqslant 3$ independent experiments. Bars to the left of the vertical line at the center of the figure represent cells moving away from the source. *, $P < 0.05$; **, $P < 0.01$; ***, $P < 0.001$ (*t* test).

None of the GPCR mutants showed phenotypes matching all of the phenotypes of *AprA* cells or the phenotypes of mutants that are insensitive to AprA. Only *grlB*$^{-}$, *grlD*$^{-}$, and *grlH*$^{-}$ cells had defects in both AprA-induced proliferation inhibition and AprA- induced chemorepulsion. These results suggest that there may be more than one AprA receptor in *D. discoideum*. Among those three mutant strains, only the *grlH* cells were insensitive to AprA-induced proliferation inhibition but not to CfaD-induced proliferation inhibition. Similar to *aprA*$^{-}$ cells, *grlH*$^{-}$ cells showed a higher death rate

after the stationary phase, a lower colony expansion rate on bacterial lawns, tighter colony edges in submerged culture, and a shorter doubling time than wild-type cells. These data suggest that GrlH may be at least one of the AprA receptors.

In this study, I tested the hypothesis that GrlH is an AprA receptor, and confirmed that AprA signaling is mediated by the GPCR GrlH in *Dictyostelium*.

2.3. Materials and Methods

2.3.1. Cell culture and strains

grlB$^-$ (DBS0350074), *grlD*$^-$ (DBS0350227), *grlE*$^-$ (DBS0350075), *grlH*$^-$ (DBS0350226), *fslA*$^-$ (DBS0350228), *fslB*$^-$ (DBS0350230), *fslK*$^-$ (DBS0350229), and *fscE*$^-$ (DBS0350232) cells were generated by homologous recombination in the wild-type Ax2 background using the vector pLPBLP [48]. The 5' homologous region and the 3' homologous region for each gene were amplified from the genomic DNA and directionally cloned into pLPBLP. The resulting construct was linearized with NotI, and 2 g of linearized DNA was electroporated into 5 x 10^6 cells [48]. The transformed cells were grown with 10 g/ml blasticidin S for 10 days, diluted, and then plated on a *Klebsiella aerogenes* lawn. Clones were isolated 5 days later, and successful gene disruption in clones was confirmed by PCR of genomic DNA using one primer inside the blasticidin resistance cassette and one primer in the genomic DNA outside the homologous region used for the knockout construct [49]. At least 2 different clones were

isolated, and phenotypes were confirmed. Parental Ax2 cells and mutants were grown as previously described [50] in SM medium with *E. coli* or in HL5 medium (Formedium Ltd., Norwich, England).

2.3.2. Assays

Proliferation in shaking culture, proliferation inhibition, chemotaxis, nucleus staining, colony expansion, spore count, and spore viability assays were done following the methods described in reference [20] except that *Escherichia coli* was also used for colony expansion. Colony edge imaging was done following the method described in reference 10 except that for GPCR mutant screening, 200 µl of HL5 medium without bacteria was added to each well. AprA and CfaD accumulation assays were done as previously described [18, 19]. Preparation of recombinant His-tagged AprA and CfaD was done following the methods described in references [18, 19]. rAprA binding to cells was measured as previously described [19], with the exception that 0, 200, 400, 800, 1,600, 2,000, or 2,400 ng/ml rAprA was added to cells and incubated with the cells for 15 min at 4°C, and biotinylated mitochondrial 3-methylcrotonyl-CoA carboxylase (MCCC1) was used as a gel loading control [51].

2.3.3. *grlH* expression

To construct a *grlH* expression vector, total RNA from vegetative Ax2 cells was

isolated using an R1054 RNA prep kit (Zymo Research, Irvine, CA) and then a cDNA library was generated using this RNA as a template with a K1651 cDNA synthesis kit (Thermo Fisher, Carlsbad, CA). PCR was done using this cDNA with primers 5'-CGCGGATCCATGAAAAATATTTTAAAAATT-3' and 5'-CCGCTCGAGTTAATTATTATTTTCTGAATCATTG-3' to generate a DNA fragment containing the *grlH* coding region. After digestion with BamHI and XhoI (NEB, Ipswich, MA), the PCR product was ligated into the corresponding sites of pDXA-3D [52] to produce expression plasmid pDXA-3D-grlH. To construct the $grlH^{-}/grlH^{OE}$ strain, *grlH* cells were transformed with pDXA-3D-grlH by electroporation following the method described in reference [53]. The expression of *grlH* was verified by reverse transcription-PCR (RT-PCR) with primers 5'-GCTTCCGAAAGAGCCACC-3' and 5'-CAATAAAGCCGCAGTGGT-3', with RNA extraction and cDNA synthesis done as described above. For a loading control, RT-PCR was done with primers for AprA (5'-CCCAAGCTTACTCCATTGGATGATTATGTC-3' and 5'-CCGCTCGAGTAAAGTTGCAGTTGAACTAGCACTATCACC-3').

2.3.4. Statistics

Statistical analyses performed with *t* tests and one-way analysis of variance (ANOVA) performed with the appropriate posttest and curve fits were done using Prism (GraphPad, San Diego, CA). Significance was defined as a *P* value of 0.05.

2.4. Results

To test the hypothesis that GrlH is an AprA receptor, I expressed *grlH* under the control of the *actin15* promoter in *grlH*$^{-}$ cells to make the rescue strain *grlH*$^{-}$/*grlH*^{OE}. *grlH* expression was observed in wild-type and *grlH*$^{-}$/*grlH*^{OE} cells but not in *grlH*$^{-}$ cells (Figure 7A). Expression of *grlH* in the *grlH*$^{-}$ cells increased the doubling time to a level similar to that of wild-type cells (Figure 7B) (Table 3), suggesting that the fast proliferation of *grlH*$^{-}$ cells is due to lack of GrlH. The *grlH*$^{-}$/*grlH*^{OE} cells had a lower maximal cell density than wild-type cells (Table 3), suggesting that GrlH may regulate cell density.

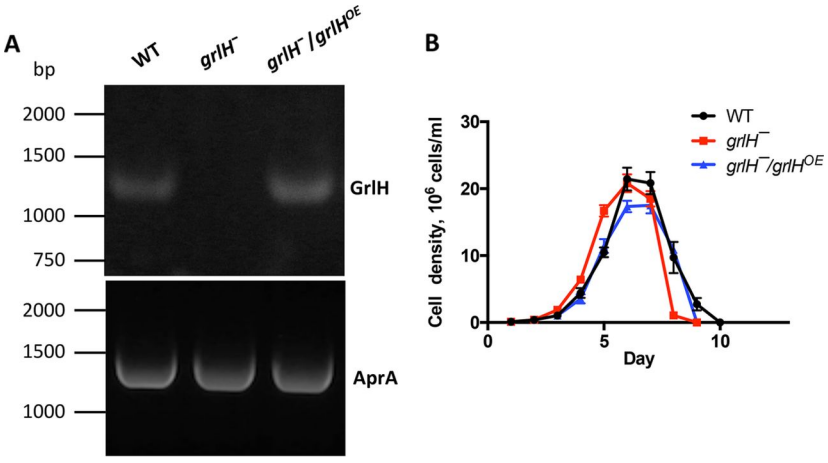

Figure 7. The effect of GrlH on proliferation.
(A) *grlH* expression (top panel) was confirmed by RT-PCR, using RT-PCR with primers for AprA as a loading control (bottom panel). (B) Cell proliferation was measured as described for Fig. 1. Values are means ± SEM; $n \geq 3$ independent experiments.

Table 3. The effect of GrlH on doubling time and stationary density.
Doubling times and maximum cell densities were calculated using the data in Fig. 7B. Values are means ± SEM; $n \geq 4$ independent experiments. *, $P < 0.05$; ***, $P < 0.001$ (compared to the wild type [one-way ANOVA, Tukey's test]). The difference between the doubling time of the *grlH*$^{-}$ mutant and that of the *grlH*$^{-}$/*grlH*^{OE} mutant was significant with $P < 0.01$; all other differences were not statistically significant (one-way ANOVA, Tukey's test).

Cell type	Doubling time, hours	Maximum observed cell density (10^6 cells/ml)
WT	14.3 ± 0.2	21.9 ± 1.7
grlH^{-}	13.0 ± 0.1 ***	20.8 ± 1.3
grlH^{-}/*grlH*^{OE}	14.1 ± 0.3	17.5 ± 1.2*

Expression of *grlH* in *grlH*$^{-}$ cells also rescued the *aprA*$^{-}$-like phenotypes of *grlH*$^{-}$ cells such as a low colony expansion rate on bacterial lawns (Figure 8) and tight colony edges (Figure 9). Expression of *grlH* in *grlH*$^{-}$ cells also restored the ability of *grlH*$^{-}$ cells to decrease proliferation in the presence of AprA (Figure 10) and to be repelled by a source of rAprA (Figure 11). These data indicate that the slower colony expansion, the tighter colony edges, and the abnormal sensitivity to rAprA of *grlH*$^{-}$ cells are due to the lack of GrlH.

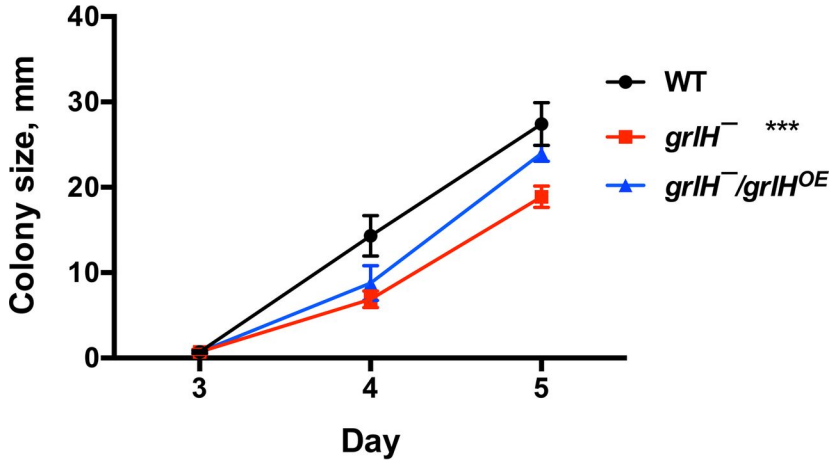

Figure 8. *grlH*⁻ and *grlH*⁻*grlH*^{OE} colony expansion.
Approximately 10 cells were plated onto plates containing *E. coli* bacteria. At least 3 colonies were measured per plate daily. Values are means ± SEM; $n \geq 3$ independent experiments. The absence of error bars indicates that the SEM was less than the size of the marker. ***, $P < 0.001$ (for the change in colony size from day 3 to day 5 compared to the wild type [one-way ANOVA, Tukey's test]). The difference between the *grlH*⁻ mutant and the *grlH*⁻/*grlH*^{OE} mutant was significant with a P value of <0.01, and there was no significant difference between WT and the *grlH*⁻/*grlH*^{OE} mutant (one-way ANOVA, Tukey's test).

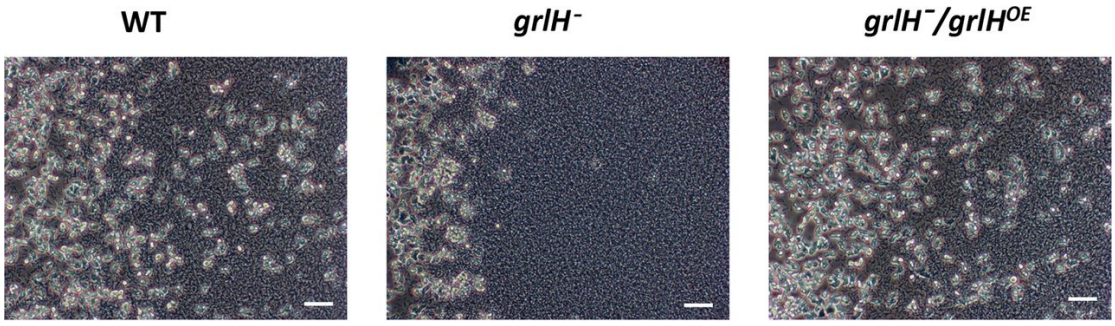

Figure 9. Colony edge formation of the *grlH*⁻ and *grlH*⁻/*grlH*^{OE} mutants.
Colonies of cells were allowed to adhere to glass well slides. Fresh SM media with *E. coli* was added to the wells, and the cells were left overnight to spread. The edges of colonies were imaged with a 10x phase-contrast objective. The right colony

edge is shown for all strains. Images are representative of results of at least three independent experiments. Bars are 50 μm.

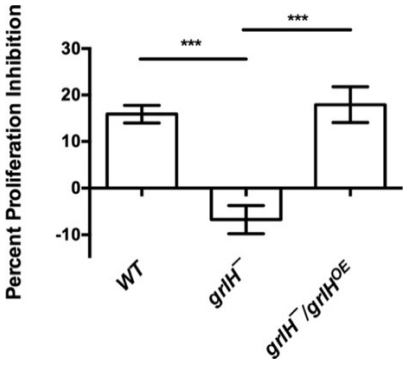

Figure 10. The effect of GrlH on AprA-induced proliferation inhibition.
The effect of AprA on proliferation was measured as described for Fig. 5. Values are means ± SEM; $n \geq 3$ independent experiments. ***, $P < 0.001$ (one-way ANOVA, Tukey's test). There is no significant difference between WT and the *grlH⁻/grlH^OE* mutant (one-way ANOVA, Tukey's test).

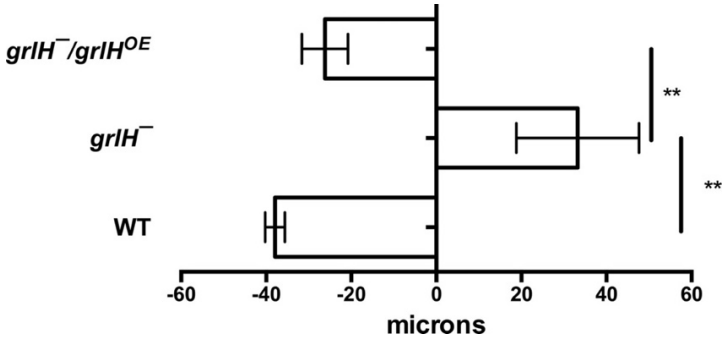

Figure 11. The effect of GrlH on AprA-induced chemorepulsion.
rAprA or an equivalent volume of buffer was added to one side of an Insall chamber. Videomicroscopy and tracking were then done as described for Fig. 5. Values are means ± SEM; $n \geq 3$ independent experiments. **, $P < 0.01$ (one-way ANOVA, Tukey's test). There is no significant difference between WT and the *grlH⁻/grlH^OE* mutant (one-way ANOVA, Tukey's test).

We previously observed that wild-type cells bind rAprA with a $B_{\max}$ of 3.1 ± 0.4 ng/ 5 x 10^5 cells and a dissociation constant (K_d) of 160 ± 50 ng/ml [19]. To directly test the hypothesis that GrlH is required for cells to bind rAprA, I did rAprA binding assays on cells. *grlH*$^-$ cells showed a decreased level of rAprA binding compared to wild-type cells, and *grlH*$^-$/*grlH*^{OE} cells showed a partially rescued level of rAprA binding (Figure 12). I measured $B_{\max}$ and K_d values for rAprA binding to wild-type cells of 3.3 ± 2.0 ng/5 x 10^5 cells and 1,600 1,200 ng/ml, respectively. For unknown reasons, the K_d value that we measured was much higher than what we had previously observed. The $B_{\max}$ and K_d values for rAprA binding to *grlH*$^-$/*grlH*^{OE} cells were 1.4 ± 0.2 ng/5 x 10^5 cells and 360 ± 100 ng/ml, respectively. The *grlH*$^-$ cells did not show saturable binding of rAprA.

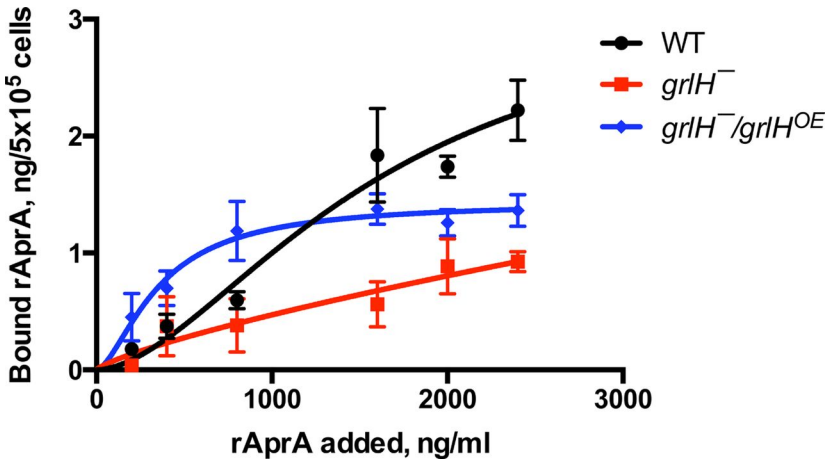

Figure 12. The effect of GrlH on AprA binding to cells.
Cells of the indicated strains were incubated with the indicated concentrations of myc-tagged rAprA at 4°C. After 15 min, cells were collected by centrifugation, resuspended in ice-cold HL5, and collected, and the bound rAprA was measured by Western blotting (with known amounts of myc-rAprA on each blot for quantitation of bands), staining for the myc tag. Values represent means ± SEM; $n \geq 3$ independent experiments. The lines represent curves fitting to a one-site binding model.

These data suggest that loss of GrlH decreases rAprA binding to cells and that binding of rAprA can be restored by expression of *grlH* in the *grlH*$^{-}$ cells.

2.5. Discussion

We previously found that AprA requires G proteins to inhibit proliferation and to induce chemorepulsion, suggesting that AprA is a ligand for a GPCR [25]. In this report, we show that, compared to wild-type cells and similarly to mutants which are insensitive to AprA, cells lacking the GPCR GrlH have a lower doubling time, a lower colony expansion rate, and tighter colony edges [17, 20, 21, 23]. An important caveat is that, in

addition to AprA, many other factors could contribute to the doubling time of cells, the colony expansion rate, and the morphology of the colony edge. In addition, cells lacking GrlH are insensitive to rAprA-induced proliferation inhibition and chemorepulsion and show reduced binding to rAprA compared to wild-type cells. Expressing GrlH in the *grlH*$^{-}$ cells rescued the phenotypes described above. Together, these data suggest that GrlH is a receptor for AprA. Although AprA is glycosylated, the effects of recombinant AprA produced in bacteria, and thus not significantly glycosylated, mimic the effects of endogenous AprA [8, 18, 19], and we observed an apparent binding of recombinant AprA to GrlH, suggesting that GrlH binds to a nonglycosylated feature of AprA.

Based on function and amino acid sequence, GPCRs can be classified into the following families: family 1, containing an β-adrenergic, odorant receptor and light receptors; family 2, containing secretins; family 3, containing metabotropic glutamate/ $GABA_B$ receptors; family 4, containing pheromone receptors; and family 5, containing frizzled/smoothened receptors [54, 55]. In humans, more than 1,000 genes encode GPCRs. In *Dictyostelium*, 61 genes encode putative GPCRs [11]. One gene, *lrlA*, belongs to family 2; 17 genes (*grlA* to *grlH* and *grlJ* to *grlR*) belong to family 3; 25 genes (*fslA* to *fslH*, *fslJ* to *fslQ*, *fscA* to *fscH*, and *fscJ*) belong to family 5; 12 genes (*cAR1* to *cAR4* and *CrlA* to *CrlH*) belong to a unique cAR/Crl (cAMP receptor/cAMP receptor like) family; 1 gene encodes a protein similar to orphan vertebrate protein GPR89; and 5 genes encode proteins with similarity to human transmembrane protein

145 [11, 46, 56, 57]. CAR1 to CAR4 are cAMP receptors, GrlB and GrlE are aminobutyric acid receptors, and GrlL (fAR1) is a folate receptor [25, 58-62]. Like GrlB, GrlE, and GrlL, GrlH is a family 3 receptor.

Several GPCR mutants other than the *grlH* mutant were insensitive to rAprA-induced proliferation inhibition or chemorepulsion or both. *grlB*$^{-}$, *grlD*$^{-}$, and *grlE*$^{-}$ cells were insensitive to rAprA-induced proliferation inhibition, and *grlB*$^{-}$, *grlD*$^{-}$, *fslB*$^{-}$, and *fscE*$^{-}$ cells were insensitive to rAprA-induced chemorepulsion. One possible explanation for those findings is that two or more receptors exist for AprA, as cells lacking GrlH did not show completely abolished rAprA binding. In support of the idea that multiple receptors might sense AprA, cells lacking GrlH were attracted to a source of recombinant AprA, indicating the presence of a non-GrlH receptor that mediates chemoattraction to AprA. If this unknown receptor is closely related to GrlH, it may be among the 17 family 3 receptors that are not GrlB, GrlE, GrlH, or GrlL. Since the recombinant AprA is not glycosylated, this unknown receptor appears to sense a nonglycosylated feature of AprA. Another possible explanation is that these receptors are activated by a different signal and that this signaling is necessary for AprA signaling. For instance, cells lacking CfaD are insensitive to rAprA-induced proliferation inhibition and chemorepulsion [17, 19]. Unlike *grlH*$^{-}$ cells, *grlB*$^{-}$, *grlD*$^{-}$, and *fslB*$^{-}$ cells were insensitive to rCfaD-induced proliferation inhibition. It is possible that the disruption of GrlB, GrlD, or FslB interrupts the CfaD signaling pathway such that *grlB*$^{-}$, *grlD*$^{-}$, and

fslB^{-} cells cannot respond properly to AprA. In addition to CfaD, there may be other factors that are necessary for AprA and CfaD signaling. Together, these results indicate that GrlH is a receptor for AprA, that there may be more than one AprA receptor, and that multiple receptors and, presumably, their associated signaling pathways regulate AprA signaling.

3. AN IMPROVED SHOTGUN ANTISENSE METHOD FOR MUTAGENESIS AND GENE IDENTIFICATION*

3.1. Summary

Shotgun expression of antisense cDNAs, where each transformed cell expresses a different antisense cDNA, has been used for mutagenesis and gene identification in *Dictyostelium discoideum*. However, the method has two limitations. First, there were too few clones in the shotgun antisense cDNA library to have an antisense cDNA for every gene in the genome. Second, the unequal transcription level of genes caused there to be many antisense cDNAs in the library for some genes, but relatively few antisense cDNAs for other genes. Here we report an improved method for generating a larger antisense cDNA library with a reduced percentage of cDNA clones from highly prevalent mRNAs, and demonstrate its utility by screening for signal transduction pathway components in *Dictyostelium discoideum*.

3.2. Methods Summary

We present an improved shotgun antisense method for generating gene expression knock-down mutants. This method incorporates a cDNA normalization step to equalize the transcript number of each gene in the antisense cDNA library.

---

* Reprinted with permission. Tang, Y., & Gomer, R. H. (2020). An improved shotgun antisense method for mutagenesis and gene identification. *BioTechniques*, *68*(3), 163-165.

3.3. Materials and Methods

Cell culture. *Dictyostelium discoideum* Ax2 cells (wild type) and REMI mutant GWDI_488_A_5 cells were from the *Dictyostelium* Stock Center (Chicago, IL) [63]. Cells were cultured in HLG0102 HL5 (Formedium, Hunstanton, UK) at 21 ˚C on a rotary shaker at 175 rpm.

cDNA synthesis and normalization. Total RNA was extracted from 5 x 10^6 cells at mid-log phase (~1 x 10^6 cells/ml) using a R1054 RNA prep kit (Zymo Research, Irvine, CA). 3 µg RNA was used for directional double-strand cDNA (ds-cDNA) library synthesis with the primers 5' - AAGCAGTGGTATCAACGCAGAGT***ACTAGT***GGGG - 3' (*SpeI* site bolded) and 5' - AAGCAGTGGTATCAACGCAGAGT***AGATCT***TTTTGTTTTTTCTTTTTTTTTTTTT VN -3' (*BglII* site bolded) using a Mint-2 cDNA synthesis kit (Evrogen, Moscow, Russia). The resultant cDNA has a *SpeI* site on the end corresponding to the 5' end of the mRNA and a *BglII* site on the other. 1.2 µg of this ds-cDNA library was then normalized using the Trimmer-2 kit (Evrogen). For the normalization, the double-stranded cDNA library was denatured to single-stranded DNA at 98 °C for 2 minutes and then allowed to hybridize to double-stranded DNA again at 68 °C for 5 hours. This hybridization process generated two populations of cDNA, successfully re-paired double-stranded DNA and unpaired single-stranded DNA. Abundant transcripts hybridize to double-stranded DNA more efficiently than rare transcripts [64]. The double-stranded cDNA, composed primarily of abundant transcripts, was then degraded by the duplex-specific nuclease

(provided from the kit). All procedures followed the manufacturers' instructions.

Construction of a normalized antisense cDNA library. The remaining single stranded cDNA, corresponding to a cDNA library with many of the abundant transcripts removed, was amplified by PCR with the primer 5' - AAGCAGTGGTATCAACGCAGAGT - 3' following the Trimmer-2 kit instructions. The enriched PCR product and the vector plasmid pDM326 containing the blasticidin resistance cassette [65] were digested for 4 hours at 37 ˚C with the restriction enzymes BglII and SpeI. Digested PCR products larger than 200 bp were purified and enriched using a Select-a-Size DNA Clean & Concentrator kit (Zymo). Digested pDM326 was gel purified using a D2500-01 Gel Extraction kit (Omega, Norcross, GA). 100 ng digested cDNA and 50 ng digested pDM326 were then ligated at 16 ˚C overnight using T4 ligase (NEB, Ipswich, MA). The ligation was concentrated with a DNA Clean & Concentrator-5 kit (Zymo) to a volume of 10 µl. The ligation was then used to transform 5-alpha electrocompetent *E. coli* cells (NEB) following the manufacturer's protocol with 1 µl purified ligation product and 25 µl competent cells per transformation. 1/10 of the total transformed cells from one transformation were plated to one LB/AMP agar plate (100 µg/ml ampicillin) to determine the library size. The total transformed cells from 10 µl ligation product were plated on 35 LB/AMP agar plates and incubated at 37 ˚C overnight. Colonies were collected using a plate scraper with 3 ml LB per plate. The collected cells were grown in 500 ml of LB to an OD 600 of ~3, and 25 ml of this culture was mixed with 25 ml of 50% glycerol in H_2O, and aliquots were stored at -80 ˚C. The remaining culture

was used for a plasmid DNA maxi-prep using a D4203 Maxi-prep kit (Zymo) and the plasmid DNA was used to transform *D. discoideum* cells.

Transformation of *Dictyostelium discoideum*. Wild-type Ax2 cells were transformed by electroporation following [66]. For each electroporation, 4 x 10^7 cells in 180 µl H50 buffer (20 mM HEPES, 50 mM KCl, 10 mM NaCl, 1 mM $MgSO_4$, 5 mM $NaHCO_3$, 1 mM NaH_2PO_4, pH 7.0) were mixed with 20 µl DNA (500 ng) and incubated on ice for 5 minutes. This mixture was then loaded into an EC2L 2-mm electroporation cuvette (Midsci, Valley Park, MO) and electroporated with a GenePulser Xcell electroporator（Bio-Rad, Hercules, CA）at 850 V and 25 µF, with 2 pulses with a 5 second gap. Electroporated cells were then cultured in 10 ml HL5/ 100 µg/ml ampicillin in a 100-mm tissue culture petri dish. 10 µg/ml blasticidin (GoldBio, St. Louis, MO) was added 16-20 hours later for selection of transformed cells. Colonies normally appeared after 5-7 days and were transferred to shaking culture for screen assays. Each plate typically contained 800 colonies.

Screen for transformants resistant to polyphosphate proliferation inhibition. Wild-type Ax2 cells and the pool of transformants were cultured in HL5 (containing 10 µg/ml blasticidin for transformants) with a cycle of 2 days of 150 µM SO169 polyphosphate (Spectrum, New Brunswick, NJ) and two days of no polyphosphate. Each cycle started with cells at 5 x 10^5 cells/ml, and after two days, cells were washed with HL5, counted, and diluted to 5 x 10^5 cells/ml again. Cell densities were counted daily to

calculate proliferation rates. After 4 to 5 cycles, compared to Ax2 cells, transformants pools which had a significantly faster proliferation rate in the presence of polyphosphate were plated on lawns of *E. coli* on SM/5 (2 g/L glucose, 2 g/L bacto peptone, 0.2 g/L yeast extract, 0.2 g/L $MgSO_4 \cdot 7H_2O$, 1.9 g/L KH_2PO_4, 1 g/L K_2HPO_4, 15 g/L agar) plates for single clone selection. Cells in plaques on the lawns were then picked and cultured in HL5 plus polyphosphate to verify the phenotype of abnormally fast proliferation in the presence of polyphosphate. Clones passing this verification were selected for further analysis.

Isolation and cloning of antisense cDNAs. The antisense cDNA plasmid was extracted from 3 x 10^6 mid-log phase transformed *Dictyostelium* cells using a ZR plasmid miniprep kit (Zymo) and then used to transform chemical competent *E. coli* (Lucigen, Middleton, WI) on the same day. After selection and growth, the antisense cDNA plasmid was then extracted from the transformed *E. coli* using the same kit as above. The antisense cDNA was digested with BglII and SpeI, gel purified, and ligated into a modified pGEM-T vector (BglII site incorporated, a gift from Dr. Beiyan Nan, Texas A&M University). The ligation was then used to transform DH5-alpha *E. coli.* The pGEM-antisense cDNA plasmid was isolated from these transformed cells and used for sequencing.

Construction of *sodC* knock-down strain by antisense repression. PCR was done using the cDNA library to generate the full-length fragment of *sodC* with the primers forward 5'- CGC***ACTAGT***ATGAGACTTTTATCTGTATTAG -3' and reverse 5'-GCG***AGATCT***TTAAAGCAAAGCAAAGATAAT -3', and a truncated version of *sodC*

with the primers forward 5'- GCG***ACTAGT***GATGGATACTGGTTACTA -3' and reverse 5'- GCG**AGATCT**TTAAAGCAAAGCAAAGATAAT -3'. PCR products were digested with BglII and SpeI and ligated into the pDM304 vector [65] in the antisense direction. pDM304-antisense-sodC was used to transform Ax2 cells by electroporation and transformants were selected with 10 μg/ml G418.

Proliferation inhibition assay. Cells at 1.5 x 10^6/ml were cultured with 0, 125 and 150 μM polyphosphate in HL5 for 24 hours and cells were then counted. The data were plotted as 100 x (density with polyphosphate – 1.5 x 10^6/ ml) / (density with no added polyphosphate – 1.5 x 10^6/ ml). Data were analyzed by t-test using Prism 7 (Graphpad, La Jolla, CA). Significance was defined as $p < 0.05$.

3.4. Results

Genetic screens are broadly used to generate and identify mutants with a desired phenotype. Techniques for genetic screens include chemical and radiation mutagenesis [67, 68], insertional mutagenesis [69, 70], CRISPR libraries [71, 72], siRNA libraries [73, 74], and shotgun antisense [75]. The basis of shotgun antisense is antisense repression. For antisense repression of a single gene, the corresponding cDNA is cloned into an expression vector plasmid in a backwards orientation and then transformed into cells. The expression vector will generate an antisense RNA that hybridizes to, and effectively neutralizes, the selected RNA sequence (typically a mRNA). This hybridization and neutralization decreases, but does not eliminate, levels of the selected RNA. Using a

transformation vector or plasmid where cells typically take up only one copy of the vector, and an antisense construct with an entire cDNA library rather than a selected cDNA then allows a mutagenesis called shotgun antisense [75].

Among the mutagenesis techniques, shotgun antisense has several benefits. First, the library is relatively easy to construct, and the mutant pool is easy to generate. It only requires RNA isolation and cDNA synthesis, followed by cloning the cDNA into an expression vector in a backwards orientation. CRISPR and siRNA libraries need careful design, and CRISPR mutagenesis requires the expression of CAS9 protein in the target cells [71, 72]. Second, shotgun antisense can be directed to target genes expressed in a specific tissue or developmental stage by using RNA isolated from a specific tissue or developmental stage. Third, as a gene knockdown technique, shotgun antisense is able to identify genes where complete disruption is lethal. Fourth, identification of the gene associated with an interesting phenotype from shotgun antisense only requires a PCR reaction on whole cells to amplify and sequence the antisense cDNA in the shotgun antisense plasmid. Fifth, antisense can repress the expression of multiple genes whose transcripts share closely related sequences, such as the three-member Discoidin I gene family in the model eukaryote *Dictyostelium discoideum* (*D. discoideum*) [76].

Shotgun antisense screens have been used for mutagenesis and gene identification in *D. discoideum* [75], but the original protocol had two disadvantages. First, there are 12,257 protein-coding genes in *D. discoideum* [77] but the size of the shotgun antisense

library from each ligation was only ~15,000 individual clones [75], so that by Poisson statistics, many genes will not have a corresponding cDNA in the library [78]. Second, the unequal transcription level of genes causes the levels of some RNAs, and corresponding cDNAs in the library, to be much less than that of other genes. In a eukaryotic cell, 20 - 40% of genes only have one to several dozen transcripts, while as few as 5 to 10 genes have several thousand transcripts [79]. Thus, if a conventional cDNA library is used for shotgun antisense, genes with rare transcripts have a low chance of generating a corresponding mutant and being identified.

To overcome these disadvantages, we developed an improved shotgun antisense technique with a cDNA normalization step to overcome the biased repression of highly prevalent mRNAs, and high-efficiency electrocompetent bacteria were used to increase the size of the library from each ligation. We checked the utility of this improved technique in a genetic screen in *D. discoideum*.

Total RNA of proliferating *D. discoideum* cells was isolated using an RNA prep kit (Zymo Research, Irvine, CA) and 3 µg of this RNA was used for directional double-strand cDNA (ds-cDNA) library synthesis using a Mint-2 cDNA synthesis kit (Evrogen, Moscow, Russia), as detailed in the supplementary file. This generates cDNAs with adapters added at the ends, with a *SpeI* site on the end corresponding to the 5' end of the mRNA and a *BglII* site on the other. 1.2 µg of this ds-cDNA library was then normalized using a Trimmer-2 kit (Evrogen) by melting the doublestranded cDNA, allowing the

abundant cDNAs to partially re-hybridize, digesting the hybridized DNA, and then amplifying the remaining DNA by PCR. Whereas the un-normalized cDNA pool showed bands after electrophoresis on agarose gels, indicating the presence of high levels of some cDNA species, there were no obvious bands after normalization, indicating that the normalization step reduced levels of these prominent cDNAs (Figure 13).

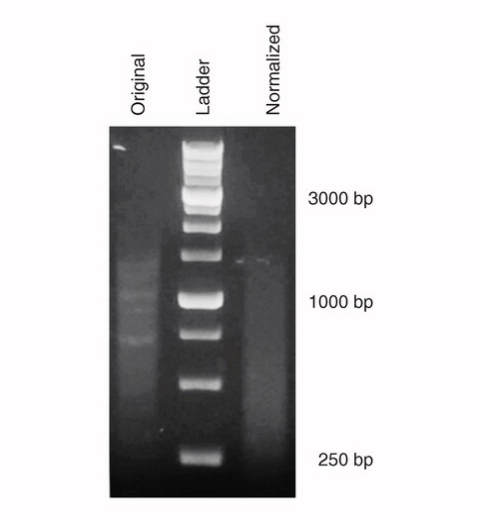

Figure 13. Normalization of cDNA removes bands corresponding to highly prevalent mRNAs.
Original cDNAs (left) and the normalized cDNAs (right) were electrophoresed on a 1.5% agarose gel in TAE buffer (Tris 40mM, Acetic Acid 20 mM and EDTA 50 mM) with a DNA ladder in the middle. Molecular masses (in bp) are at right.

The normalized ds-cDNA was then amplified by PCR with primers matching the adapters as detailed in the supplementary file. The enriched PCR product and the vector plasmid pDM326 containing the blasticidin resistance cassette [65] were digested with the

restriction enzymes BglII and SpeI, ligated with T4 ligase (NEB, Ipswich, MA) and then concentrated with a DNA Clean & Concentrator-5 kit (Zymo) to a volume of 10 µl, as detailed in the supplementary file. The ligation was then used to transform 5-alpha electrocompetent *E. coli* cells (NEB) with 1 µl purified ligation product and 25 µl competent cells per transformation. 1/10 of the total transformed cells from one transformation were plated on a LB/AMP agar plate (100 µg/ml ampicillin) to determine the library size. There were ~800 colonies after overnight incubation at 37 ℃. Thus, the library from each ligation contained ~80,000 independent clones (800 x 10 x 10) [78]. The total transformed cells from 10 µl ligation product were plated on 35 LB/AMP agar plates and incubated at 37 ˚C overnight. The next day, we picked 16 colonies for plasmid minipreps and then did a BglII and SpeI double digestion of the plasmids. Electrophoresis showed that all of the plasmids had ~250 bp to ~ 1000 bp insertions. The remaining colonies were collected by a plate scraper with 3 ml LB per plate. The collected cells were grown in a 500-ml culture to an OD 600 of ~3, and 25 ml of this culture was mixed with 25 ml of 50% glycerol in H_2O, and aliquots were stored at -80 ˚C. The remaining culture was used for a plasmid DNA maxi-prep using a Maxi-prep kit (Zymo) and the plasmid DNA was used to transform *D. discoideum* cells by electroporation [66].

Electroporated cells were then transferred into 10 ml HL5/ 100 µg/ml ampicillin in a 100-mm tissue culture petri dish. 10 µg/ml blasticidin (GoldBio, St. Louis, MO) was added 16-20 hours later for selection of transformed cells. Colonies normally appeared after 5-7 days and were transferred to shaking culture for screen assays. Each plate

typically contained 800 colonies.

Polyphosphate inhibits the proliferation of *Dictyostelium* cells through a signal transduction pathway involving the receptor GrlD (metabotropic **G**lutamate **R**eceptor-**L**ike protein **D**) [39]. As a check of the utility of the new shotgun antisense library, we screened for mutants resistant to polyphosphate. Each transformation generated 3 pools with ~ 800 individual clones per pool, and these pools were cultured in 150 μM polyphosphate for 2 days, allowed to recover for 2 days in the absence of polyphosphate, and the cycle was then repeated. After 4 cycles, we observed that cells in 3 of 20 pools screened, representing ~16,000 clones screened, proliferated faster than control untransformed cells in the presence of polyphosphate. In this screening, most transformed cells showed normal sensitivity to polyphosphate compared to untransformed cells. These transformed cells (they have a vector with other inserts) served as controls to rule out the effect of vector transformation on cells.

Cells from these 3 pools were cloned and tested for abnormally fast proliferation in the presence of polyphosphate. Antisense cDNA plasmids were extracted from the clones which passed the verification, and the antisense cDNA inserts were sequenced. The lengths of the antisense cDNAs were 244 bp to 406 bp. We found 4 antisense cDNAs (two from one pool, and one from each of the other 2 pools). One cDNA sequence matched the *Dictyostelium* gene *ai2a* (homing endonuclease, DDB_G0294421), one matched *ddcB* (diaminopimelate decarboxylase, DDB_G0276067), one matched *sodC* (superoxide

dismutase, DDB_G0282993) and one matched DDB_G0273573 (AAA+ATPase, core domain-containing protein).

To check the utility of the new shotgun antisense technique, we checked the identification of SodC and the AAA+ATPase as proteins affecting polyphosphate inhibition of proliferation. For SodC, we generated two *sodC* knock-down strains by antisense repression, one with full length antisense mRNA (sodC AS1) and the other one with a truncated antisense mRNA (sodC AS2). The detailed construction procedure is in the supplementary file. For the AAA+ATPase, we obtained a mutant (GWDI_488_A_5; henceforth AAA+ATPase^{REMI}) with an insertion of a plasmid at bp 13710 in the 16893 bp long coding sequence. Compared to wild type cells, these three mutants, and the corresponding original clones from the shotgun antisense screen, had reduced sensitivity to proliferation inhibition by polyphosphate (Figure 14). This indicates that the modified shotgun antisense mutagenesis described here can successfully generate and identify mutants.

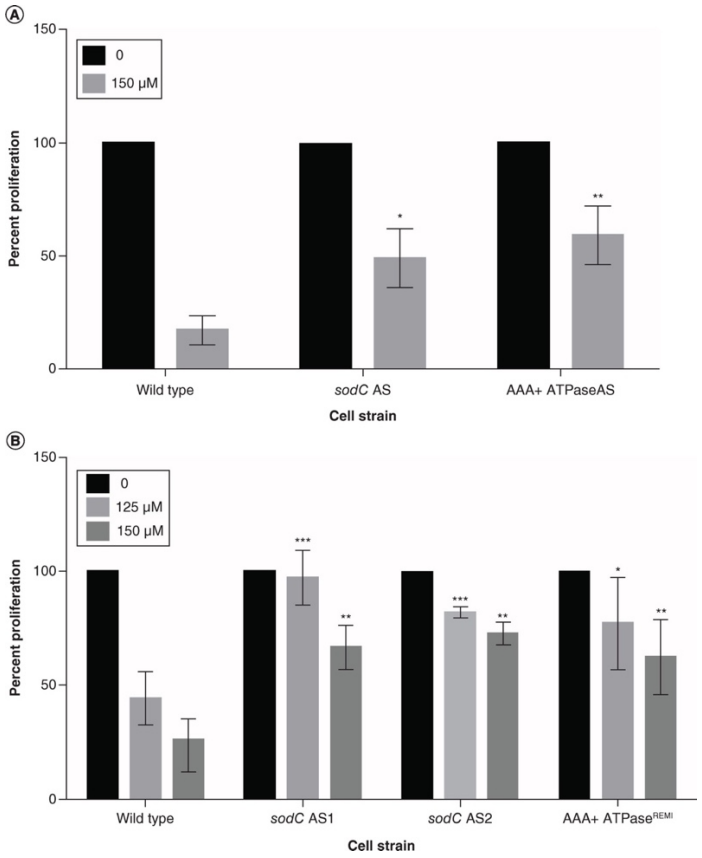

Figure 14. Identification of polyphosphate-resistant mutants from a shotgun antisense screen.
(A) Wild-type cells and two clones from the shotgun antisense screen were tested for proliferation in the presence or absence of 150-µM polyphosphate. (B) Wild-type cells, two SodC antisense transformants generated by constructing specific antisense transformants and a mutant with an insertion in the AAA-ATPase gene were tested for proliferation in the presence of 0-, 125- or 150-µM polyphosphate. For (A & B), percent proliferation is the cell density at 24 h as a percent of the cell density with no added polyphosphate. All values are mean ± standard deviation, $n \geq 3$. *$p < 0.05$, **$p < 0.01$ and ***$p < 0.001$ compared with wild-type cells at the same polyphosphate concentration (unpaired *t*-test, correcting for multiple comparisons using the Holm – Sidak method).

A limitation of this study is that there is no straightforward way to perform a comparative study between this modified method and the 1996 shotgun antisense method.

A comparison would require multiple genetic screens to saturation using the two protocols, and then identification of the resulting mutants. Despite this limitation, the shogun antisense protocol presented here has two theoretical improvements. First, the modified shotgun antisense cDNA library has a larger size (~80,000 individual clones) than that made before (~15,000 individual clones), so that by Poisson statistics, many more genes will have a corresponding cDNA in the library [78]. Second, the addition of cDNA normalization for the shotgun antisense cDNA library reduces bias of gene repression and thus helps increase the chance of generating mutants corresponding to genes with low transcription levels. Together, these modifications should increase the utility of shotgun antisense for mutagenesis and gene identification.

4. AN AUTOCRINE NEGATIVE FEEDBACK LOOP INHIBITS *D. DISCOIDEUM* PROLIFERATION THROUGH AN IP3/ CA^{2+} PATHWAY

4.1. Summary

Very little is known about how tissues can regulate their size. In one possible mechanism, cells in a tissue secrete a factor that inhibits their proliferation, and as the tissue gets bigger, the concentration of the factor increases. If the factor inhibits proliferation at some concentration, the resulting negative feedback loop will limit tissue size. Despite evidence for such factors, very few have been identified and their signal transduction pathways are poorly understood. We previously found that *Dictyostelium discoideum* accumulates extracellular polyphosphate to inhibit its proliferation, and that this requires the G protein coupled receptor GrlD and the small GTPase RasC. Here we show that cells lacking the G protein components Gα3 and Gβ, the Ras guanine nucleotide exchange factor GefA, Phosphatase and tensin homolog (PTEN), Phospholipase C (PLC, which produces IP3 from PIP2), Inositol 1,4,5-trisphosphate receptor-like protein A (IplA, which acts as a calcium channel activated by IP3), Polyphosphate kinase 1(Ppk1), PiaA (cytosolic regulator of adenylate cyclase), Protein kinase A, or Growth-differentiation transition family members 1 and 2 have significantly reduced sensitivities to polyphosphate-induced proliferation inhibition. Polyphosphate upregulates IP3, and this requires GrlD, GefA, PTEN, PLC, PiaA, PKA-C, and Gdt 1 and 2. Polyphosphate also upregulates cytosolic Ca^{2+}, and this requires GrlD, Gα3, Gβ, GefA, RasC, PLC, IplA,

Ppk1, PiaA, PKA-C, and Gdt 1 and 2. These data suggest that polyphosphate inhibits the proliferation of *D. discoideum* through an IP3/Ca^{2+} pathway.

4.2. Introduction

A longstanding idea in developmental biology is that the size of a tissue or group of cells, or the spatial density of a specific cell type, could be limited by an autocrine proliferation inhibitor, where the concentration of the inhibitor increases as the size of the tissue or cell group, or density of cells, increases [1-3]. Although a considerable amount is known about signals and pathways that promote cell proliferation, relatively little is known about autocrine proliferation inhibiting signals and their signal transduction pathways.

Polyphosphate is a linear polymer of phosphate residues and is present in all kingdoms of life [26-28]. In bacteria, polyphosphate functions as energy and phosphate storage [26], potentiates survival in some high stress conditions [30], and potentiates biofilm formation [31, 32]. In mammals, polyphosphate inhibits bone calcification [33], potentiates pro-inflammatory responses [34], potentiates mTOR activation of plasma cells [35], accelerates blood coagulation [38], inhibits the proliferation of leukemia cells [36], and induces apoptosis [37].

The eukaryotic social amoeba *Dictyostelium discoideum* grows on soil surfaces and eventually overgrows its food supply and starves. *Dictyostelium* accumulates

extracellular polyphosphate as cells grow and proliferate [9]. At very high cell densities, when the cells are about to starve, the accumulated extracellular polyphosphate reaches ~150 μM, and this concentration of polyphosphate inhibits cytokinesis (and thus cell proliferation), possibly to prevent the formation of small cells, and therefore just before starvation increases the percentage of large cells with relatively large reserves of stored nutrients [9].

Polyphosphate regulates the proliferation of *D. discoideum* by different signaling pathways depending on nutrient levels [39]. In 100% HL5 (the common rich medium for culturing *Dictyostelium*), loss of the G protein coupled receptor GrlD, a metabotropic Glutamate Receptor-Like receptor, partially reduced the sensitivity of cells to polyphosphate, and loss of the small GTPase RasC did not reduce the sensitivity of cells to polyphosphate [39]. However, in 25% HL5, a low nutrient condition for *D. discoideum* cells, loss of GrlD or RasC blocked the sensitivity of cells to polyphosphate [39].

The above results suggest that polyphosphate uses a signal transduction pathway in 25% HL5 to inhibit proliferation. In this report, we screened 49 available signal transduction pathway mutants for insensitivity to polyphosphate-induced proliferation inhibition in 25% HL5. In combination with biochemical assays, we found evidence for a pathway involving inositol 1,4,5-trisphosphate and cytosolic calcium that mediates autocrine proliferation inhibition in *Dictyostelium.*

4.3. Materials and methods

4.3.1. Cell culture and strains

Dictyostelium discoideum strains were obtained from the *Dictyostelium* stock center [80] and were wild-type Ax2, *grlD*$^{-}$ (DBS0350227) [39], *rasC*$^{-}$ (DBS0236853) [81], *gefA*$^{-}$ (DBS0236896) [82], *gβ*$^{-}$ (DBS0236531) [83], *gα1*$^{-}$ (DBS0236088) [84], *gα2*$^{-}$ (DBS0236575) [85], *gα3*$^{-}$ (DBS0235986) [86], *gα4*$^{-}$ (DBS0235984) [87], *gα5*$^{-}$ (DBS0236451) [88], *gα7*$^{-}$ (DBS0236106) [89], *gα8*$^{-}$ (DBS0236107) [89], *gα9*$^{-}$ (DBS0236109) [90], *aprA*$^{-}$ (DBS0235509) [8], *cfaD*$^{-}$ (DBS0302444) [91], *pakD*$^{-}$ (DBS0350281) [92], *rblA*$^{-}$ (DBS0236877) [93], *cnrN*$^{-}$ (DBS0302655) [94], *qkgA*$^{-}$ (DBS0236839) [95], *bzpN*$^{-}$ (DBS0349965) [96], *scrA*$^{-}$ (DBS0236926) [97], *elmoE*$^{-}$ (DBS0350065) [98], *gcA*$^{-}$/*sgcA*$^{-}$ (DBS0302679) [99], *racC*$^{-}$ (DBS0350272) [100], *plA2*$^{-}$ (DBS0238068) [101], *pikA*$^{-}$/*pikB*$^{-}$ (DBS0236766) [102], *dagA*$^{-}$ (DBS0235559) [103], *pten*$^{-}$ (DBS0236830) [104], *pten*$^{-}$/*pten-GFP* (DBS0236831) [104], *plC*$^{-}$ (DBS0236793) [105], *plC*$^{-}$/*plC* (DBS0236795) [106], *iplA*$^{-}$ (DBS0236260) [107], *Dd5p4*$^{-}$ (DBS0266692) [108], *erk1*$^{-}$ (DBS0350622) [109], *erk1*$^{-}$/*erk2*$^{-}$ (DBS0351256) [110], *mekA*$^{-}$ (DBS0236541) [111], *smkA*$^{-}$ (DBS0236938) [111], *i6kA*$^{-}$ (DBS0236426), *ppk1*$^{-}$ (DBS0350686) [28], *csaA*$^{-}$ (DBS0236957) [112], *smlA*$^{-}$ (DBS0236939) [75], *piaA*$^{-}$ (DBS0349879) [113], *lst8*$^{-}$ (DBS0236517) [114], *pkaC*$^{-}$ (DBS0236783) [115], *pkcA*$^{-}$ (DBS0350916) [116], *amtA*$^{-}$ (DBS0235497) [117], *sibA*$^{-}$ (DBS0236935) [118], *tpC2* (A gift from Pierrec Cosson, University of Geneva, Geneva, Switzerland) [119], *trpp* (A gift from Pierrec Cosson, University of Geneva, Geneva, Switzerland) [119], *mcln* (DBS0350059) [120], *wasA*$^{-}$ (A gift from Robert Insall, Beatson Institute for Cancer

Research, Glasgow, UK) [121], *gdt1*$^{-}$/*gdt2*$^{-}$ (A gift from Adam Kuspa, Baylor College of Medicine), *gdt2*$^{-}$ (A gift from Adam Kuspa, Baylor College of Medicine), *gdt4*$^{-}$ (A gift from Adam Kuspa, Baylor College of Medicine). As described previously, all mutants were confirmed by PCR [122]. Cells were cultured at 21 ℃ in shaking culture at 175 rpm in HL5 (Formedium Ltd, Norwich, England). Cell densities were counted by hemocytometer.

4.3.2. Proliferation inhibition and nuclei counts

0.474 grams of ~46-mer (average length) S0169 sodium polyphosphate (Spectrum, New Brunswick, NJ) was dissolved in 10 ml of PBM (20 mM KH_2PO_4, 0.01 mM $CaCl_2$, 1 mM $MgCl_2$, pH 6.1) to make a 10 mM stock; the final pH was 6.1 and the pH was thus not adjusted. Mid-log phase cells cultured in HL5 were collected by centrifugation at 1000 x g for 3 minutes and washed once by resuspending in PBM and centrifugation at 1000 x g for 3 minutes, and then resuspended in fresh HL5 to 6 x 10^6 cells/ml. 100 µl of these cells were mixed with 300 µl of PBM or HL5 containing the indicated concentrations of polyphosphate in a well of a type 353047 24-well plate (Corning, Corning, NY) and incubated in a humid box for 24 hours. Cell density was counted at 24 hours and the cell density normalized to the density with no added polyphosphate was calculated. The doubling time and maximal density of each strain was calculated following [39] and the number of nuclei per cell was counted following [8]. Curve fits and IC50 calculations were done using Prism (Graphpad, San Diego, CA), with nonlinear regression (sigmoidal dose-response, variable slope, top constrained to 100).

4.3.3. Extraction and measurement of inositol (1,4,5)-trisphosphate

Cells were grown to mid-log phase (1-4 x 10^6 cells/ ml), counted, and ~2 x 10^7 cells were collected by centrifugation and washed with PBM as described above, and then resuspended and incubated in 10 ml 25% HL5 diluted with PBM with 0 or 150 µM polyphosphate in shaking culture at 175 rpm. After 4 hours, cells were collected by centrifugation at 1000 x g for 3 minutes and resuspended in 110 µl of the supernatant from the centrifugation in 1.7 ml Eppendorf tubes. 10 µl of resuspended cells were taken out for cell counts and the remaining cells were mixed with 100 µl 3.5% perchloric acid and incubated on ice for 15 minutes. 50 µl of 50% saturated $KHCO_3$ were then added to the 200 µl mix to neutralize the lysates, and CO_2 was allowed to escape. The material was then clarified by centrifugation at 14,000 x g for 5 minutes at 4 ℃. 200 µl of the supernatant of each tube was transferred to new pre-chilled 1.7 ml tubes and stored at 0 ℃. The IP3 levels in the clarified lysates were measured with a type 2515875 IP3 ELISA kit (MyBioSource, San Diego, CA) less than 1 week after extraction.

4.3.4. Measurement of cytosolic free Ca^{2+}

3 x 10^6 mid-log phase cells were collected by centrifugation at 1000 x g for 3 minutes and washed with ice-cold Sorensen's buffer (14.7 mM KH_2PO_4, 2 mM Na_2HPO_4, pH 6.1) twice (each time collecting cells by centrifugation and resuspension), and then resuspended in 95 µl ice-cold Sorensen's buffer. 90 µl of washed cells were then mixed with 10 µl 25 mg/ml BAPTA-1 dextran 10,000 MW (Invitrogen, Eugene, OR), loaded

into an EC2L 2-mm electroporation cuvette (Midsci, Valley Park, MO) and pulsed once with 850 V at 10 μF and 200 Ω in a GenePulser Xcell electroporator (Bio-Rad, Hercules, CA). The cells were then collected by centrifugation and resuspended in 1 ml HL5, and incubated for 30 minutes at 21 ℃ in shaking culture at 175 rpm. The cells were then diluted and incubated at 1 x 10^6 cells/ml with 150 μM polyphosphate or an equal volume of PBM in 25% HL5 for 3.5 hours. The cells were then diluted to 0.3 x 10^6 cells/ml with 150 μM polyphosphate or an equal volume of PBM in 25% HL5 and 300 μl of diluted cells were allowed to adhere in the well of a 94.6190.802 8-well tissue culture chamber (Sarstedt, Nümbrecht, Germany) for 30 minutes. Cells were imaged with a 40x objective on a Ti2 Eclipse inverted epifluorescence microscope (Nikon, Melville, NY). Fluorescence intensity was analyzed by ImageJ.

4.3.5. Statistics

Statistical analyses were done using Prism (GraphPad). Significance was defined as $p < 0.05$.

4.4. Results

4.4.1. In addition to a G protein-coupled receptor and a Ras protein, a Ras GEF potentiates polyphosphate inhibition of cell proliferation

We previously observed that polyphosphate inhibits the proliferation of wild-type cells, and that the loss of GrlD, RasC, or Ppk1 reduces the ability of polyphosphate to inhibit proliferation [9, 39], suggesting the existence of a polyphosphate signal

transduction pathway. To identify additional components of the polyphosphate proliferation inhibition pathway, 49 available mutants were screened for sensitivity to polyphosphate-induced proliferation inhibition. The data were graphed in 9 groups: previously reported polyphosphate signal transduction pathway components (Figure 15A), G protein subunits (Figure 15B), AprA pathway components (Figure 15C), selected cAMP chemoattraction pathway components (Figure 15D), PLC/IP3 pathway components (Figure 15E), MAPK pathway/polyphosphate synthesis pathway components (Figure 15F), growth-development transition components (Figure 15G), TOR complex components/protein kinases (Figure 15H), and mechanotransduction components (Figure 15I). The initial cell density was 1.5 x 10^6 cells/ ml, and cells were counted 24 hours later. The data were plotted as 100 x (density with polyphosphate – 1.5 x 10^6/ ml) / (density with no added polyphosphate – 1.5 x 10^6/ ml). This would then be 100 if the polyphosphate had no effect on cell proliferation, and 0 if the polyphosphate caused no increase in cell density beyond the initial 1.5 x 10^6 cells/ ml. Compared to no added polyphosphate, 125 μM and 150 μM polyphosphate reduced the increase in cell density of Ax2 (wild-type) cells to ~ 30% and ~ 18%, respectively, Figure 15). At 24 hours, the density of the Ax2 cells with no polyphosphate was 3.9 ± 0.1 x 10^6 cells/ ml (mean ± SEM, n = 7; Table 4. Some mutants have abnormal proliferation rate in 25% HL5.), so the 18% cell density increase at 24 hours represents a change in doubling time from the control value of 17.7 ± 0.7 hours to 81.3 ± 16.7 hours.

Table 4. Some mutants have abnormal proliferation rate in 25% HL5.
The indicated cell lines were tested for proliferation for 24 hours. Cells were cultured in 25% HL5, starting with 1.5 x 10^6 cells/ml. All values are mean ± SEM, n ⩾ 3 independent experiments. *, $p < 0.05$, **, $p < 0.01$, ***, $p < 0.001$ (t-test).

Strain	Cell Density at 24 hr, 10^6 cells/ml	Doubling Time, hours
Ax2	3.9 ± 0.1	17.7 ± 0.7
grlD$^-$	3.3 ± 0.8 *	20.8 ± 0.9 *
rasC$^-$	5.7 ± 0.5 *	13.2 ± 1.5 *
gefA$^-$	5.6 ± 0.3 **	12.8 ± 0.9 **
gβ$^-$	4.1 ± 0.3	17.1 ± 0.9
gα1$^-$	6.4 ± 0.4 ***	11.6 ± 0.4 ***
gα2$^-$	3.5 ± 0.3	22 ± 2.6
gα3$^-$	5.2 ± 0.5 **	13.6 ± 0.8 **
gα4$^-$	4.7 ± 0.6	15.3 ± 1.6
gα5$^-$	4.6 ± 0.4	16 ± 2.2
gα7$^-$	3 ± 0.2 *	26.9 ± 4.9 *
gα8$^-$	3.4 ± 0.5	21.1 ± 1.7
gα9$^-$	5.5 ± 0.4 **	13.1 ± 0.8 **
aprA$^-$	5 ± 0.4 *	14.1 ± 0.9 *
cfaD$^-$	5.8 ± 0.2 ***	12.5 ± 0.7 ***
pakD$^-$	3.8 ± 0.5	18 ± 0.9
rblA$^-$	5.7 ± 1 **	12.6 ± 0.7 ***
cnrN$^-$	5.3 ± 0.5	16 ± 3.3
qkgA$^-$	6.7 ± 0.6 ***	11.3 ± 0.5 ***
BzpN$^-$	4.8 ± 0.4	15.1 ± 1.7
scrA$^-$	4.3 ± 0.5	16.6 ± 1.4
ElmoE$^-$	4.7 ± 0.1	14.9 ± 1.3
gcA$^-$*/sgcA*$^-$	3.9 ± 0.3	17.4 ± 0.5
wasA$^-$	7.3 ± 0.2 ***	10.5 ± 0.2 ***
racC$^-$	3.5 ± 0.3	20.1 ± 1.3
plaA$^-$	4.9 ± 0.2 **	14.3 ± 0.7 **
pikA$^-$*/pikB*$^-$	3 ± 0.1 **	24 ± 1.8 **
dagA$^-$	4.5 ± 0.1 *	15.3 ± 0.3 *
pten$^-$	3.9 ± 0.3	17.5 ± 0.5
pten$^-$*/pten-GFP*	3.1 ± 0.1 **	22.6 ± 1.0 **
plC$^-$	5.2 ± 0.3 **	13.8 ± 0.7 **
plC$^-$*/plC*	6.1 ± 0.3 ***	11.9 ± 0.5 ***
iplA$^-$	4.4 ± 0.5	15.8 ± 0.9

Dd5P4^{-}	3.4 ± 0.3		22.8 ± 4.4	
erk1^{-}	5.3 ± 0.6	***	13.3 ± 0.5	***
erk1^{-}*/ekr2*$^{-}$	3.9 ± 0.3		19.5 ± 3.2	
mekA^{-}	3.7 ± 0.2		19.1 ± 1.8	
smkA^{-}	4.9 ± 0.3	**	14.3 ± 0.8	*
i6kA^{-}	5.9 ± 0.4	***	12.3 ± 0.5	***
ppk1^{-}	4.6 ± 0.5		15.5 ± 1.2	
gdt1^{-}*/gdt2*$^{-}$	3.8 ± 0.3		20.1 ± 2.5	
gdt2^{-}	4 ± 0.3		17.5 ± 1.2	
gdt4^{-}	4.2 ± 0.3		16.9 ± 0.4	
csaA^{-}	4.2 ± 0		16.5 ± 1.4	
smlA^{-}	4 ± 0.3		16.9 ± 0.2	
amtA^{-}	4.2 ± 0.2		16.8 ± 1.4	
piaA^{-}	2 ± 0.4	***	79.4 ± 22.2	*
lst8^{-}	3.1 ± 0.2	*	25.1 ± 4.9	
pkaC^{-}	3.6 ± 0.2		19.4 ± 1.3	
pkcA^{-}	3.2 ± 0.4	*	22 ± 1.8	*
sibA^{-}	4.1 ± 0.3		16.9 ± 0.9	
tpC2^{-}	4.1 ± 0.5		16.9 ± 1.2	
trpp^{-}	4.8 ± 0.4	*	14.8 ± 1.4	
mclN^{-}	4.5 ± 0.4		15.5 ± 1.1	

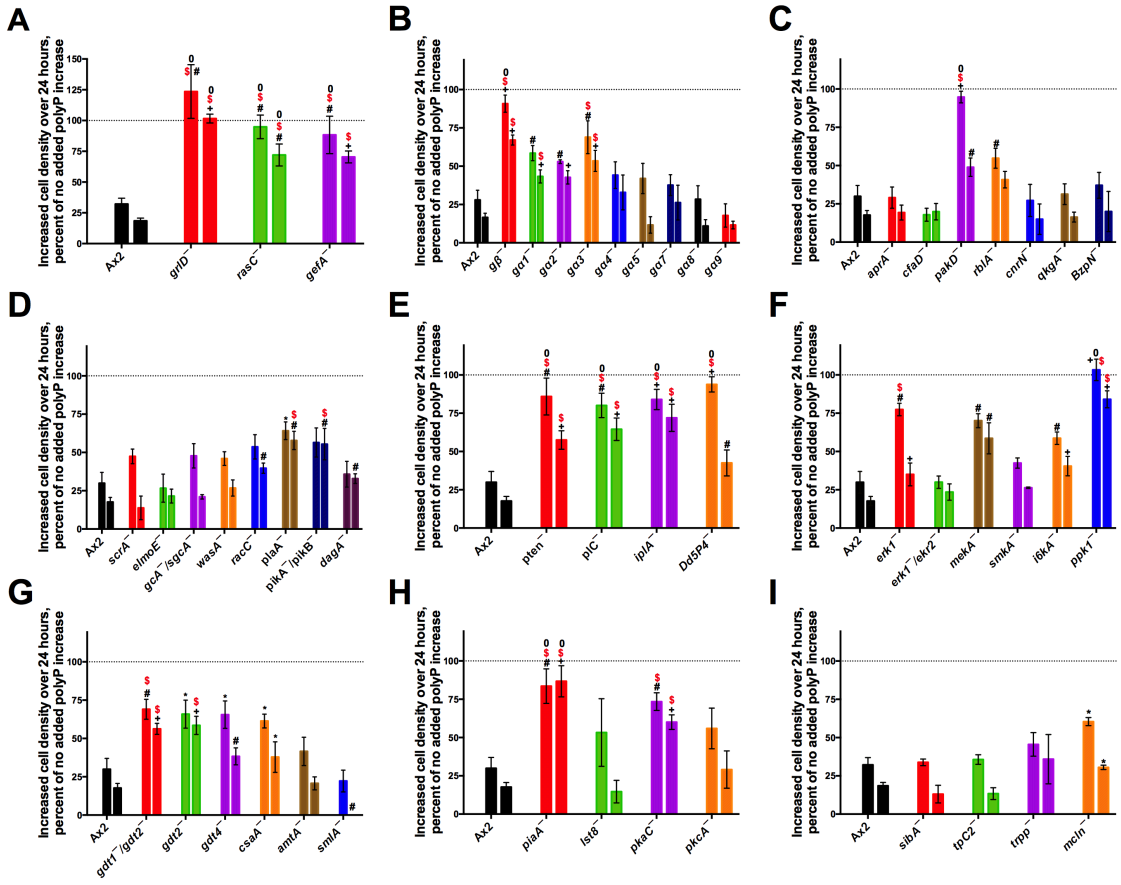

Figure 15. Some signal transduction pathway components are needed for polyphosphate inhibition of proliferation in 25% HL5.
The indicated cell lines were tested for proliferation with 0, 125 or 150 µM polyphosphate for 24 hours. The increase in cell density over 24 hours was normalized to no added polyphosphate for the indicated strain. For each strain, the left bar is with 125 µM and the right bar is with 150 µM polyphosphate. All values are mean ± SEM, n ≥ 3 independent experiments. * indicates $p < 0.05$, #, $p < 0.01$, +, $p < 0.001$, compared to Ax2 cells with the same concentration of polyphosphate (t-test). $ indicates $p < 0.05$ (one-way ANOVA, multiple comparisons with Dunnett's test within the panel). 0 indicates not significantly different from 100 (one-sample t-test).

As previously reported, compared to Ax2 cells, cells lacking the putative polyphosphate receptor GrlD [39] or the Ras protein RasC [81] showed abolished

sensitivity (no significant difference compared to no added polyphosphate by t-test) to 125 and 150 μM polyphosphate (Figure 15A). Cells lacking GefA, a Ras guanine nucleotide exchange factor for RasC but not RasB, RasD, RasG or Rap1 [82], also showed reduced sensitivity to polyphosphate (Figure 15A).

4.4.2. Gβ and three Gα subunits potentiate polyphosphate inhibition of cell proliferation

Cells lacking the heterotrimeric G protein subunits Gβ [83], Gα1 [84], Gα2 [85], or Gα3 [86] showed reduced sensitivity to polyphosphate inhibition of cell proliferation (Figure 15B). Cells lacking Gα's 4, 5, 7, 8, or 9 did not have significantly abnormal sensitivity to polyphosphate. Whereas cells lacking the putative receptor GrlD appeared to be completely insensitive to polyphosphate, none of these mutants showed complete insensitivity, suggesting that there is an additional pathway downstream of GrlD that does not involve Gβ, that GrlD may activate multiple Gα subunits, or that GrlD regulates the expression of other receptors that also mediate polyphosphate sensing.

4.4.3. The AprA pathway components PakD and RblA potentiate polyphosphate inhibition of cell proliferation

AprA is a secreted autocrine proliferation repressor and chemorepellent [8]. Cells lacking the AprA pathway components retinoblastoma orthologue RblA [93] and the p21-activated kinase family member PakD [92] showed reduced sensitivity to polyphosphate (Figure 15C). Compared to wild-type cells, cells lacking AprA, CfaD (a secreted factor

that binds to AprA and then slows cell proliferation [91]), CnrN (a PTEN-like phosphatase involved in AprA sensing [22, 94, 122]), QkgA (a LRRK family protein kinase that is required for AprA induced proliferation inhibition and chemorepulsion [95]), or BzpN (a transcription factor that is required for AprA induced proliferation repression [96]) did not show significantly abnormal sensitivities to polyphosphate, indicating that many AprA pathway components are not used by polyphosphate to inhibit proliferation.

4.4.4. The cAMP chemoattraction pathway components RacC, PlaA, PikA and B, and DagA potentiate polyphosphate inhibition of cell proliferation

Cells lacking the cAMP chemoattraction pathway components Rho GTPase RacC [100], phospholipase A2 PlaA [101], the phosphatidylinositol kinases PikA and B [102], or the cytosolic regulator of adenylate cyclase DagA [103] showed modestly reduced sensitivity to 150 μM polyphosphate (Figure 15D). Compared to wild-type cells, cells lacking ScrA (an adaptor protein that regulates actin polymerization [97]), ElmoE (engulfment and cell motility protein, which transduces signals from chemoattractant receptors to the cytoskeleton [98]), GcA and SgcA (membrane bound and soluble guanylyl cyclases, respectively [99]), or WasA (an adaptor protein that regulates actin polymerization [121]) did not show significantly abnormal sensitivity to polyphosphate, indicating that many of the components of the cAMP pathway are not used by polyphosphate to inhibit proliferation.

4.4.5. The PLC/IP3 pathway components PTEN, PLC, IplA, and Dd5P4 potentiate polyphosphate inhibition of cell proliferation

Cells lacking the phosphatase and tensin homolog PTEN [104], the phospholipase C PLC [105], the inositol 1,4,5-trisphosphate receptor-like protein IplA [107], or the inositol 5-phosphatase 4 Dd5P4 [108] showed abolished sensitivity to 125 μM and reduced sensitivity to 150 μM polyphosphate (Figure 15E). PTEN catalyzes the conversion of phosphatidylinositol (3,4,5)-trisphosphate (PIP3) to phosphatidylinositol (4,5)-bisphosphate (PIP2) [123] , and PLC catalyzes the hydrolysis of PIP2 to diacylglycerol (DAG) and inositol 1,4,5-trisphosphate (IP3) [123]. IplA is a potential IP3 receptor in *D. discoideum* [107]. Dd5P4 dephosphorylates PIP3, PIP2 and IP3 [124]. These results suggest that the PLC/IP3 pathway affects or is involved in polyphosphate inhibition of cell proliferation, and that IP3 might be a second messenger in the polyphosphate signal transduction pathway.

4.4.6. The MAPK/Erk pathway component Erk1 and MekA potentiates polyphosphate inhibition of cell proliferation

Cells lacking the extracellular signal-regulated kinase Erk1 [109] or the Erk1 kinase MekA [111] showed reduced sensitivity to polyphosphate inhibition of cell proliferation (Figure 15F). Deleting the suppressor of MekA, SmkA [111], did not alter the sensitivity to polyphosphate (Figure 15F). These results suggest that the MekA-Erk1 pathway is involved in polyphosphate proliferation inhibition.

4.4.7. The polyphosphate synthesis pathway components I6kA and Ppk1 potentiate polyphosphate inhibition of cell proliferation

The inositol phosphate kinase I6kA does not appear to affect intracellular polyphosphate levels at cell densities below ~1 x10^7/ml) but plays a role in upregulating intracellular polyphosphate at cell densities ≥ 2 x 10^7/ml [9]. The polyphosphate kinase Ppk1 is essential for intracellular polyphosphate production at all cell stages [28]. Cells lacking I6kA showed reduced sensitivity to 125 μM and 150 μM polyphosphate. Cells lacking Ppk1 showed abolished sensitivity to 125 μM polyphosphate and strongly reduced sensitivity to 150 μM polyphosphate (Figure 15F). The correlation between intracellular polyphosphate synthesis and sensitivity to extracellular polyphosphate suggests that intracellular polyphosphate plays a role in polyphosphate inhibition of cell proliferation.

4.4.8. The growth-differentiation transition components Gdts and CsaA potentiate polyphosphate inhibition of cell proliferation

The growth-differentiation transition family of proteins (Gdts) are *Dictyostelium*-specific tyrosine kinase-like proteins, classified by their sequence similarity and their participation in development [125]. Gdt1 and Gdt2 are negative regulators for the *Dictyostelium* growth-differentiation transition process [125, 126], but there is no report about the function of Gdt4 yet. Cells lacking the growth-differentiation transition family member 2, both 1 and 2, or 4, or cells lacking the contact site A protein CsaA showed reduced sensitivity to both 125 μM and 150 μM polyphosphate (Figure 15G). Polyphosphate primes cells for development by, for instance, increasing expression of

CsaA [112]. Cells lacking the ammonium transporter AmtA [117] did not show altered sensitivity to polyphosphate. These results suggest that the polyphosphate-regulated development-related components may also play a role in cell proliferation.

4.4.9. The cell aggregates size regulator SmlA attenuates polyphosphate inhibition of cell proliferation

The small aggregate formation protein SmlA regulates the size of cell aggregates and fruiting bodies during development by inhibiting the extracellular accumulation of the group size-regulating factor Counting Factor [75, 127]. Cells lacking SmlA showed a normal sensitivity to 125 μM polyphosphate, but for unknown reasons appeared to be hypersensitive to 150 μM polyphosphate (after 24 hours, this polyphosphate concentration caused the cell density to decrease from 1.5 x 10^6 cells/ ml to 1.2 ± 0.2 x 10^6 cells/ ml, mean ± SEM, n = 4) (Figure 15G).

4.4.10. The TORC2 component PiaA and protein kinase PKA-C potentiate polyphosphate inhibition of cell proliferation

Dictyostelium Tor complex 2 (TORC2) composed of Tor, PiaA, Lst8 and Rip3 regulates the adenylate cyclase ACA [114, 128] and protein kinase B/ Akt activation [114, 129] and is essential for cell aggregation [114, 130]. Cells lacking the TORC2 component PiaA (Rictor) but not Lst8 showed abolished sensitivity to both 125 μM and 150 μM polyphosphate, suggesting that PiaA is an essential component of the polyphosphate proliferation inhibition pathway (Figure 15H). Cells lacking the cAMP-dependent protein

kinase catalytic subunit PKA-C showed reduced sensitivity to polyphosphate inhibition of cell proliferation, suggesting that cAMP might be a messenger in the polyphosphate proliferation inhibition pathway (Figure 15H). Compared to wild-type cells, cells lacking Lst8 and protein kinase C (PKCA) did not show significantly abnormal sensitivities to polyphosphate, indicating that some components of the PKCA pathway are not used by polyphosphate (Figure 15H).

4.4.11. The mechanotransduction component Mcln potentiates polyphosphate inhibition of proliferation

Cells lacking the mechanotransduction component Mcln (an ortholog of mucolipin) [119] showed reduced sensitivity to 125 μM and 150 μM polyphosphate (Figure 15I). Compared to wild-type cells, cells lacking the mechanotransduction components SibA (an integrin beta-like protein) [119], TPC2 (a two-pore calcium channel protein 2) [119] or TrpP (the transient receptor potential cation channel protein) [119], did not show significantly abnormal sensitivities to polyphosphate (Figure 15I). These results suggest that many components of the mechanotransduction pathway are not used by polyphosphate to inhibit proliferation.

4.4.12. Gα3, Gβ, GefA, PTEN, PLC, IplA, Ppk1, PiaA, PKA-C, and Gdt 1 and 2 potentiate polyphosphate inhibition of cell proliferation in both 25% and 100% HL5

With the stricter one-way ANOVA test (multiple comparisons with Dunnett's

test), cells lacking GrlD, Gα3, Gβ, GefA, RasC, PTEN, PLC, IplA, Ppk1, PiaA, PKA-C, or Gdt 1 and 2 showed significantly reduced sensitivity to both 125 and 150 μM polyphosphate (Figure 15 A, B, E, F, G, and H). Cells lacking PakD, Dd5P4, or Erk1 showed significantly reduced sensitivity to 125 μM polyphosphate but not 150 μM polyphosphate (Figure 15 C, E, and F), and cells lacking Gα1, PlA2, Pik A and B, or Gdt2 showed significantly reduced sensitivity to 150 μM polyphosphate but not 125 μM polyphosphate (Figure 15 B, D, and G).

To confirm that disruption of the genes encoding Gα3, Gβ, GefA, PTEN, PLC, IplA, Ppk1, PiaA, PKA-C, or Gdt 1 and 2 reduces the sensitivity to polyphosphate, mutant and available rescue strains were tested for sensitivity to polyphosphate with a more extensive dose-response curve in the nutrient-low condition 25% HL5 (Figure 16). Compared to Ax2 cells, cells lacking Gα3, Gβ, GefA, PTEN, PLC, IplA, Ppk1, PiaA, PKA-C, or Gdt 1 and 2 showed a reduced sensitivity to physiological levels of polyphosphate (150 μM or less) (Figure 16). The IC50s of polyphosphate proliferation inhibition on these knock-out mutant strains were significantly higher than that of Ax2 cells in 25% HL5 (Table 5). Expressing PTEN in *pten*$^{-}$ cells and PLC in *plC*$^{-}$ cells rescued or partially rescued the sensitivity to polyphosphate (Figure 16 C and D, Table 5).

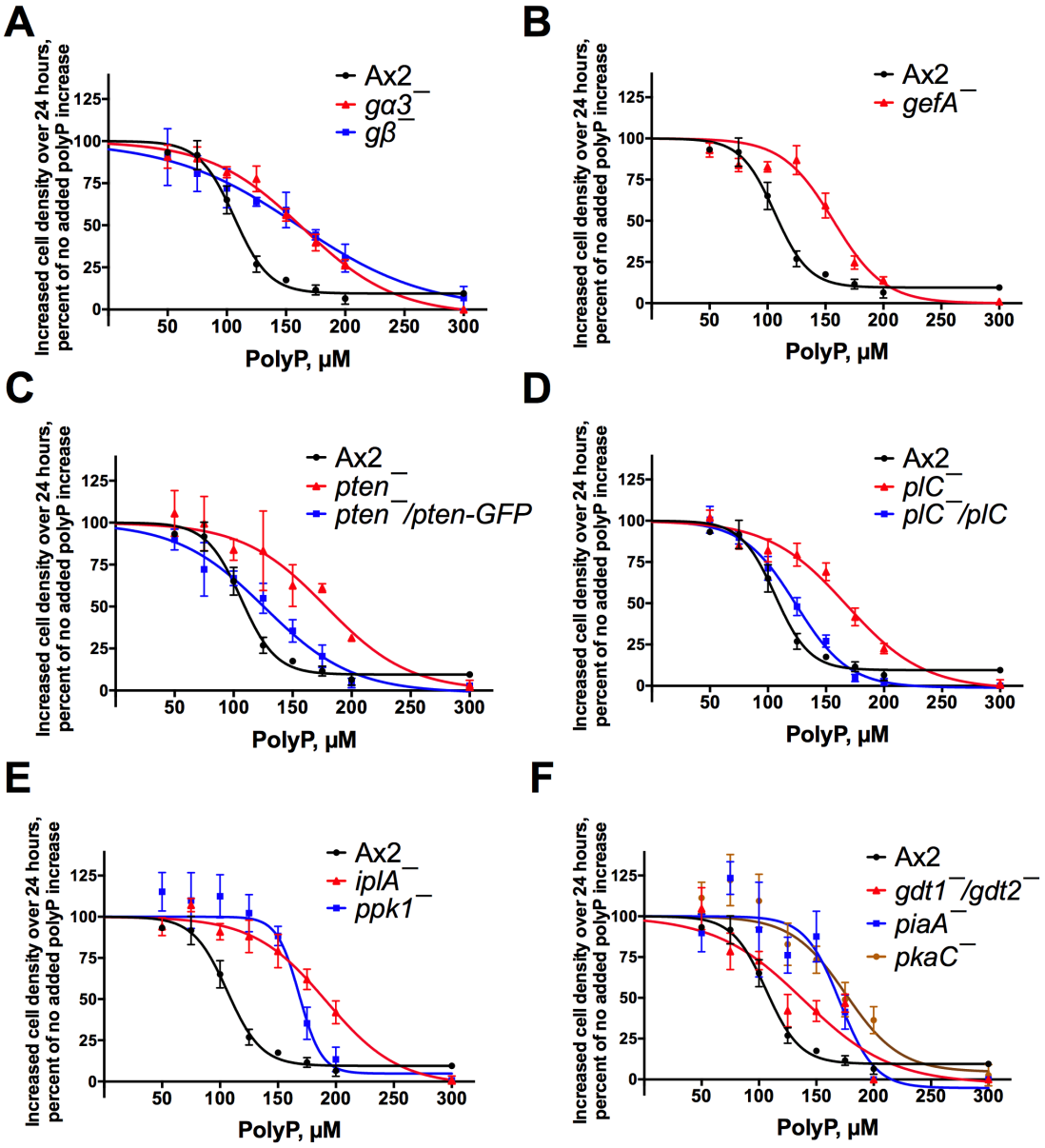

Figure 16. Some mutants have abnormal sensitivities to polyphosphate in 25% HL5.

The indicated cell lines were tested for proliferation in 25% HL5 with the indicated concentrations of polyphosphate for 24 hours. The increase in cell density over 24 hours was normalized to the increase with no added polyphosphate. Curve fits were done using Prism with nonlinear regression (sigmoidal dose-response, variable slope, top constrained to 100). Values are mean ± SEM, n ≥ 3.

Table 5. Deletion of some potential polyphosphate pathway components increases the IC50 for polyphosphate inhibition of proliferation.
IC50s were calculated from Figure S1 and S2, using Prism with nonlinear regression (sigmoidal dose-response, variable slope, top constrained to 100). All values are mean ± SEM, n ≥ 3 independent experiments. * indicates $p < 0.05$, **, $p < 0.01$, *** $p < 0.001$ compared to Ax2 (t-test). ^, $p < 0.05$, ^^, $p<0.01$, ^^^, $p < 0.001$ compared to Ax2 (one-way ANOVA, Tukey's test among Ax2, *plC*$^{-}$ and *plC*$^{-}$*/plC*, or Ax2, *pten*$^{-}$ and *pten*$^{-}$*/pten-GFP*). @, $p < 0.001$ compared to *plC*$^{-}$ (one-way ANOVA, Tukey's test among Ax2, *plC*$^{-}$ and *plC*$^{-}$*/plC*). #, $p < 0.001$ compared to *pten*$^{-}$ (one-way ANOVA, Tukey's test among Ax2, *pten*$^{-}$ and *pten*$^{-}$*/pten-GFP*).

Strain	IC50 in 25% HL5, µM	IC50 in 100% HL5, µM
Ax2	106 ± 3	117 ± 10
gα3^{-}	164 ± 6 ***	> 200
gβ^{-}	160 ± 20 *	> 200
gefA^{-}	158 ± 15 **	177 ± 35
pten^{-}	178 ± 15 ^^	> 200
pten^{-}*/pten-GFP*	127 ± 8 #	91 ± 7
plC^{-}	168 ± 6 ^^^	> 200
plC^{-}*/plC*	124 ± 3 ^ @	130 ± 3
iplA^{-}	192 ± 8 ***	188 ± 41
ppk1^{-}	168 ± 5 ***	189 ± 48
piaA^{-}	167 ± 10 ***	> 200
pkaC^{-}	175 ± 10 ***	> 200
gdt1^{-}*/2*$^{-}$	139 ± 11 *	159 ± 22

To determine if these proteins are also involved in the polyphosphate signal transduction pathway in a nutrient-rich condition, the corresponding knockout strains were tested for sensitivity to polyphosphate with dose-response curves in 100% HL5 (Figure 17). In 100% HL5, compared to Ax2 cells, cells lacking Gα3, Gβ, GefA, PTEN, PLC, IplA, Ppk1, PiaA, PKA-C, or Gdt 1 and 2 also showed a reduced sensitivity to polyphosphate (Figure 17). In 100% HL5, the proliferation-inhibition curves of *gβ*$^{-}$ and *pkaC*$^{-}$ did not converge, and the fitting for curves of *gα3*$^{-}$, *gefA*$^{-}$, *pten*$^{-}$, *plC*$^{-}$, *iplA*$^{-}$,

ppk1^{-}, and *piaA*$^{-}$ were ambiguous. The IC50s of polyphosphate proliferation inhibition on these knock-out mutant strains were higher than that of Ax2 cells (Table 5). Expressing PTEN in *pten*$^{-}$ cells and PLC in *plC*$^{-}$ cells appeared to partially rescue or rescue the sensitivity to polyphosphate (Figure 17 C and D, Table 5). Together, these results support the idea that Gα3, Gβ, GefA, PTEN, PLC, IplA, Ppk1, PiaA, PKA-C, and Gdt 1 and 2 affect the polyphosphate proliferation inhibition signal transduction pathway in both low and high nutrient conditions.

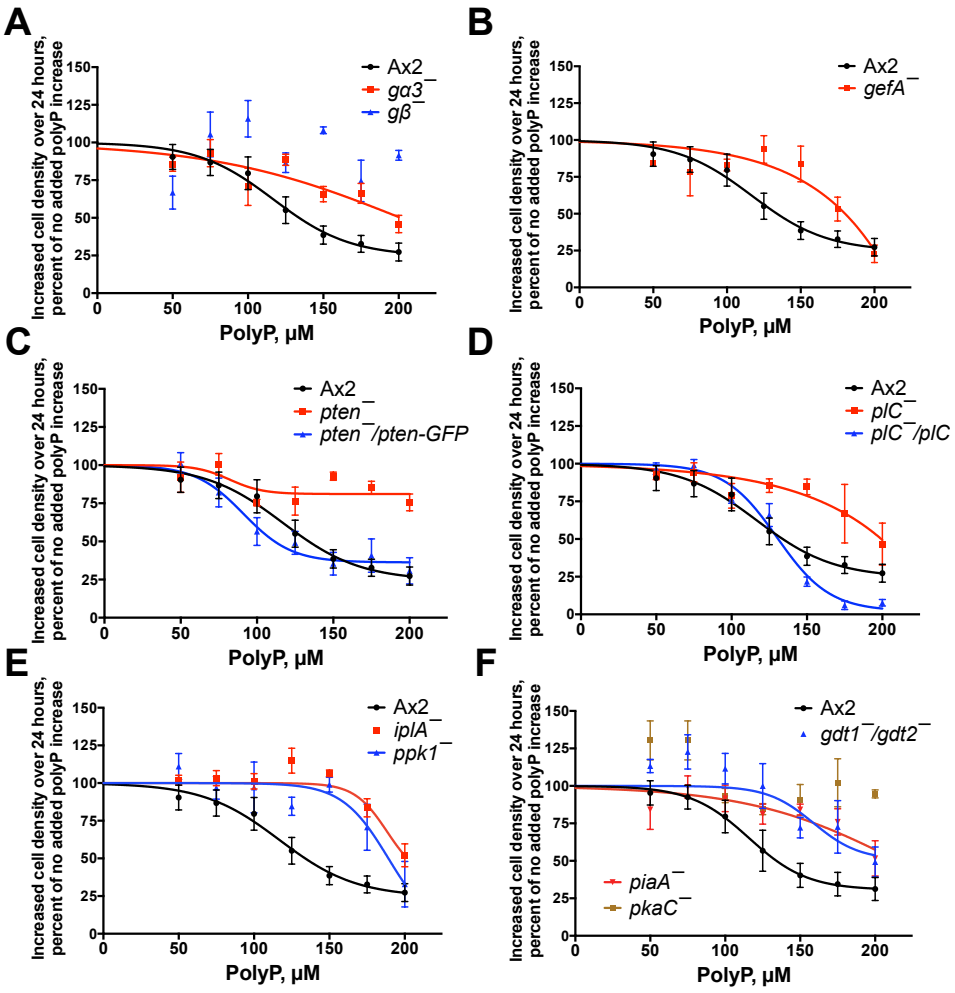

Figure 17. Some mutants have abnormal sensitivities to polyphosphate in 100% HL5. The indicated cell lines were tested for proliferation in 100% HL5 as in Figure 16. Values are mean ± SEM, n ≥ 3.

4.4.13. Gα3, Gβ, GefA, PTEN, PLC, IplA, Ppk1, PiaA, PKA-C, and Gdt 1 and 2 affect cell proliferation

To assess the effect of the disruption of these genes on general cell proliferation, we assayed proliferation curves of the above strains in 100% HL5 in shaking culture

(Figure 18), except for *gβ*$^{-}$ cells, which were assayed previously [25]. The doubling times at low cell density (0.5 ~ 6 x 10^6/ml) and high cell density (6 x 10^6/ml to maximal cell density or plateau) were calculated. At low cell densities, where the extracellular polyphosphate concentration is expected to be low, cells lacking GefA, PTEN, PLC, Ppk1, or PKA-C had a longer doubling time compared to Ax2 cells (Table 6), and cells lacking Gβ have a shorter doubling time [25]. Expressing PTEN in *pten*$^{-}$ cells rescued the phenotype, and expressing PLC in *plC*$^{-}$ cells shortened the doubling time (Table 6). At high cell densities, where the extracellular polyphosphate concentration is expected to be high, cells lacking Gβ, GefA, IplA, Ppk1, or PiaA had shorter doubling times compared to Ax2 cells ([25], Table 6). Expressing PLC in *plC*$^{-}$ cells caused a shorter doubling time compared to Ax2 cells (Table 6). These data suggest that GefA, PTEN, PLC, Ppk1, and PKA-C promote cell proliferation at low cell densities, and Gβ ([25]), GefA, IplA, Ppk1, and PiaA slow cell proliferation at high cell densities. The maximal cell density of cells lacking Gβ, GefA, IplA, Ppk1, or PiaA is abnormally high ([25], Figure 18 A, D and F, Table 6), and cells lacking Gα3, PTEN, PLC, PKA-C, or Gdt 1 and 2 is abnormally low (Figure 18 B, C, E and F, Table 6). Expressing PTEN in *pten*$^{-}$ cells and PLC in *plC*$^{-}$ cells rescued or reversed the phenotype (Figure 18 B and C, Table 6). These data suggest that these proteins affect the proliferation of *D. discoideum* cells.

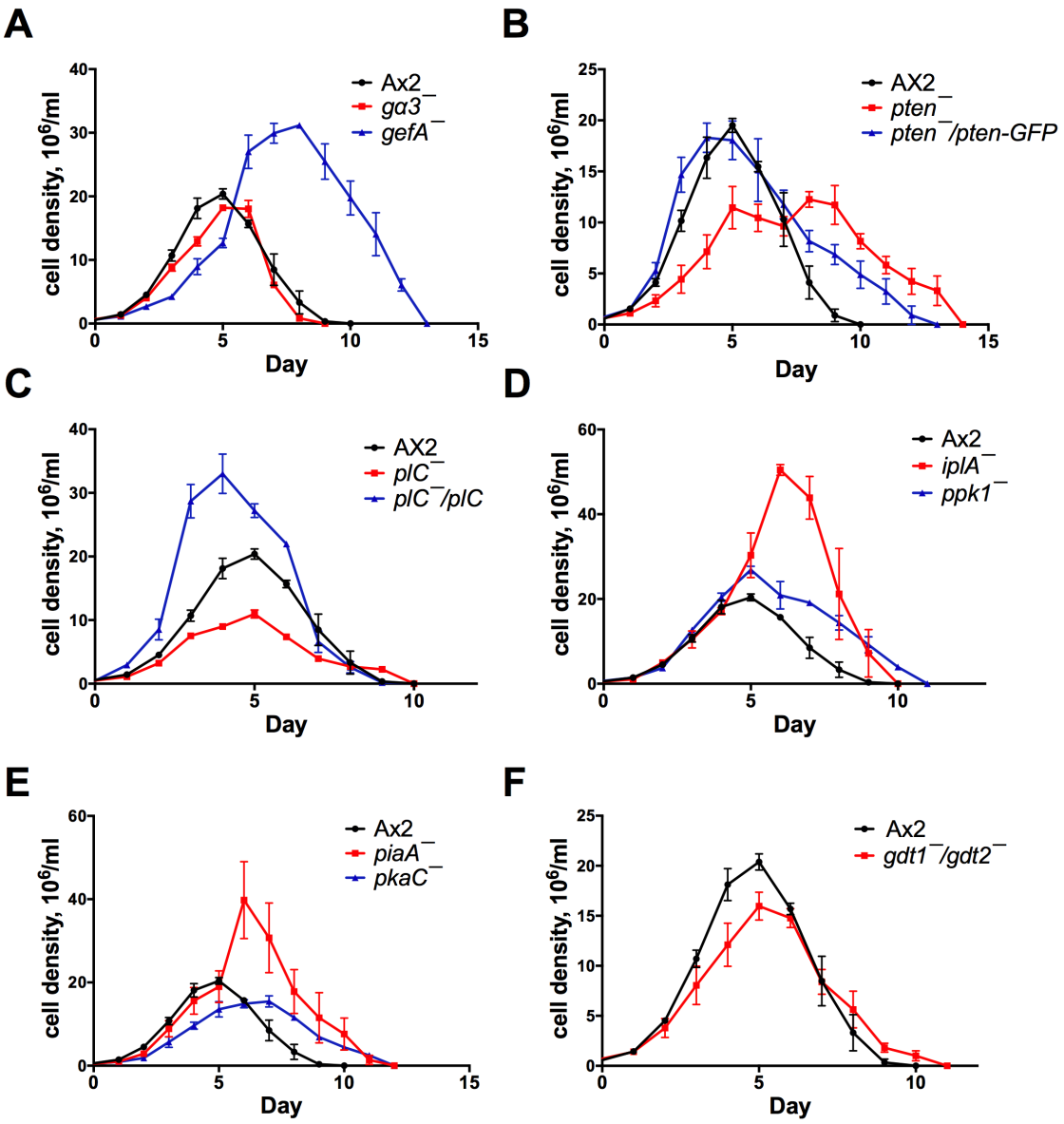

Figure 18. Some mutants have abnormal growth curves in HL5.
Log phase cells were grown in liquid shaking culture starting at ~5 x 10^5 cells/ml and counted daily. All values are mean ± SEM, n ≥ 3 independent experiments.

Table 6. Deletion of some potential polyphosphate pathway components alters doubling time and maximal cell density.
For the data in Figure 18, doubling times were calculated for low cell densities (0.5 to 6 million/ml) and high cell densities (6 million/ml to maximal density reached). Values are mean ± SEM, n ≥ 3 independent experiments. *, $p < 0.05$, **, $p < 0.01$, *** $p < 0.001$ compared to Ax2 (t-test). ^, $p < 0.05$, ^^, $p<0.01$ compared to Ax2 (one-way ANOVA, Tukey's test among Ax2, *pten*$^-$ and *pten*$^-$*/pten-GFP* or Ax2, *plC*$^-$ and *plC*$^-$*/plC*). #, $p < 0.05$ compared to *pten*$^-$ (one-way ANOVA, Tukey's test among Ax2, *pten*$^-$ and *pten*$^-$*/pten-GFP*). @, $p < 0.01$ compared to *plC*$^-$ (one-way ANOVA, Tukey's test among Ax2, *plC*$^-$ and *plC*$^-$*/plC*).

Strain	Doubling Time, hours (Low Density)	Doubling Time, hours (High Density)	Maximal Density
Ax2	16.3 ± 1.1	32.4 ± 1.7	21.8 ± 0.7
gα3$^-$	19.1 ± 0.6	33.0 ± 0.9	19.1 ± 0.4 *
gefA$^-$	26.3 ± 1.2 **	27.2 ± 1.2 *	31.8 ± 0.5 ***
pten$^-$	29.4 ± 4.4 ^	33.8 ± 4.0	13.8 ± 1.1 ^^^
pten$^-$*/pten-GFP*	17.6 ± 1.3 #	32.9 ± 3.5	22.5 ± 0.7 #
plC$^-$	21.2 ± 0.9 ^	41.8 ± 5.0	11.0 ± 0.6 ^^
plC$^-$*/plC*	9.0 ± 0.6 ^^ @	20.9 ± 1.2 ^ @	33.0 ± 3.1 ^^ @
iplA$^-$	14.9 ± 0.5	25.2 ± 1.7 *	52.0 ± 1.3 ***
ppk1$^-$	19.9 ± 0.9 *	25.3 ± 1.1 *	27.3 ± 0.7 **
piaA$^-$	19.4 ± 1.6	23.7 ± 2.2 *	38.4 ± 9.1
pkaC$^-$	22.7 ± 0.7 **	36.1 ± 9.5	17.3 ± 0.8 *
gdt1$^-$*/2*$^-$	21.7 ± 3.8	35.0 ± 4.0	15.4 ± 1.2 *

4.4.14. Polyphosphate upregulates inositol 1,4,5-trisphosphate

PLC catalyzes the hydrolysis of PIP2 to diacylglycerol (DAG) and inositol 1,4,5-trisphosphate (IP3) [123, 131]. PLC and the putative IP3 receptor IplA potentiate polyphosphate proliferation inhibition, suggesting that IP3 might mediate polyphosphate proliferation inhibition. To examine this, we measured the effect of polyphosphate on IP3 levels with an IP3 ELISA kit. The baseline IP3 levels we measured are far less than levels previously reported using an isotope dilution kit that has been discontinued by the

manufacturer (pg vs μg level per 10^7 cells) [132, 133]. Both kits detect IP3 levels based on competition binding strategy, but the isotope kit used an IP3 binding protein prepared from bovine adrenal cortex, and the ELISA kit uses an anti-IP3 antibody. We hypothesize that the difference between the measured IP3 levels could be caused by the specificity of the anti-IP3 antibody being much higher than that of the bovine IP3 binding protein.

Polyphosphate increased IP3 in Ax2, *gα3*$^-$, *gβ*$^-$, *rasC*$^-$, *iplA*$^-$, and *ppk1*$^-$ cells, and decreased IP3 in *pkaC*$^-$ cells (Figure 19). The upregulation of IP3 for *gβ*$^-$ cells is slight but statistically significant. Polyphosphate did not significantly affect IP3 levels in *grlD*$^-$, *gefA*$^-$, *pten*$^-$, *plC*$^-$, *piaA*$^-$ and *gdt1*$^-$/*gdt2*$^-$ cells, and expressing PTEN in *pten*$^-$ cells and PLC in *plC*$^-$ cells partially rescued the response (Figure 19). Compared to Ax2 cells, the baseline IP3 levels of *grlD*$^-$, *plC*$^-$/*plC*, and *ppk1*$^-$ cells were significantly higher, and the baseline IP3 levels of *piaA*$^-$ and *gdt1*$^-$/*gdt2*$^-$ were significantly lower (Figure 19). These results indicate that polyphosphate upregulates IP3 in *D. discoideum* and that this upregulation requires GrlD, GefA, PTEN, PLC, PiaA, PKA-C, and Gdt 1 and 2, and that polyphosphate does not require Gα3, Gβ, RasC, IplA, or Ppk1 to upregulate IP3.

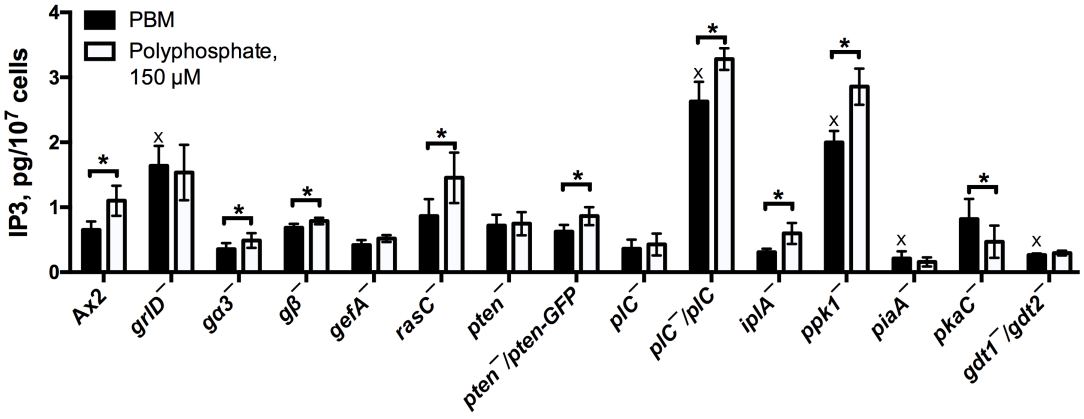

Figure 19. Polyphosphate upregulates inositol 1,4,5-trisphosphate (IP3) levels. Cells were cultured with 0 or 150 µM polyphosphate in 25% HL5 for 4 hours, collected by centrifugation, and IP3 in the cells was measured. All values are mean ± SEM, n ≥ 3 independent experiments. * indicates $p < 0.05$ (paired t-test). X indicates $p<0.05$ compared to Ax2 with no added polyphosphate (t-test).

4.4.15. Polyphosphate upregulates cytosolic free Ca^{2+}

IP3 activates IP3 receptors on the endoplasmic reticulum, leading to Ca^{2+} release from the endoplasmic reticulum lumen to the cytosol in many organisms [123]. In *D. discoideum*, the putative IP3 receptor IplA is localized mostly in cytoplasmic organelles and at very low levels at the plasma membrane, and is involved in Ca^{2+} entry into the cytosol in response to chemoattractants [107, 134]. As a partial test of the hypothesis that the GrlD-PLC-IP3-IplA-Ca^{2+} pathway is used by polyphosphate to regulate proliferation, we examined the effect of polyphosphate on cytosolic Ca^{2+}. BAPTA-1 dextran, which shows an increased fluorescence in the presence of Ca^{2+} [135], was loaded into *Dictyostelium* cells by electroporation. This technique loads the BAPTA-dextran into the cytosol [135, 136]. The BAPTA-1 dextran loaded cells were then incubated with or

without polyphosphate and Ca^{2+} levels were analyzed based on the total fluorescence per cell (representing the total Ca^{2+} amount) (Figure 20A) and the mean fluorescence per μm^2 of cells (Figure 20B) to exclude the impact of cell size/surface area. By both measurements, polyphosphate increased cytosolic free Ca^{2+} in Ax2 cells (Figure 20 and Figure 21).

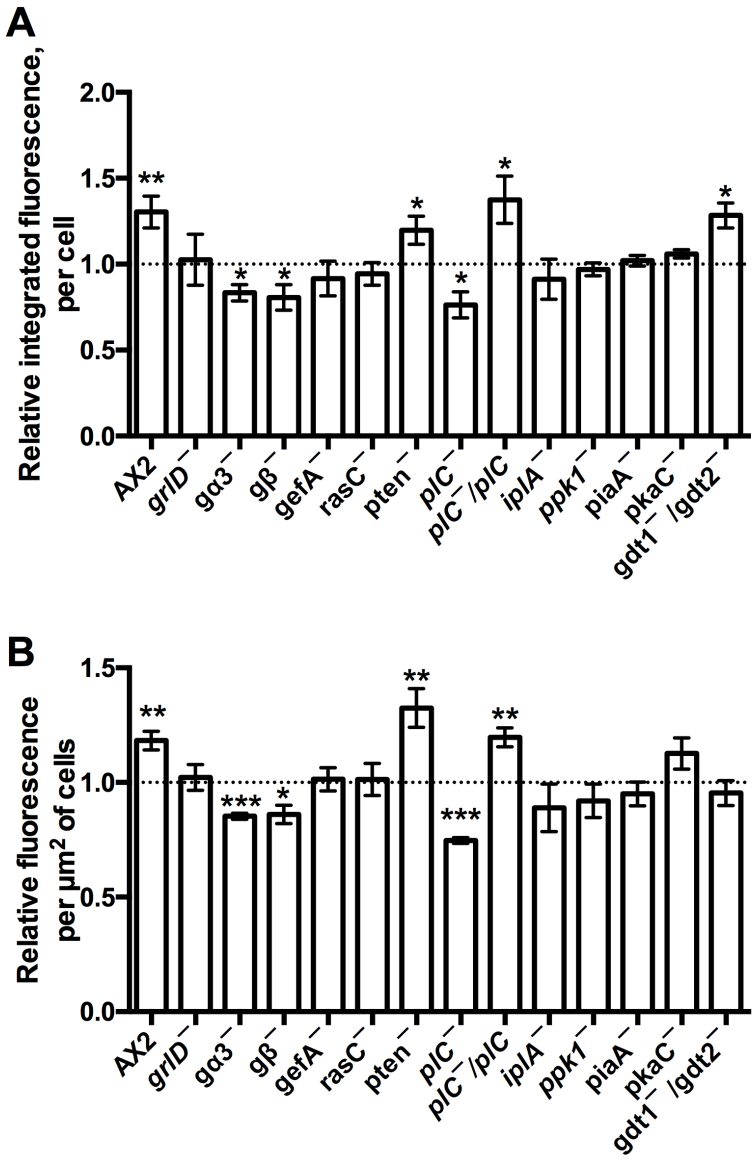

Figure 20. Polyphosphate upregulates cytosolic Ca^{2+}.
Cells were cultured with 0 or 150 μM polyphosphate in 25% HL5 for 4 hours. Cells were cultured with 0 or 150 μM polyphosphate in 25% HL5 for 4 hours. After dye uptake, calcium levels were measured by microscopy, examining > 30 cells per sample. The ratio of fluorescence intensity with 150 μM polyphosphate to the intensity with no polyphosphate was calculated. The integrated fluorescence ratio is shown in **A**, and the fluorescence ratio per μm^2 in cell images is shown in **B**. All values are mean ± SEM, n ≥ 3 independent experiments. * indicates $p < 0.05$, **, $p < 0.01$, *** $p < 0.001$ compared to no polyphosphate (t-test).

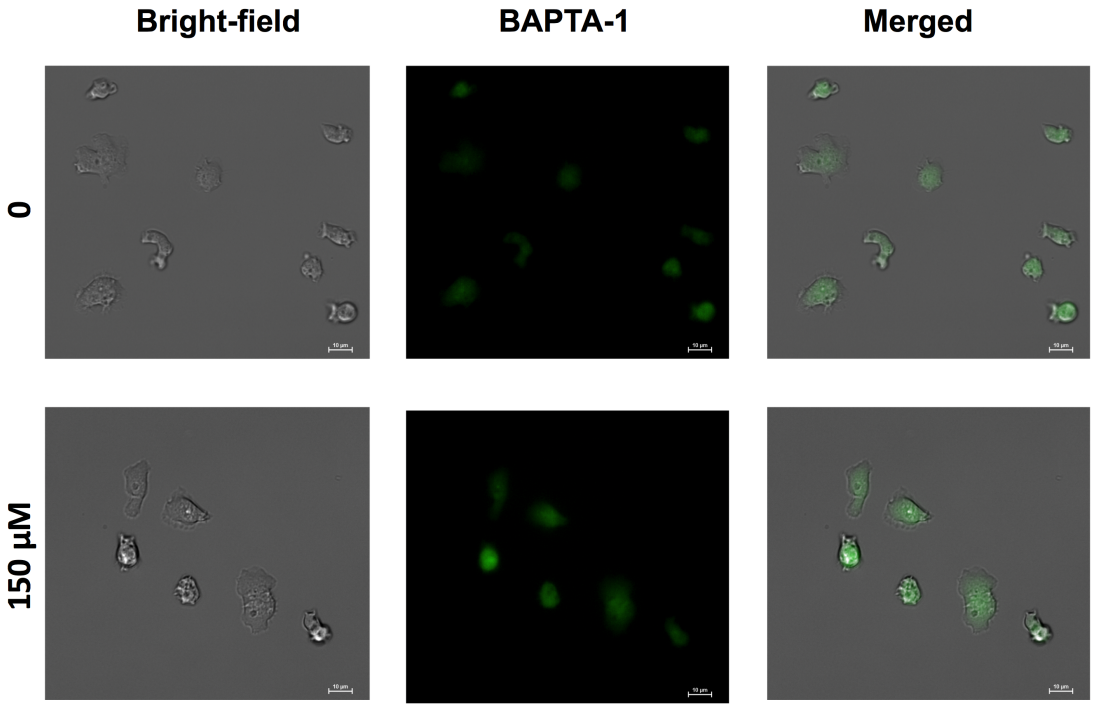

Figure 21. Polyphosphate upregulates cytosolic Ca^{2+}.
Wild-type cells were loaded with BAPTA-1 dextran by electroporation. BAPTA-1 loaded cells were then cultured with 0 or 150 µM polyphosphate for 4 hours in 25% HL5 and were imaged with a 40x objective on a Ti2 Eclipse inverted epifluorescence microscope (Nikon). Images are representative of 3 independent experiments. Bars are 10 µm.

Polyphosphate did not significantly affect cytosolic free Ca^{2+} in cells lacking GrlD, GefA, RasC, IplA, Ppk1, PiaA, or PKA-C (Figure 20), increased Ca^{2+} in cells lacking PTEN, and reduced Ca^{2+} in cells lacking Gα3, Gβ, or PLC (Figure 20). Expressing PLC in *plC*$^{-}$ cells rescued the response to polyphosphate (Figure 20). Polyphosphate increased the total cytosolic Ca^{2+} amount per cell but not the concentration per μm^2, in cells lacking Gdt1 and Gdt2 (Figure 20). Overall, these data suggest that polyphosphate upregulates

cytosolic free Ca^{2+} of *D. discoideum*, and this requires GrlD, Gα3, Gβ, GefA, RasC, PLC, IplA, Ppk1, PiaA, PKA-C and Gdt 1 and 2.

4.4.16. Polyphosphate inhibits cytokinesis

Polyphosphate inhibits the proliferation of cells by inhibiting cytokinesis, causing an increased number of multinucleated cells [9]. To determine if the signal transduction components identified above are needed for the effect of polyphosphate on cytokinesis, we measured the number of nuclei per cell in the presence or absence of polyphosphate. For wild-type cells, polyphosphate increased nuclei per cell (Table 7). This effect was not observed in cells lacking GrlD, Gα3, Gβ, GefA, RasC, PTEN, PLC, IplA, Ppk1, PiaA, PKA-C, or Gdt1 and Gdt2 (Table 7). Expressing PTEN in *pten*$^-$ cells and PLC in *plC*$^-$ cells rescued or partially rescued the sensitivity to polyphosphate (Table 7). These data suggest that the potential signaling components identified above are needed for polyphosphate inhibition of cytokinesis.

Table 7. The potential polyphosphate pathway components are needed for polyphosphate induced cell multinucleation.

Nuclei number and percent of cells with 1, 2 and 3 or more nuclei was measured by counts of DAPI (4', 6-diamidino-2-phenylindole)-stained cells. Cells were examined by epifluorescence microscope with a 40x lens, and for each condition, at least 100 cells were counted. Values are mean ± SEM, n ≥ 3 independent experiments. *, $p < 0.05$, **, $p < 0.01$ and ***, $p < 0.001$, compared to no polyphosphate (t-test).

Cell type	[polyP] μM	Nuclei/100 cells	Percent of cells with n nuclei		
			1	2	3+
Ax2	0	108 ± 2	93.2 ± 1.5	6.5 ± 1.3	0.3 ± 0.2
	150	123 ± 3 **	79.4 ± 2.1***	18.7 ± 1.5***	1.9 ± 0.8
grlD$^-$	0	104 ± 1	96.2 ± 1.2	3.8 ± 1.2	0 ± 0
	150	105 ± 2	95.3 ± 1.4	4.7 ± 1.2	0 ± 0
gα3$^-$	0	110 ± 4	90.5 ± 2.9	8.8 ± 2.5	0.7 ± 0.4
	150	111 ± 3	89.7 ± 2.4	9.6 ± 2.3	0.6 ± 0.2
gβ$^-$	0	101 ± 1	98.9 ± 0.3	1.1 ± 0.3	0 ± 0
	150	102 ± 1	98.3 ± 0.7	1.4 ± 0.6	0 ± 0
gefA$^-$	0	110 ± 3	90.5 ± 2.3	9.0 ± 2.1	0.5 ± 0.4
	150	118 ± 6	83.1 ± 4.2	16.0 ± 3.8	1.0 ± 0.5
rasC$^-$	0	116 ± 4	86.8 ± 2.2	11.3 ± 1.5	1.9 ± 0.7
	150	117 ± 5	85.9 ± 3.0	12.5 ± 2.5	1.6 ± 0.5
pten$^-$	0	120 ± 2	82.4 ± 1.9	16.0 ± 1.9	1.6 ± 0.1
	150	116 ± 4	86.4 ± 2.6	12.1 ± 2.0	1.5 ± 0.7
pten$^-$*/pten-GFP*	0	114 ± 6	87.2 ± 4.2	12.1 ± 3.9	0.7 ± 0.3
	150	123 ± 5	79.9 ± 3.2***	17.7 ± 2.9	2.3 ± 0.3*
plC$^-$	0	106 ± 3	94.1 ± 2.5	5.9 ± 2.5	0 ± 0
	150	110 ± 4	89.7 ± 3.0	10.3 ± 3.0	0 ± 0
plC$^-$*/plC*	0	106 ± 1	94.6 ± 1.0	5.3 ± 0.9	0.2 ± 0.2
	150	121 ± 4 *	81.4 ± 2.6**	16.6 ± 2.0**	2.0 ± 0.7**
iplA$^-$	0	103 ± 1	97.3 ± 0.5	2.7 ± 0.5	0 ± 0
	150	104 ± 1	96.5 ± 1.0	3.5 ± 1.0	0 ± 0
ppk1$^-$	0	106 ± 2	94.9 ± 0.9	4.7 ± 0.8	0.4 ± 0.2
	150	111 ± 2	90.6 ± 1.8	8.5 ± 2	0.9 ± 0.4
piaA$^-$	0	102 ± 1	98.4 ± 0.5	1.6 ± 0.5	0 ± 0
	150	104 ± 1	96.0 ± 1.0	4.0 ± 1.0	0 ± 0
pkaC$^-$	0	105 ± 1	96.2 ± 0.9	3.1 ± 1.0	0.6 ± 0.6
	150	105 ± 1	95.5 ± 0.5	4.0 ± 0.7	0.5 ± 0.3
gdt1$^-$*/2*$^-$	0	139 ± 11	74.0 ± 4.2	18.7 ± 1.8	7.3 ± 2.5
	150	143 ± 8	64.4 ± 6.0	29.7 ± 5.2	5.8 ± 1.2

4.5. Discussion

We screened 49 signal transduction pathway mutants for sensitivity to polyphosphate-induced proliferation inhibition. We found that Gα1, Gα2, Gα3, Gβ, GefA, PakD, RblA, RacC, PlaA, Pik A and B, DagA, PTEN, PLC, IplA, Dd5p4, Erk1, MekA, I6kA, Ppk1, Gdt 1, 2 and 4, CsaA, PiaA, PKA-C and Mcln potentiate polyphosphate inhibition of cell proliferation, suggesting that a complex signal transduction pathway mediates this example of an autocrine proliferation inhibition mechanism. Compared to Ax2 cells, *gα3*$^{-}$, *gβ*$^{-}$, *gefA*$^{-}$, *rasC*$^{-}$, *pten*$^{-}$, *plC*$^{-}$, *iplA*$^{-}$, *ppk1*$^{-}$, *pkaC*$^{-}$ and *gdt1*$^{-}$*/2*$^{-}$ cells showed strongly reduced sensitivity to polyphosphate proliferation inhibition, but not as abolished as *grlD*$^{-}$ cells. These results suggest that there are branched signaling pathways downstream of GrlD responding to extracellular polyphosphate.

The polyphosphate signal transduction pathway appears to use components that regulate proliferation in other systems. Ras, PLC and IP3-induced Ca^{2+} release promote proliferation, and PTEN and PKA inhibit proliferation in mammalian systems [137-143]. Inhibition of Ras, PLC or IP3-induced Ca^{2+} release inhibit cell proliferation in various cell types [139, 144-146]. Overexpression of PTEN inhibits cell proliferation in many cancer cell lines [140, 141, 147], and activation of PKA inhibits vascular smooth cell proliferation induced by injury [142, 143]

Polyphosphate is a prestarvation factor that primes *Dictyostelium* cells for development [36], and many signal transduction pathway components affecting the

Dictyostelium growth-development transition also affect polyphosphate inhibition of proliferation. This is not unexpected, as *Dictyostelium* cells stop proliferation and initiate development at approximately the same time.

Many components of the AprA and cAMP signal transduction pathways did not affect polyphosphate inhibition of cell proliferation. For those components in these two pathways that potentiated polyphosphate induced proliferation inhibition, the effect on polyphosphate inhibition was relatively mild. PiaA and Lst8 are both Tor complex 2 components [114] but *piaA*$^{-}$ cells showed some impairment of polyphosphate signaling, while *lst8*$^{-}$ cells showed no significant inhibition, suggesting that PiaA and Lst8 have independent functions.

We tested the effect of the mutants that attenuate polyphosphate proliferation inhibition on proliferation in shaking culture. *gefA*$^{-}$, *pten*$^{-}$, *plC*$^{-}$, *ppk1*$^{-}$, and *pkaC*$^{-}$ cells proliferated abnormally slowly and *gβ*$^{-}$ cells ([25]) proliferated abnormally quickly at low cell densities, and *gβ*$^{-}$([25]), *gefA*$^{-}$, *iplA*$^{-}$, *ppk1*$^{-}$, and *piaA*$^{-}$ cells proliferated abnormally quickly at high cell densities. The maximal cell density of *gβ*$^{-}$, *gefA*$^{-}$, *iplA*$^{-}$, *ppk1*$^{-}$, and *piaA*$^{-}$ cells was abnormally high, and that of *gα3*$^{-}$, *pten*$^{-}$, *plC*$^{-}$, *pkaC*$^{-}$, or *gdt1*$^{-}$/*2*$^{-}$ cells was abnormally low. Compared to Ax2 cells, we expected that mutant cells with reduced sensitivity to polyphosphate would proliferate faster and reach higher maximal cell densities. However, *pten*$^{-}$, *plC*$^{-}$, *pkaC*$^{-}$, and *gdt1*$^{-}$/*2*$^{-}$ proliferated slower and had a lower maximal cell density. The accumulated extracellular polyphosphate of these four mutants

might be abnormally high, or the proteins knocked out could be required for regulating proliferation through other pathways.

Polyphosphate inhibits cytokinesis and thus causes an increased percentage of multinucleated cells [9]. The effect of GrlD, Gα3, Gβ, GefA, RasC, PTEN, PLC, IplA, Ppk1, PiaA, PKA-C, and Gdt 1 and 2 on polyphosphate inhibition of cytokinesis was tested. The data indicate that all of these proteins are required for polyphosphate inhibition of cytokinesis (Table 7). As cytokinesis is a key component of proliferation, this result is not unexpected.

Polyphosphate proliferation inhibition is potentiated by proteins in the PLC/IP3 pathway. We found that polyphosphate upregulates cellular IP3 levels and this requires GrlD, GefA, PTEN, PLC, PiaA, PKA-C and Gdt 1 and 2, and that Gα3, Gβ, RasC, IplA and Ppk1 are not required for polyphosphate upregulating IP3. Together, these results suggest that polyphosphate activates a signal transduction pathway that upregulates IP3 levels.

IP3 activates IP3 receptors on the endoplasmic reticulum, leading to Ca^{2+} release from the endoplasmic reticulum lumen to the cytosol in many organisms [123]. We found that polyphosphate upregulates cytosolic Ca^{2+} levels and this requires GrlD, Gα3, Gβ, GefA, RasC, PLC, IplA, Ppk1, PiaA and PKA-C. Polyphosphate upregulated the total Ca^{2+} level per cell but not the concentration (Ca^{2+} level per μm^2 of cells) in *gdt1*$^{-}$*/gdt2*$^{-}$

cells. This indicates that polyphosphate increased the size of *gdt1*$^{-}$/*gdt2*$^{-}$ cells (1.2 $\pm$ 0.05 fold increase) in 4 hours.

Polyphosphate upregulated both IP3 levels and cytosolic Ca^{2+} levels of Ax2 cells but did not significantly alter either IP3 levels or cytosolic Ca^{2+} levels of *grlD*$^{-}$, *gefA*$^{-}$, *piaA*$^{-}$ and *gdt1*$^{-}$/*2*$^{-}$ cells. These results suggest that GrlD, GefA, PiaA, and Gdt 1 and 2 function upstream of elevating IP3 in the polyphosphate pathway. As expected, polyphosphate upregulated IP3 levels and did not alter cytosolic Ca^{2+} levels in cells lacking the inositol 1,4,5-trisphosphate receptor-like protein IplA. In cells lacking RasC or Ppk1, polyphosphate upregulated IP3 but did not affect cytosolic Ca^{2+}. In cells lacking Gα3 or Gβ, polyphosphate upregulated IP3 but downregulated cytosolic Ca^{2+}. In cells lacking PKA-C, polyphosphate downregulated IP3 but did not affect cytosolic Ca^{2+}. A possible explanation is that Gα3, Gβ, RasC, Ppk1 and PKA-C are required for IP3 to activate the IplA receptor to release Ca^{2+} to the cytosol, and that GrlD might use components in addition to G proteins to transduce extracellular signals. Unexpectedly, the IP3 levels of cells lacking PTEN or PLC were not altered by polyphosphate, but the cytosolic Ca^{2+} of cells lacking PTEN or PLC was upregulated or downregulated, respectively. These results suggest that polyphosphate can regulate cytosolic Ca^{2+} levels through a pathway not involving IP3.

Ppk1 mediates intracellular polyphosphate production, and the intracellular polyphosphate of *ppk1*$^{-}$ cells is undetectable [28]. How intracellular polyphosphate or

Ppk1 affect the extracellular polyphosphate-induced proliferation inhibition is unclear. As polyphosphate can bind to free divalent cations such as Ca^{2+} and Mg^{2+} [26], we hypothesized that intracellular polyphosphate might bind to elevated cytosolic free Ca^{2+} and then the polyphosphate/Ca^{2+} complex could function as a second messenger. If this is the case, compared to Ax2 cells, cells lacking Ppk1 will show a higher increase of the fluorescence signal with the BAPTA-1 dextran method after stimulating with polyphosphate, as polyphosphate bound Ca^{2+} could not be detected by BAPTA-1. However, cells lacking Ppk1 lost the polyphosphate induced cytosolic free Ca^{2+} increase (Figure 20), while still showing a polyphosphate-induced IP3 increase (Figure 19). This result disproved our hypothesis of a polyphosphate - Ca^{2+} elevation and a Ca^{2+} bound polyphosphate pathway. This indicates that Ppk1/intracellular polyphosphate functions downstream of IP3 and upstream of Ca^{2+} elevation.

Besides proliferation inhibition, polyphosphate inhibits proteasome activity, promotes aggregation, and regulates actin polymerization in *Dictyostelium* cells [39]. In both 25% and 100% HL5, polyphosphate reduces proteasome activity, and this requires GrlD and RasC [39]. However, in 25% HL5 but not 100% HL5, MG132-induced inhibition of proteasome activity inhibits proliferation [39]. In HCT116 cells, the proteasome inhibitor MG132 increases intracellular Ca^{2+} levels [148], and in mouse embryonic fibroblasts, chelating calcium by BAPTA-AM decreases proteasome activity, while increasing intracellular Ca^{2+} with 2 mM extracellular Ca^{2+} and ionomycin treatment increases proteasome activity [149]. In *Dictyostelium*, whether there is a crosstalk in the

polyphosphate signal transduction pathway between proteasome activity and IP3/Ca^{2+} levels is unclear.

In this work, we identified 10 signaling components in the polyphosphate pathway, and showed that polyphosphate appears to use the IP3/Ca^{2+} pathway to inhibit *Dictyostelium* proliferation. An intriguing possibility is that similar mechanisms may be used in other eukaryotes for autocrine proliferation inhibition and group and tissue size regulation.

5. CONCLUSIONS AND FUTURE DIRECTIONS

5.1. Conclusions

A longstanding idea in developmental biology is that the size of a tissue or group of cells, or the spatial density of a specific cell type, could be limited by an autocrine proliferation inhibitor, named as chalone, where the concentration of the inhibitor increases as the size of the tissue or cell group, or density of cells, increases [1-3]. Although a considerable amount is known about signals and pathways that promote cell proliferation, relatively little is known about such autocrine proliferation inhibiting signals and their signal transduction pathways. In the social amoeba *Dictyostelium discoideum*, two molecules, the autocrine proliferation repressor protein A (AprA) and the extracellular inorganic polyphosphate, were identified as chalones [8, 9].

Our lab previously found that in *Dictyostelium discoideum* AprA inhibits proliferation and induces chemorepulsion and this requires G proteins. This suggests that AprA is a ligand for a GPCR [25]. In the work presented in this dissertation, I show that, compared to wild-type cells and similarly to mutants which are insensitive to AprA, cells lacking the GPCR GrlH have a lower doubling time, a lower colony expansion rate, and tighter colony edges [17, 20, 21, 23]. In addition, cells lacking GrlH are insensitive to rAprA-induced proliferation inhibition and chemorepulsion and show reduced binding to rAprA compared to wild-type cells. Expressing GrlH in the *grlH*$^{-}$ cells rescued the phenotypes described above. Together, these data suggest that GrlH is a receptor for

AprA.

We previously found that polyphosphate regulates the proliferation of *D. discoideum* by different signaling pathways depending on nutrient levels [39]. In 100% HL5, loss of the G protein coupled receptor GrlD, a metabotropic Glutamate Receptor-Like receptor, partially reduced the sensitivity of cells to polyphosphate, and loss of the small GTPase RasC did not reduce the sensitivity of cells to polyphosphate [39]. However, in 25% HL5, a low nutrient condition for *D. discoideum* cells, loss of GrlD or RasC blocked the sensitivity of cells to polyphosphate [39]. These results suggest that polyphosphate uses a signal transduction pathway in 25% HL5 to inhibit proliferation.

In the work presented in this dissertation, I identify that several signal transduction pathway components required for polyphosphate inhibition of proliferation, and I show evidence for a pathway involving inositol 1,4,5-trisphosphate and cytosolic calcium that mediates polyphosphate-induced proliferation inhibition in *Dictyostelium.*

In 100% HL5, SodC and the AAA+ATPase were identified as signaling components affecting polyphosphate inhibition of proliferation using the modified shotgun antisense screen. Compared to Ax2 cells, cells with reduced expression of SodC or AAA+ATPase, or with an AAA+ATPase gene disruption, showed reduced sensitivity to proliferation inhibition by polyphosphate (Figure 14).

In 25% HL5, 49 available signal transduction pathway mutants were screened for insensitivity to polyphosphate-induced proliferation inhibition. I show that cells lacking the G protein components Gα3 or Gβ, the Ras guanine nucleotide exchange factor GefA, Phosphatase and tensin homolog (PTEN), Phospholipase C (PLC, which produces IP3 from PIP2), Inositol 1,4,5-trisphosphate receptor-like protein A (IplA, which acts as a calcium channel activated by IP3), Polyphosphate kinase 1(Ppk1), PiaA (cytosolic regulator of adenylate cyclase), Protein kinase A, or Growth-differentiation transition family members 1 and 2 have a significantly reduced sensitivity to polyphosphate induced proliferation inhibition. Polyphosphate inhibits cytokinesis and thus causes an increased percentage of multinucleated cells [9] and this requires GrlD, Gα3, Gβ, GefA, RasC, PTEN, PLC, IplA, Ppk1, PiaA, PKA-C, and Gdt 1 and 2. Polyphosphate upregulates IP3, and this requires GrlD, GefA, PTEN, PLC, PiaA, PKA-C, and Gdt 1 and 2. Polyphosphate also upregulates cytosolic Ca^{2+}, and this requires GrlD, Gα3, Gβ, GefA, RasC, PLC, IplA, Ppk1, PiaA, PKA-C, and Gdt 1 and 2. These data suggest that polyphosphate inhibits the proliferation of *D. discoideum* through an IP3/Ca^{2+} pathway.

5.2. Future directions

5.2.1. Identification of additional receptors required for AprA signaling

A future direction for this project is to identify the additional receptors required for AprA signaling. Several GPCR mutants other than the *grlH* mutant were insensitive to rAprA- induced proliferation inhibition or chemorepulsion or both. *grlB*$^{-}$, *grlD*$^{-}$, and

grlE^{-} cells were insensitive to rAprA-induced proliferation inhibition, and *grlB*$^{-}$, *grlD*$^{-}$, *fslB*$^{-}$, and *fscE*$^{-}$ cells were insensitive to rAprA-induced chemorepulsion.

One possible explanation for those findings is that two or more receptors exist for AprA, as cells lacking GrlH did not show completely abolished rAprA binding. In support of the idea that multiple receptors might sense AprA, cells lacking GrlH were attracted to a source of recombinant AprA, indicating the presence of a non-GrlH receptor that mediates chemoattraction to AprA. Since the recombinant AprA is not glycosylated, this unknown receptor appears to sense a nonglycosylated feature of AprA.

Another possible explanation is that these receptors are activated by a different signal and that this signaling is necessary for AprA signaling. For instance, cells lacking CfaD are insensitive to rAprA-induced proliferation inhibition and chemorepulsion [17, 19]. Unlike *grlH*$^{-}$ cells, *grlB*$^{-}$, *grlD*$^{-}$, and *fslB*$^{-}$ cells were insensitive to rCfaD-induced proliferation inhibition. It is possible that the disruption of GrlB, GrlD, or FslB interrupts the CfaD signaling pathway such that *grlB*$^{-}$, *grlD*$^{-}$, and *fslB*$^{-}$ cells cannot respond properly to AprA. In addition to CfaD, there may be other factors that are necessary for AprA and CfaD signaling.

Together, these data indicate that there may be more than one AprA receptor, and that multiple receptors and, presumably, their associated signaling pathways regulate AprA signaling.

5.2.2. Further study on the mechanism of polyphosphate proliferation inhibition pathway

In the work I presented in this dissertation, 10 new signaling components in the polyphosphate pathway were identified, and polyphosphate using IP3/Ca^{2+} pathway inhibiting *Dictyostelium* cell proliferation was suggested. The detailed mechanism of these components regulating IP3 and Ca^{2+} release, and the mechanism of increased cytosolic Ca^{2+} inhibiting proliferation need to be clarified in future studies. To identify other possibly existing pathways of polyphosphate inhibition of cell proliferation, more mutants need be tested for sensitivity to polyphosphate.

Besides proliferation inhibition, polyphosphate inhibits proteasome activity, promotes aggregation, and regulates actin polymerization in *Dictyostelium* cells [39]. In both 25% and 100% HL5, polyphosphate reduces proteasome activity, and this requires GrlD and RasC [39]. However, in 25% HL5 but not 100% HL5, MG132-induced inhibition of proteasome activity inhibits proliferation [39]. How cells sense the nutrient levels and then alter their polyphosphate-response mechanism is an intriguing project to study.

REFERENCES

1. Roisin-Bouffay C, Gomer RH. [How to reach the right size?]. *Med Sci (Paris)* 20(2), 219-224 (2004).

2. Gomer RH, Jang W, Brazill D. Cell density sensing and size determination. *Dev Growth Differ* 53(4), 482-494 (2011).

3. Consalvo KM, Rijal R, Tang Y, Kirolos SA, Smith MR, Gomer RH. Extracellular signaling in Dictyostelium. *Int J Dev Biol* 63(8-9-10), 395-405 (2019).

4. Metcalf D. Restricted Growth Capacity of Multiple Spleen Grafts. *Transplantation* 2 387-392 (1964).

5. Nadal C. Control of liver growth by growth inhibitors (chalones). *Arch Toxicol Suppl* doi:10.1007/978-3-642-67265-1_11(2), 131-142 (1979).

6. Huang Z, Chen X, Chen D. Myostatin: a novel insight into its role in metabolism, signal pathways, and expression regulation. *Cell Signal* 23(9), 1441-1446 (2011).

7. Lui JC, Baron J. Mechanisms limiting body growth in mammals. *Endocr Rev* 32(3), 422-440 (2011).

8. Brock DA, Gomer RH. A secreted factor represses cell proliferation in Dictyostelium. *Development* 132(20), 4553-4562 (2005).

9. Suess PM, Gomer RH. Extracellular Polyphosphate Inhibits Proliferation in an Autocrine Negative Feedback Loop in Dictyostelium discoideum. *J Biol Chem* 291(38), 20260-20269 (2016).

10. Escalante R, Vicente JJ. Dictyostelium discoideum: a model system for differentiation and patterning. *Int J Dev Biol* 44(8), 819-835 (2000).

11. Eichinger L, Pachebat JA, Glockner G *et al*. The genome of the social amoeba Dictyostelium discoideum. *Nature* 435(7038), 43-57 (2005).

12. Goldberg JM, Manning G, Liu A *et al*. The dictyostelium kinome--analysis of the protein kinases from a simple model organism. *PLoS genetics* 2(3), e38 (2006).

13. Mesquita A, Cardenal-Munoz E, Dominguez E *et al*. Autophagy in Dictyostelium: Mechanisms, regulation and disease in a simple biomedical model. *Autophagy* doi:10.1080/15548627.2016.1226737 1-17 (2016).

14. Adachi H, Hasebe T, Yoshinaga K, Ohta T, Sutoh K. Isolation of Dictyostelium discoideum cytokinesis mutants by restriction enzyme-mediated integration of the blasticidin S resistance marker. *Biochemical and biophysical research communications* 205(3), 1808-1814 (1994).

15. Spann TP, Brock DA, Lindsey DF, Wood SA, Gomer RH. Mutagenesis and gene identification in Dictyostelium by shotgun antisense. *Proceedings of the National Academy of Sciences of the United States of America* 93(10), 5003-5007 (1996).

16. Chisholm RL, Gaudet P, Just EM *et al*. dictyBase, the model organism database for Dictyostelium discoideum. *Nucleic Acids Res* 34(Database issue), D423-427 (2006).

17. Phillips JE, Gomer RH. A secreted protein is an endogenous chemorepellant in Dictyostelium discoideum. *Proceedings of the National Academy of Sciences of the United States of America* 109(27), 10990-10995 (2012).

18. Bakthavatsalam D, Brock DA, Nikravan NN, Houston KD, Hatton RD, Gomer RH. The secreted Dictyostelium protein CfaD is a chalone. *J Cell Sci* 121(Pt 15), 2473-2480 (2008).

19. Choe JM, Bakthavatsalam D, Phillips JE, Gomer RH. Dictyostelium cells bind a secreted autocrine factor that represses cell proliferation. *BMC Biochem* 10 4 (2009).

20. Phillips JE, Gomer RH. The ROCO kinase QkgA is necessary for proliferation inhibition by autocrine signals in Dictyostelium discoideum. *Eukaryot Cell* 9(10), 1557-1565 (2010).

21. Bakthavatsalam D, White MJ, Herlihy SE, Phillips JE, Gomer RH. A retinoblastoma orthologue is required for the sensing of a chalone in Dictyostelium discoideum. *Eukaryot Cell* 13(3), 376-382 (2014).

22. Herlihy SE, Tang Y, Gomer RH. A Dictyostelium secreted factor requires a PTEN-like phosphatase to slow proliferation and induce chemorepulsion. *Plos One* 8(3), e59365 (2013).

23. Phillips JE, Gomer RH. The p21-activated kinase (PAK) family member PakD is required for chemorepulsion and proliferation inhibition by autocrine signals in Dictyostelium discoideum. *Plos One* 9(5), e96633 (2014).

24. Phillips JE, Huang E, Shaulsky G, Gomer RH. The putative bZIP transcription factor BzpN slows proliferation and functions in the regulation of cell density by autocrine signals in Dictyostelium. *Plos One* 6(7), e21765 (2011).

25. Bakthavatsalam D, Choe JM, Hanson NE, Gomer RH. A Dictyostelium chalone uses G proteins to regulate proliferation. *BMC Biol* 7 44 (2009).

26. Kornberg A, Rao NN, Ault-Riche D. Inorganic polyphosphate: a molecule of many functions. *Annu Rev Biochem* 68 89-125 (1999).

27. Rao NN, Gomez-Garcia MR, Kornberg A. Inorganic polyphosphate: essential for growth and survival. *Annu Rev Biochem* 78 605-647 (2009).

28. Livermore TM, Chubb JR, Saiardi A. Developmental accumulation of inorganic polyphosphate affects germination and energetic metabolism in Dictyostelium discoideum. *Proceedings of the National Academy of Sciences of the United States of America* 113(4), 996-1001 (2016).

29. Schröder HC, Müller WE. *Inorganic polyphosphates: biochemistry, biology, biotechnology*. Springer Science & Business Media, 23, (2012).

30. Crooke E, Akiyama M, Rao NN, Kornberg A. Genetically altered levels of inorganic polyphosphate in Escherichia coli. *J Biol Chem* 269(9), 6290-6295 (1994).

31. Rashid MH, Rumbaugh K, Passador L *et al*. Polyphosphate kinase is essential for biofilm development, quorum sensing, and virulence of Pseudomonas aeruginosa. *Proceedings of the National Academy of Sciences of the United States of America* 97(17), 9636-9641 (2000).

32. Chen W, Palmer RJ, Kuramitsu HK. Role of polyphosphate kinase in biofilm formation by Porphyromonas gingivalis. *Infect Immun* 70(8), 4708-4715 (2002).

33. Schroder HC, Kurz L, Muller WE, Lorenz B. Polyphosphate in bone. *Biochemistry (Mosc)* 65(3), 296-303 (2000).

34. Hassanian SM, Avan A, Ardeshirylajimi A. Inorganic polyphosphate: a key modulator of inflammation. *J Thromb Haemost* 15(2), 213-218 (2017).

35. Wang L, Fraley CD, Faridi J, Kornberg A, Roth RA. Inorganic polyphosphate stimulates mammalian TOR, a kinase involved in the proliferation of mammary cancer cells. *Proceedings of the National Academy of Sciences of the United States of America* 100(20), 11249-11254 (2003).

36. Suess PM, Watson J, Chen W, Gomer RH. Extracellular polyphosphate signals through Ras and Akt to prime Dictyostelium discoideum cells for development. *J Cell Sci* 130(14), 2394-2404 (2017).

37. Hernandez-Ruiz L, Gonzalez-Garcia I, Castro C, Brieva JA, Ruiz FA. Inorganic polyphosphate and specific induction of apoptosis in human plasma cells. *Haematologica* 91(9), 1180-1186 (2006).

38. Smith SA, Mutch NJ, Baskar D, Rohloff P, Docampo R, Morrissey JH. Polyphosphate modulates blood coagulation and fibrinolysis. *Proceedings of the National Academy of Sciences of the United States of America* 103(4), 903-908 (2006).

39. Suess PM, Tang Y, Gomer RH. The putative G protein–coupled receptor GrlD mediates extracellular polyphosphate sensing in Dictyostelium discoideum. *Molecular biology of the cell* 30(9), 1118-1128 (2019).

40. Elgjo K, Reichelt KL. Chalones: from aqueous extracts to oligopeptides. *Cell Cycle* 3(9), 1208-1211 (2004).

41. Weiss P, Kavanau JL. A model of growth and growth control in mathematical terms. *J Gen Physiol* 41(1), 1-47 (1957).

42. Bullough WS, Laurence EB. Melanocyte chalone and mitotic control in melanomata. *Nature* 220(5163), 137-138 (1968).

43. Bullough WS, Laurence EB. Control of mitosis in mouse and hamster melanomata by means of the melanocyte chalone. *Eur J Cancer* 4(6), 607-615 (1968).

44. Heidel AJ, Lawal HM, Felder M *et al*. Phylogeny-wide analysis of social amoeba genomes highlights ancient origins for complex intercellular communication. *Genome Res* 21(11), 1882-1891 (2011).

45. Parikh A, Miranda ER, Katoh-Kurasawa M *et al*. Conserved developmental transcriptomes in evolutionarily divergent species. *Genome Biol* 11(3), R35 (2010).

46. Raisley B, Zhang M, Hereld D, Hadwiger JA. A cAMP receptor-like G protein-coupled receptor with roles in growth regulation and development. *Dev Biol* 265(2), 433-445 (2004).

47. Muinonen-Martin AJ, Veltman DM, Kalna G, Insall RH. An improved chamber for direct visualisation of chemotaxis. *Plos One* 5(12), e15309 (2010).

48. Faix J, Kreppel L, Shaulsky G, Schleicher M, Kimmel AR. A rapid and efficient method to generate multiple gene disruptions in Dictyostelium discoideum using a single selectable marker and the Cre-loxP system. *Nucleic Acids Res* 32(19), e143 (2004).

49. Charette SJ, Cosson P. Preparation of genomic DNA from Dictyostelium discoideum for PCR analysis. *Biotechniques* 36(4), 574-575 (2004).

50. Brock DA, Gomer RH. A cell-counting factor regulating structure size in Dictyostelium. *Genes Dev* 13(15), 1960-1969 (1999).

51. Davidson AJ, King JS, Insall RH. The use of streptavidin conjugates as immunoblot loading controls and mitochondrial markers for use with Dictyostelium discoideum. *Biotechniques* 55(1), 39-41 (2013).

52. Ehrenman K, Yang G, Hong WP *et al*. Disruption of aldehyde reductase increases group size in dictyostelium. *J Biol Chem* 279(2), 837-847 (2004).

53. Gaudet P, Pilcher KE, Fey P, Chisholm RL. Transformation of Dictyostelium discoideum with plasmid DNA. *Nat Protoc* 2(6), 1317-1324 (2007).

54. Fredriksson R, Lagerstrom MC, Lundin LG, Schioth HB. The G-protein-coupled receptors in the human genome form five main families. Phylogenetic analysis, paralogon groups, and fingerprints. *Mol Pharmacol* 63(6), 1256-1272 (2003).

55. Howard AD, Mcallister G, Feighner SD *et al*. Orphan G-protein-coupled receptors and natural ligand discovery. *Trends Pharmacol Sci* 22(3), 132-140 (2001).

56. Prabhu Y, Eichinger L. The Dictyostelium repertoire of seven transmembrane domain receptors. *Eur J Cell Biol* 85(9-10), 937-946 (2006).

57. Manahan CL, Iglesias PA, Long Y, Devreotes PN. Chemoattractant signaling in dictyostelium discoideum. *Annu Rev Cell Dev Biol* 20 223-253 (2004).

58. Prabhu Y, Mondal S, Eichinger L, Noegel AA. A GPCR involved in post aggregation events in Dictyostelium discoideum. *Dev Biol* 312(1), 29-43 (2007).

59. Anjard C, Loomis WF. GABA induces terminal differentiation of Dictyostelium through a GABAB receptor. *Development* 133(11), 2253-2261 (2006).

60. Pan M, Xu X, Chen Y, Jin T. Identification of a Chemoattractant G-Protein-Coupled Receptor for Folic Acid that Controls Both Chemotaxis and Phagocytosis. *Dev Cell* 36(4), 428-439 (2016).

61. Wu Y, Janetopoulos C. Systematic analysis of gamma-aminobutyric acid (GABA) metabolism and function in the social amoeba Dictyostelium discoideum. *J Biol Chem* 288(21), 15280-15290 (2013).

62. Wang Y, Chen CL, Iijima M. Signaling mechanisms for chemotaxis. *Dev Growth Differ* 53(4), 495-502 (2011).

63. Fey P, Dodson RJ, Basu S, Chisholm RL. One stop shop for everything Dictyostelium: dictyBase and the Dicty Stock Center in 2012. In: *Dictyostelium Discoideum Protocols*, (Ed.^(Eds).Springer 59-92 (2013).

64. Hames BD, Higgins SJ. *Nucleic acid hybridisation: a practical approach*. IRL Press, (1985).

65. Veltman DM, Akar G, Bosgraaf L, Van Haastert PJ. A new set of small, extrachromosomal expression vectors for Dictyostelium discoideum. *Plasmid* 61(2), 110-118 (2009).

66. Gaudet P, Pilcher KE, Fey P, Chisholm RL. Transformation of Dictyostelium discoideum with plasmid DNA. *Nature protocols* 2(6), 1317 (2007).

67. Singer B, Kusmierek JT. Chemical Mutagenesis. *Annual Review of Biochemistry* 51 655-693 (1982).

68. Frankenbergschwager M. Induction, Repair and Biological Relevance of Radiation-Induced DNA Lesions in Eukaryotic Cells. *Radiat Environ Bioph* 29(4), 273-292 (1990).

69. Adachi H, Hasebe T, Yoshinaga K, Ohta T, Sutoh K. Isolation of Dictyostelium-Discoideum Cytokinesis Mutants by Restriction Enzyme-Mediated Integration of the Blasticidin-S Resistance Marker, (Vol 205, Pg 1808, 1994). *Biochemical and biophysical research communications* 208(3), 1181-1181 (1995).

70. Carlson CM, Largaespada DA. Insertional mutagenesis in mice: New perspectives and tools. *Nat Rev Genet* 6(7), 568-580 (2005).

71. Shalem O, Sanjana NE, Hartenian E *et al*. Genome-Scale CRISPR-Cas9 Knockout Screening in Human Cells. *Science* 343(6166), 84-87 (2014).

72. Wang T, Wei JJ, Sabatini DM, Lander ES. Genetic Screens in Human Cells Using the CRISPR-Cas9 System. *Science* 343(6166), 80-84 (2014).

73. Echeverri CJ, Perrimon N. High-throughput RNAi screening in cultured cells: a user's guide. *Nat Rev Genet* 7(5), 373-384 (2006).

74. Gonczy P, Echeverri C, Oegema K *et al*. Functional genomic analysis of cell division in C-elegans using RNAi of genes on chromosome III. *Nature* 408(6810), 331-336 (2000).

75. Spann TP, Brock DA, Lindsey DF, Wood SA, Gomer RH. Mutagenesis and gene identification in Dictyostelium by shotgun antisense. *Proceedings of the National Academy of Sciences* 93(10), 5003-5007 (1996).

76. Crowley TE, Nellen W, Gomer RH, Firtel RA. Phenocopy of Discoidin I-Minus Mutants by Antisense Transformation in Dictyostelium. *Cell* 43(3), 633-641 (1985).

77. Eichinger L, Pachebat JA, Glockner G *et al*. The genome of the social amoeba Dictyostelium discoideum. *Nature* 435(7038), 43-57 (2005).

78. Clarke L, Carbon J. Colony Bank Containing Synthetic Col El Hybrid Plasmids Representative of Entire Escherichia-Coli Genome. *Cell* 9(1), 91-99 (1976).

79. Alberts B, Bray D, Lewis J, Raff M, Roberts K, Watson J. Molecular biology of the cell Garland. *New York* 18-19 (1994).

80. Fey P, Dodson RJ, Basu S, Chisholm RL. One stop shop for everything Dictyostelium: dictyBase and the Dicty Stock Center in 2012. *Methods Mol Biol* 983 59-92 (2013).

81. Lim CJ, Spiegelman GB, Weeks G. RasC is required for optimal activation of adenylyl cyclase and Akt/PKB during aggregation. *EMBO J* 20(16), 4490-4499 (2001).

82. Kae H, Kortholt A, Rehmann H *et al*. Cyclic AMP signalling in Dictyostelium: G-proteins activate separate Ras pathways using specific RasGEFs. *EMBO Rep* 8(5), 477-482 (2007).

83. Lilly P, Wu LJ, Welker DL, Devreotes PN. A G-Protein Beta-Subunit Is Essential for Dictyostelium Development. *Gene Dev* 7(6), 986-995 (1993).

84. Dharmawardhane S, Cubitt AB, Clark AM, Firtel RA. Regulatory role of the G alpha 1 subunit in controlling cellular morphogenesis in Dictyostelium. *Development* 120(12), 3549-3561 (1994).

85. Kumagai A, Pupillo M, Gundersen R, Miake-Lye R, Devreotes PN, Firtel RA. Regulation and function of G alpha protein subunits in Dictyostelium. *Cell* 57(2), 265-275 (1989).

86. Brandon MA, Podgorski GJ. G alpha 3 regulates the cAMP signaling system in Dictyostelium. *Molecular Biology of the Cell* 8(9), 1677-1685 (1997).

87. Hadwiger JA, Srinivasan J. Folic acid stimulation of the Galpha4 G protein-mediated signal transduction pathway inhibits anterior prestalk cell development in Dictyostelium. *Differentiation* 64(4), 195-204 (1999).

88. Hadwiger JA, Natarajan K, Firtel RA. Mutations in the Dictyostelium heterotrimeric G protein alpha subunit G alpha5 alter the kinetics of tip morphogenesis. *Development* 122(4), 1215-1224 (1996).

89. Wu L, Gaskins C, Zhou K, Firtel RA, Devreotes PN. Cloning and targeted mutations of G alpha 7 and G alpha 8, two developmentally regulated G protein alpha-subunit genes in Dictyostelium. *Mol Biol Cell* 5(6), 691-702 (1994).

90. Brzostowski JA, Johnson C, Kimmel AR. Galpha-mediated inhibition of developmental signal response. *Curr Biol* 12(14), 1199-1208 (2002).

91. Bakthavatsalam D, Brock DA, Nikravan NN, Houston KD, Hatton RD, Gomer RH. The secreted Dictyostelium protein CfaD is a chalone. *Journal of Cell Science* 121(15), 2473-2480 (2008).

92. Garcia M, Ray S, Brown I, Irom J, Brazill D. PakD, a putative p21-activated protein kinase in Dictyostelium discoideum, regulates actin. *Eukaryot Cell* 13(1), 119-126 (2014).

93. Macwilliams H, Doquang K, Pedrola R *et al*. A retinoblastoma ortholog controls stalk/spore preference in Dictyostelium. *Development* 133(7), 1287-1297 (2006).

94. Tang YT, Gomer RH. A Protein with Similarity to PTEN Regulates Aggregation Territory Size by Decreasing Cyclic AMP Pulse Size during Dictyostelium discoideum Development. *Eukaryotic Cell* 7(10), 1758-1770 (2008).

95. Abe T, Langenick J, Williams JG. Rapid generation of gene disruption constructs by in vitro transposition and identification of a Dictyostelium protein kinase that regulates its rate of growth and development. *Nucleic Acids Res* 31(18), (2003).

96. Phillips JE, Huang EY, Shaulsky G, Gomer RH. The Putative bZIP Transcripton Factor BzpN Slows Proliferation and Functions in the Regulation of Cell Density by Autocrine Signals in Dictyostelium. *Plos One* 6(7), (2011).

97. Blagg SL, Stewart M, Sambles C, Insall RH. PIR121 regulates pseudopod dynamics and SCAR activity in Dictyostelium. *Curr Biol* 13(17), 1480-1487 (2003).

98. Yan J, Mihaylov V, Xu X *et al*. A Gbetagamma effector, ElmoE, transduces GPCR signaling to the actin network during chemotaxis. *Dev Cell* 22(1), 92-103 (2012).

99. Roelofs J, Snippe H, Kleineidam RG, Van Haastert PJ. Guanylate cyclase in Dictyostelium discoideum with the topology of mammalian adenylate cyclase. *Biochem J* 354(Pt 3), 697-706 (2001).

100. Han JW, Leeper L, Rivero F, Chung CY. Role of RacC for the regulation of WASP and phosphatidylinositol 3-kinase during chemotaxis of Dictyostelium. *J Biol Chem* 281(46), 35224-35234 (2006).

101. Chen L, Iijima M, Tang M *et al*. PLA2 and PI3K/PTEN pathways act in parallel to mediate chemotaxis. *Dev Cell* 12(4), 603-614 (2007).

102. Chung CY, Potikyan G, Firtel RA. Control of cell polarity and chemotaxis by Akt/PKB and PI3 kinase through the regulation of PAKa. *Mol Cell* 7(5), 937-947 (2001).

103. Lilly PJ, Devreotes PN. Chemoattractant and GTP gamma S-mediated stimulation of adenylyl cyclase in Dictyostelium requires translocation of CRAC to membranes. *J Cell Biol* 129(6), 1659-1665 (1995).

104. Iijima M, Devreotes P. Tumor suppressor PTEN mediates sensing of chemoattractant gradients. *Cell* 109(5), 599-610 (2002).

105. Keizer-Gunnink I, Kortholt A, Van Haastert PJ. Chemoattractants and chemorepellents act by inducing opposite polarity in phospholipase C and PI3-kinase signaling. *J Cell Biol* 177(4), 579-585 (2007).

106. Drayer AL, Meima ME, Derks MW, Tuik R, Van Haastert PJ. Mutation of an EF-hand Ca(2+)-binding motif in phospholipase C of Dictyostelium discoideum: inhibition of activity but no effect on Ca(2+)-dependence. *Biochem J* 311 (Pt 2) 505-510 (1995).

107. Traynor D, Milne JL, Insall RH, Kay RR. Ca(2+) signalling is not required for chemotaxis in Dictyostelium. *EMBO J* 19(17), 4846-4854 (2000).

108. Loovers HM, Veenstra K, Snippe H, Pesesse X, Erneux C, Van Haastert PJ. A diverse family of inositol 5-phosphatases playing a role in growth and development in Dictyostelium discoideum. *J Biol Chem* 278(8), 5652-5658 (2003).

109. Nguyen HN, Raisley B, Hadwiger JA. MAP kinases have different functions in Dictyostelium G protein-mediated signaling. *Cell Signal* 22(5), 836-847 (2010).

110. Schwebs DJ, Pan M, Adhikari N, Kuburich NA, Jin T, Hadwiger JA. Dictyostelium Erk2 is an atypical MAPK required for chemotaxis. *Cell Signal* 46 154-165 (2018).

111. Mendoza MC, Du F, Iranfar N *et al*. Loss of SMEK, a novel, conserved protein, suppresses MEK1 null cell polarity, chemotaxis, and gene expression defects. *Mol Cell Biol* 25(17), 7839-7853 (2005).

112. Harloff C, Gerisch G, Noegel AA. Selective elimination of the contact site A protein of Dictyostelium discoideum by gene disruption. *Genes Dev* 3(12A), 2011-2019 (1989).

113. Tang M, Iijima M, Kamimura Y, Chen L, Long Y, Devreotes P. Disruption of PKB signaling restores polarity to cells lacking tumor suppressor PTEN. *Mol Biol Cell* 22(4), 437-447 (2011).

114. Lee S, Comer FI, Sasaki A *et al*. TOR complex 2 integrates cell movement during chemotaxis and signal relay in Dictyostelium. *Mol Biol Cell* 16(10), 4572-4583 (2005).

115. Mann SK, Firtel RA. A developmentally regulated, putative serine/threonine protein kinase is essential for development in Dictyostelium. *Mech Dev* 35(2), 89-101 (1991).

116. Mohamed W, Ray S, Brazill D, Baskar R. Absence of catalytic domain in a putative protein kinase C (PkcA) suppresses tip dominance in Dictyostelium discoideum. *Dev Biol* 405(1), 10-20 (2015).

117. Singleton CK, Kirsten JH, Dinsmore CJ. Function of ammonium transporter A in the initiation of culmination of development in Dictyostelium discoideum. *Eukaryot Cell* 5(7), 991-996 (2006).

118. Cornillon S, Gebbie L, Benghezal M *et al*. An adhesion molecule in free-living Dictyostelium amoebae with integrin beta features. *EMBO Rep* 7(6), 617-621 (2006).

119. Lima WC, Vinet A, Pieters J, Cosson P. Role of PKD2 in rheotaxis in Dictyostelium. *Plos One* 9(2), e88682 (2014).

120. Lima WC, Leuba F, Soldati T, Cosson P. Mucolipin controls lysosome exocytosis in Dictyostelium. *J Cell Sci* 125(Pt 9), 2315-2322 (2012).

121. Davidson AJ, Amato C, Thomason PA, Insall RH. WASP family proteins and formins compete in pseudopod- and bleb-based migration. *J Cell Biol* 217(2), 701-714 (2018).

122. Rijal R, Consalvo KM, Lindsey CK, Gomer RH. An endogenous chemorepellent directs cell movement by inhibiting pseudopods at one side of cells. *Mol Biol Cell* 30(2), 242-255 (2019).

123. Bruce A, Johnson A, Lewis J, Raff M, Roberts K, Walter P. Molecular Biology of the Cell 5th edn (New York: Garland Science). (2007).

124. Loovers HM, Kortholt A, De Groote H, Whitty L, Nussbaum RL, Van Haastert PJ. Regulation of phagocytosis in Dictyostelium by the inositol 5-phosphatase OCRL homolog Dd5P4. *Traffic* 8(5), 618-628 (2007).

125. Chibalina MV, Anjard C, Insall RH. Gdt2 regulates the transition of Dictyostelium cells from growth to differentiation. *BMC Dev Biol* 4 8 (2004).

126. Zeng C, Anjard C, Riemann K, Konzok A, Nellen W. gdt1, a new signal transduction component for negative regulation of the growth-differentiation transition in Dictyostelium discoideum. *Mol Biol Cell* 11(5), 1631-1643 (2000).

127. Sharma SK, Brock DA, Ammann RR *et al*. The cdk5 homologue, crp, regulates endocytosis and secretion in dictyostelium and is necessary for optimum growth and differentiation. *Dev Biol* 247(1), 1-10 (2002).

128. Rosel D, Khurana T, Majithia A, Huang X, Bhandari R, Kimmel AR. TOR complex 2 (TORC2) in Dictyostelium suppresses phagocytic nutrient capture independently of TORC1-mediated nutrient sensing. *J Cell Sci* 125(Pt 1), 37-48 (2012).

129. Liao XH, Buggey J, Kimmel AR. Chemotactic activation of Dictyostelium AGC-family kinases AKT and PKBR1 requires separate but coordinated functions of PDK1 and TORC2. *J Cell Sci* 123(Pt 6), 983-992 (2010).

130. Cai H, Das S, Kamimura Y, Long Y, Parent CA, Devreotes PN. Ras-mediated activation of the TORC2-PKB pathway is critical for chemotaxis. *J Cell Biol* 190(2), 233-245 (2010).

131. Berridge MJ, Irvine RF. Inositol phosphates and cell signalling. *Nature* 341(6239), 197-205 (1989).

132. Brazill DT, Lindsey DF, Bishop JD, Gomer RH. Cell density sensing mediated by a G protein-coupled receptor activating phospholipase C. *J Biol Chem* 273(14), 8161-8168 (1998).

133. Williams RS, Eames M, Ryves WJ, Viggars J, Harwood AJ. Loss of a prolyl oligopeptidase confers resistance to lithium by elevation of inositol (1,4,5) trisphosphate. *EMBO J* 18(10), 2734-2745 (1999).

134. Europe-Finner GN, Newell PC. Inositol 1, 4, 5-trisphosphate induces calcium release from a non-mitochondrial pool in amoebae of Dictyostelium. *Biochimica et Biophysica Acta (BBA)-Molecular Cell Research* 887(3), 335-340 (1986).

135. Paredes RM, Etzler JC, Watts LT, Zheng W, Lechleiter JD. Chemical calcium indicators. *Methods* 46(3), 143-151 (2008).

136. Schlatterer C, Knoll G, Malchow D. Intracellular calcium during chemotaxis of Dictyostelium discoideum: a new fura-2 derivative avoids sequestration of the indicator and allows long-term calcium measurements. *Eur J Cell Biol* 58(1), 172-181 (1992).

137. Cordova-Alarcon E, Centeno F, Reyes-Esparza J, Garcia-Carranca A, Garrido E. Effects of HRAS oncogene on cell cycle progression in a cervical cancer-derived cell line. *Arch Med Res* 36(4), 311-316 (2005).

138. Berridge MJ. Inositol trisphosphate and calcium signalling mechanisms. *Biochim Biophys Acta* 1793(6), 933-940 (2009).

139. Stallings JD, Zeng YX, Narvaez F, Rebecchi MJ. Phospholipase C-delta1 expression is linked to proliferation, DNA synthesis, and cyclin E levels. *J Biol Chem* 283(20), 13992-14001 (2008).

140. Zhao H, Dupont J, Yakar S, Karas M, Leroith D. PTEN inhibits cell proliferation and induces apoptosis by downregulating cell surface IGF-IR expression in prostate cancer cells. *Oncogene* 23(3), 786-794 (2004).

141. Chu EC, Tarnawski AS. PTEN regulatory functions in tumor suppression and cell biology. *Med Sci Monit* 10(10), RA235-241 (2004).

142. Indolfi C, Avvedimento EV, Di Lorenzo E *et al*. Activation of cAMP-PKA signaling in vivo inhibits smooth muscle cell proliferation induced by vascular injury. *Nat Med* 3(7), 775-779 (1997).

143. Hewer RC, Sala-Newby GB, Wu YJ, Newby AC, Bond M. PKA and Epac synergistically inhibit smooth muscle cell proliferation. *J Mol Cell Cardiol* 50(1), 87-98 (2011).

144. Indolfi C, Avvedimento EV, Rapacciuolo A *et al*. Inhibition of cellular ras prevents smooth muscle cell proliferation after vascular injury in vivo. *Nat Med* 1(6), 541-545 (1995).

145. Kaproth-Joslin KA, Li X, Reks SE, Kelley GG. Phospholipase C delta 1 regulates cell proliferation and cell-cycle progression from G1- to S-phase by control of cyclin E-CDK2 activity. *Biochem J* 415(3), 439-448 (2008).

146. Szatkowski C, Parys JB, Ouadid-Ahidouch H, Matifat F. Inositol 1,4,5-trisphosphate-induced Ca2+ signalling is involved in estradiol-induced breast cancer epithelial cell growth. *Mol Cancer* 9 156 (2010).

147. Sun Y, Tian H, Wang L. Effects of PTEN on the proliferation and apoptosis of colorectal cancer cells via the phosphoinositol-3-kinase/Akt pathway. *Oncol Rep* 33(4), 1828-1836 (2015).

148. Williams JA, Hou Y, Ni HM, Ding WX. Role of intracellular calcium in proteasome inhibitor-induced endoplasmic reticulum stress, autophagy, and cell death. *Pharm Res* 30(9), 2279-2289 (2013).

149. Uvarov AV, Mesaeli N. Enhanced ubiquitin-proteasome activity in calreticulin deficient cells: a compensatory mechanism for cell survival. *Biochim Biophys Acta* 1783(6), 1237-1247 (2008).

150. Walborg EF, Tsuchida S, Weeden DS *et al*. Identification of Dipeptidyl Peptidase-Iv as a Protein Shared by the Plasma-Membrane of Hepatocytes and Liver Biomatrix. *Exp Cell Res* 158(2), 509-518 (1985).

151. Cordero OJ, Salgado FJ, Nogueira M. On the origin of serum CD26 and its altered concentration in cancer patients. *Cancer Immunol Immun* 58(11), 1725-1749 (2009).

152. Yu DM, Slaitini L, Gysbers V *et al*. Soluble CD26 / dipeptidyl peptidase IV enhances human lymphocyte proliferation in vitro independent of dipeptidyl peptidase enzyme activity and adenosine deaminase binding. *Scand J Immunol* 73(2), 102-111 (2011).

153. Ohnuma K, Hosono O, Dang NH, Morimoto C. Dipeptidyl Peptidase in Autoimmune Pathophysiology. *Adv Clin Chem* 53 51-84 (2011).

154. Nauck MA, Vardarli I, Deacon CF, Holst JJ, Meier JJ. Secretion of glucagon-like peptide-1 (GLP-1) in type 2 diabetes: what is up, what is down? *Diabetologia* 54(1), 10-18 (2011).

155. Roy A, Kucukural A, Zhang Y. I-TASSER: a unified platform for automated protein structure and function prediction. *Nat Protoc* 5(4), 725-738 (2010).

156. Roy A, Yang J, Zhang Y. COFACTOR: an accurate comparative algorithm for structure-based protein function annotation. *Nucleic Acids Res* 40(Web Server issue), W471-477 (2012).

157. Zhang Y. I-TASSER server for protein 3D structure prediction. *BMC Bioinformatics* 9 40 (2008).

158. Whisstock JC, Lesk AM. Prediction of protein function from protein sequence and structure. *Q Rev Biophys* 36(3), 307-340 (2003).

159. Lee D, Redfern O, Orengo C. Predicting protein function from sequence and structure. *Nat Rev Mol Cell Biol* 8(12), 995-1005 (2007).

160. Kim SH, Shin DH, Choi IG, Schulze-Gahmen U, Chen S, Kim R. Structure-based functional inference in structural genomics. *J Struct Funct Genomics* 4(2-3), 129-135 (2003).

161. Holm L, Sander C. Mapping the protein universe. *Science* 273(5275), 595-603 (1996).

162. Chandra NR, Prabu MM, Suguna K, Vijayan M. Structural similarity and functional diversity in proteins containing the legume lectin fold. *Protein Eng* 14(11), 857-866 (2001).

163. Herlihy SE, Pilling D, Maharjan AS, Gomer RH. Dipeptidyl peptidase IV is a human and murine neutrophil chemorepellent. *J Immunol* 190(12), 6468-6477 (2013).

164. Misumi Y, Hayashi Y, Arakawa F, Ikehara Y. Molecular-Cloning and Sequence-Analysis of Human Dipeptidyl Peptidase-Iv, a Serine Proteinase on the Cell-Surface. *Biochimica Et Biophysica Acta* 1131(3), 333-336 (1992).

165. Thoma R, Loffler B, Stihle M, Huber W, Ruf A, Hennig M. Structural basis of proline-specific exopeptidase activity as observed in human dipeptidyl peptidase-IV. *Structure* 11(8), 947-959 (2003).

166. Proost P, Menten P, Struyf S, Schutyser E, De Meester I, Van Damme J. Cleavage by CD26/dipeptidyl peptidase IV converts the chemokine LD78beta into a most efficient monocyte attractant and CCR1 agonist. *Blood* 96(5), 1674-1680 (2000).

167. Matteucci E, Giampietro O. Dipeptidyl peptidase-4 (CD26): knowing the function before inhibiting the enzyme. *Curr Med Chem* 16(23), 2943-2951 (2009).

168. Brock DA, Gomer RH. A cell-counting factor regulating structure size in Dictyostelium. *Gene Dev* 13(15), 1960-1969 (1999).

169. Crawford JR, Pilling D, Gomer RH. FcgammaRI mediates serum amyloid P inhibition of fibrocyte differentiation. *Journal of leukocyte biology* 92(4), 699-711 (2012).

170. Brock DA, Hatton RD, Giurgiutiu D-V, Scott B, Ammann R, Gomer RH. The different components of a multisubunit cell number-counting factor have both unique and overlapping functions. *Development* 129(15), 3657-3668 (2002).

171. Cox N, Pilling D, Gomer RH. DC-SIGN activation mediates the differential effects of SAP and CRP on the innate immune system and inhibits fibrosis in mice. *Proceedings of the National Academy of Sciences of the United States of America* 112(27), 8385-8390 (2015).

172. Fan H, Meng W, Kilian C, Grams S, Reutter W. Domain‐Specific N‐Glycosylation of the Membrane Glycoprotein Dipeptidylpeptidase IV (CD26) Influences its Subcellular Trafficking, Biological Stability, Enzyme Activity and Protein Folding. *European Journal of Biochemistry* 246(1), 243-251 (1997).

173. Casset F, Hamelryck T, Loris R *et al*. Nmr, Molecular Modeling, and Crystallographic Studies of Lentil Lectin-Sucrose Interaction. *Journal of Biological Chemistry* 270(43), 25619-25628 (1995).

174. Benz I, Schmidt MA. Glycosylation with heptose residues mediated by the aah gene product is essential for adherence of the AIDA‐I adhesin. *Molecular microbiology* 40(6), 1403-1413 (2001).

175. Lindenthal C, Elsinghorst EA. Identification of a glycoprotein produced by enterotoxigenic Escherichia coli. *Infect Immun* 67(8), 4084-4091 (1999).

176. Sherlock O, Dobrindt U, Jensen JB, Munk Vejborg R, Klemm P. Glycosylation of the self-recognizing Escherichia coli Ag43 autotransporter protein. *Journal of bacteriology* 188(5), 1798-1807 (2006).

177. North MJ, Franek KJ, Cotter DA. Differential Secretion of Dictyostelium-Discoideum Proteinases. *J Gen Microbiol* 136 827-833 (1990).

178. North MJ, Scott KI, Lockwood BC. Multiple Cysteine Proteinase Forms during the Life-Cycle of Dictyostelium-Discoideum Revealed by Electrophoretic Analysis. *Biochemical Journal* 254(1), 261-268 (1988).

179. Aertgeerts K, Ye S, Shi L *et al*. N-linked glycosylation of dipeptidyl peptidase IV (CD26): effects on enzyme activity, homodimer formation, and adenosine deaminase binding. *Protein science : a publication of the Protein Society* 13(1), 145-154 (2004).

180. Arya R, Bhattacharya A, Saini KS. Dictyostelium discoideum-a promising expression system for the production of eukaryotic proteins. *Faseb J* 22(12), 4055-4066 (2008).

181. Brazill DT, Caprette DR, Myler HA *et al*. A protein containing a serine-rich domain with vesicle fusing properties mediates cell cycle-dependent cytosolic pH regulation. *J Biol Chem* 275(25), 19231-19240 (2000).

182. Maruyama T, Kanaji T, Nakade S, Kanno T, Mikoshiba K. 2APB, 2-aminoethoxydiphenyl borate, a membrane-penetrable modulator of Ins(1,4,5)P3-induced Ca2+ release. *J Biochem* 122(3), 498-505 (1997).

183. Ma HT, Patterson RL, Van Rossum DB, Birnbaumer L, Mikoshiba K, Gill DL. Requirement of the inositol trisphosphate receptor for activation of store-operated Ca2+ channels. *Science* 287(5458), 1647-1651 (2000).

184. Yoshioka K, Takahashi H, Homma T *et al*. A novel fluorescent derivative of glucose applicable to the assessment of glucose uptake activity of Escherichia coli. *Biochim Biophys Acta* 1289(1), 5-9 (1996).

185. Zou C, Wang Y, Shen Z. 2-NBDG as a fluorescent indicator for direct glucose uptake measurement. *J Biochem Biophys Methods* 64(3), 207-215 (2005).

APPENDIX A

FUNCTIONAL SIMILARITIES BETWEEN THE *DICTYOSTELIUM* PROTEIN APRA AND THE HUMAN PROTEIN DIPEPTIDYL-PEPTIDASE IV[*]

Autocrine proliferation repressor protein A (AprA) is a protein secreted by *Dictyostelium discoideum* cells. Although there is very little sequence similarity between AprA and any human protein, AprA has a predicted structural similarity to the human protein Dipeptidyl Peptidase IV (DPPIV). AprA is a chemorepellent for *Dictyostelium* cells, and DPPIV is a chemorepellent for neutrophils. This led us to investigate if AprA and DPPIV have additional functional similarities. We find that like AprA, DPPIV is a chemorepellent for, and inhibits the proliferation of, *D. discoideum* cells, and that AprA binds some DPPIV binding partners such as fibronectin. Conversely, rAprA has DPPIV-like protease activity. These results indicate a functional similarity between two eukaryotic chemorepellent proteins with very little sequence similarity, and emphasize the usefulness of using a predicted protein structure to search a protein structure database, in addition to searching for proteins with similar sequences.

Introduction

AprA is a secreted *Dictyostelium discoideum* protein that inhibits the proliferation of *D. discoideum* cells [8, 17]. AprA functions in conjunction with another

[*] Reprinted with permission. Herlihy, S. E., Tang, Y., Phillips, J. E., & Gomer, R. H. (2017). Functional similarities between the dictyostelium protein AprA and the human protein dipeptidyl-peptidase IV. Protein Science, 26(3), 578-585. Copyright © 2016, The Protein Society.

secreted protein called CfaD, which also inhibits the proliferation of *D. discoideum* cells [18]. Loss of the AprA or CfaD proteins results in cells that proliferate faster and reach a higher density than wild type cells [8, 18]. The addition of recombinant AprA (rAprA) or CfaD (rCfaD) to wild type cells causes a significant reduction in proliferation [18, 19]. In addition to its ability to inhibit *D. discoideum* cell proliferation, AprA causes chemorepulsion of *D. discoideum* cells [17]. Cells at the edge of wild type colonies move away from the dense colony center while cells at the edge of an *aprA*$^{-}$ colony form a tight edge with little movement outward [20]. Both wild type and *aprA*$^{-}$ cells move away from a source of rAprA [17].

DPPIV is a human glycoprotein that can be found in both a transmembrane as well as an extracellular soluble form [150]. The membrane form is on some lymphocytes and epithelial cells and has a number of binding partners including adenosine deaminase, fibronectin, and collagen [151-153]. The soluble form is found in most bodily fluids [151, 153]. Both the membrane and soluble forms have serine protease activity, and cleave proteins or peptides with a proline or alanine at the second position of the N-terminus [150]. One of the major functions of DPPIV is the cleavage of glucagon-like peptide-1 (GLP-1), which normally increases the secretion of insulin to promote glucose uptake [154]. DPPIV cleavage of GLP-1 inhibits this process, and inhibitors of DPPIV are used as treatment for type 2 diabetes [154].

Protein structure prediction can reveal protein function that was not obvious from sequence analysis. Structure prediction can be extremely accurate [155-160]. Structure based classification can help identify related proteins that have low sequence similarities [161, 162]. For instance, lectins, which bind carbohydrates, contain a characteristic structural fold [162]. Although the fold is present in many different protein families with proteins that bind carbohydrates, there is little sequence similarity within the fold [162]. These studies are evidence that structural and functional properties may be comparable even when sequence similarities are lacking.

The AprA protein has no significant amino acid sequence similarity to human proteins. We previously found that the predicted structure of AprA has similarity to the crystal structure of DPPIV [163]. AprA causes chemorepulsion of *D. discoideum* cells, and we observed that DPPIV causes chemorepulsion of human and mouse neutrophils [17, 163].

DPPIV is a serine peptidase, with a characteristic serine protease catalytic triad in the crystal structure [164, 165], and DPPIV cleaves peptides or proteins with a proline or alanine in the second position at the N-terminus [166, 167]. The predicted structure of AprA has a similar serine peptidase catalytic triad (Figure 22) [163]. Previous lab members found that conditioned media collected from log-phase wild type or *aprA*$^{-}$ cells were assayed for DPPIV activity. Wild type conditioned media had significantly more DPPIV-like protease activity, with a K_m of 720 ± 150 μM and a V_{max} of 20 ± 1 μM/hour

(mean ± SEM, n=3), than conditioned media from *aprA*$^{-}$ cells (Figure 2A). The subtracted curve (the *aprA*$^{-}$ values subtracted from the WT values) had a K_m of 590 ± 480 μM and a V_{max} of 10 ± 2 μM/hour (n=3). This suggests that AprA may have DPPIV-like activity, or that AprA may regulate something that has DPPIV-like peptidase activity.

In this report, we examine whether other functional similarities exist between AprA and DPPIV, and show that AprA has a DPPIV-like peptidase activity, and that DPPIV can both inhibit the proliferation and induce chemorepulsion of *D. discoideum* cells. Together, this indicates conserved properties of two eukaryotic chemorepulsion signals with very different amino acid sequences albeit with possibly similar structures.

Materials and Methods

Cell culture

Cells were cultured following Brock et al. [168] in HL5 medium (Formedium Ltd, Norwich, England) using wild-type Ax2 cells, *aprA*$^{-}$ strain DB60T3-8 [8] and *cfaD*$^{-}$ strain DB27C-1 [18]. Proliferation inhibition and chemorepulsion assays were done as previously described [22].

Recombinant DPPIV and AprA

Recombinant DPPIV was purchased from Enzo Life Sciences (Farmingdale, NY). Recombinant AprA was expressed in, and purified from, *E.coli* as previously described [18]. To express recombinant AprA in HEK 293 cells, the DNA encoding the secretion

signal sequence of human Serum Amyloid P (SAP) was amplified by PCR using hSAP-pcDNA3.1^{-} [169] as a template and the primers 5' ATAGGCGCGCCATGAACAAGCCGCTGC-3' and 5' ATTAAGCTTAGCAAAGGCTTCCAGG-3'. This was digested with Asc I and Hind III and ligated into the corresponding sites of pCMV-AC-His (Origene, Rockville, MD) to generate pCMV6-SAPSec-His. PCR was then done using a vegetative Ax2 cDNA library and the primers 5'-CCCAAGCTTACTCCATTGGATGATTATGTC-3' and 5'-CCGCTCGAGTAAAGTTGCAGTTGAACTAGCACTATCACC-3' to generate DNA containing the AprA coding region without the AprA secretion signal. After digestion with Hind III and Xho I, the PCR product was ligated into the corresponding sites of pCMV6-SAPSec-His to generate pCMV6-SAP-AprA-His. After sequencing to verify the integrity of the insert, the recombinant plasmid was transfected into HEK 293 cells, and recombinant AprA was purified as previously described [170, 171].

Western blots and AprA binding

Proteins were electrophoresed on 4 – 20% Tris-Glycine gels (Lonza, Rockland, ME) following the manufacturer's instructions. For Western blots, biotinylated *Lens culinaris* agglutinin (Vector Laboratories, Burlingame, CA) was used following the manufacturer's directions. For rAprA binding, 10% fetal calf serum (VWR, Houston, TX) or 100 µg/ml of bovine collagen I (Santa Cruz Biotechnology, Dallas, TX), human collagen IV (Sigma-Aldrich, St. Louis, MO) or human plasma fibronectin (Corning, Corning, NY) in PBS buffer were added to wells of a 96-well tissue culture plate (Corning)

and incubated overnight at 4°C. Wells were washed with PBST (3.2 mM Na_2HPO_4, 0.5 mM KH_2PO_4, 1.3 mM KCl, 135 mM NaCl, 0.05% Tween 20, pH 7.4) three times and blocked with 4% BSA in PBM (20 mM KH_2PO_4, 10 µM $CaCl_2$, 1 mM $MgCl_2$, pH 6.1 with KOH) for 1 hour. Wells were incubated with 10 µg/ml rAprA (+ wells) or 4% BSA (- wells) in PBST for 1 hour. Wells were washed with PBST six times and then incubated with 1.14 µg/ml affinity-purified rabbit anti-AprA antibodies [8] for 1 hour, then washed six times with PBST and incubated with 1:5000 HRP-conjugated donkey anti-rabbit antibody (Biolegend, San Diego, CA) in PBST for 30 minutes. Bound antibody was then reacted with 100 µl TMB (Biolegend, San Diego, CA). The reaction was stopped by adding 100 µl of 1 N HCl, and reaction products were detected with a SynergyMx plate reader (Biotek, Winooski, VT) at 450 nm. Subtracted values ('+' – '-') were calculated.

DPPIV activity assay

For enzymatic activity assays, conditioned media from log phase *D. discoideum* cells were clarified by centrifugation at 3000 x g for 4 minutes. DPPIV-like enzymatic activity of conditioned media, buffer (20 mM sodium phosphate, pH 7.4) or rAprA in buffer were measured using pNA substrate (H-Gly-Pro-pNA·p-tosylate) (Enzo Life Sciences, Farmingdale, NY) for 1 hour at room temperature and the reaction product was detected at 410 nm with an Ultrospec 2100 pro spectrophotometer (for conditioned media) (Amersham Biosciences, Piscataway, NJ) or a SynergyMx plate reader (for recombinant AprA).

Statistics

Statistical analysis was performed using GraphPad Prism 4 software (GraphPad, San Diego, CA). Statistical significance between two groups was determined by t tests or Mann-Whitney tests, or between multiple groups using 1-way ANOVA with Dunnett's test. Significance was defined as $p < 0.05$.

Results

Like DPPIV, rAprA has protease activit

To directly test whether AprA has DPPIV-like activity, I examined the DPPIV-like protease activity of recombinant AprA. As glycosylation of DPPIV is required for its peptidase activity [172], I expressed AprA in, and purified recombinant AprA from, HEK 293 cells (293-rAprA) and *E. coli* (bac-rAprA; this is the form of rAprA that we previously observed to both inhibit proliferation and induce chemorepulsion of *Dictyostelium* cells [8, 17]). After electrophoresis on SDS-PAGE gels, 293-rAprA showed a larger apparent molecular mass than bac-rAprA (Figure 23B, top). Western blots stained with *Lens culinaris* agglutinin, which detects sequences containing α-linked mannose or α-linked D-glucose residues [173], indicated that 293-rAprA and DPPIV are glycosylated, while bac-rAprA showed much less glycosylation (Figure 23B middle and bottom). The smeared bac-rAprA band in the middle panel is two bands, which was revealed by a high contrast view (Figure 23B bottom). Since there are some glycosylated proteins in *E. coli* [174-176], this may be due either to some glycosylation of the bac-rAprA, or non-specific staining by the lectin. The apparently lower level of lectin

staining of rDPPIV compared to 293-rAprA may be due to differences in glycosylation content or composition.

Both 293-rAprA and bac-rAprA had DPPIV-like peptidase activity (Figure 23C). The 293-AprA showed a K_m of 100 ± 65 μM and a V_{max} of 9 ± 1 μM/(hour*μg) (n=3), while bac-rAprA, showed a K_m of 220 ± 120 μM and a V_{max} of 4 ± 1 μM/(hour*μg) (n=7). Although the K_m's were not significantly different (and were not significantly different from the 'WT-*aprA*$^-$' activity described above), the bac-rAprA V_{max} was significantly lower than that of 293-rAprA ($p < 0.05$, t-test). Together, these data suggest that AprA has DPPIV-like enzymatic activity, and that glycosylation of AprA potentiates this activity.

Like DPPIV, rAprA can bind fibronectin

DPPIV binds to fibronectin and collagen [151, 153]. To determine if AprA also has a similar binding activity, fibronectin, collagen, or 10% serum were coated on plates and the ability of rAprA to bind them was assessed. Previous lab member found that bac-rAprA was able to bind plasma fibronectin (Figure 24A). The bac-rAprA also appeared to weakly bind collagen. Although the anti-AprA antibodies used in this assay recognize both bac-rAprA and 293-rAprA on Western blots (data not shown), in parallel assays, I found that 293-rAprA showed no significant binding to fibronectin or collagen (Figure 24B). These data suggest that rAprA has some DPPIV-like binding activity, and that AprA glycosylation is not required for this binding.

rAprA is unable to chemorepulse human neutrophils

DPPIV causes chemorepulsion of human neutrophils [163]. To determine if AprA also causes chemorepulsion of human neutrophils, bac-rAprA or 293-rAprA were assayed for their ability to cause chemorepulsion. Neither bac-rAprA nor 293-rAprA could cause biased movement of human neutrophils (Figure 25A). Neutrophils are the only cell type that we observed DPPIV to have a chemorepellent effect on [163], and since neutrophils do not proliferate in culture, we were unable to determine if AprA affects neutrophil proliferation. 293-rAprA could not induce chemorepulsion of *D. discoideum* cells (Figure 25B), suggesting that glycosylation is not involved in the chemorepulsion activity of AprA.

Like AprA, DPPIV can inhibit the proliferation of D. discoideum cells

Bac-rAprA inhibits the proliferation of *D. discoideum* cells [19]. To determine if recombinant DPPIV (rDPPIV) affects the proliferation of *D. discoideum* cells, my colleague did the proliferation assay for D. discoideum cells with rDPPIV. Like bac-rAprA and rCfaD, 300 ng/ml rDPPIV inhibited the proliferation of *D. discoideum* cells (Figure 26A), and this inhibition was observed at rDPPIV concentrations ranging from 1 to 1000 ng/ml ((Figure 26B). My colleague found that rDPPIV was also able to inhibit the proliferation of cells lacking AprA or CfaD ((Figure 26C). However, I was unable to detect any significant ability of 293-rAprA to inhibit (or increase) *D. discoideum* proliferation. Together, these data indicate that for unknown reasons, 293-rAprA is unable to affect *D.*

discoideum proliferation, that rDPPIV can inhibit *D. discoideum* proliferation, and that this inhibition by rDPPIV does not require AprA or CfaD.

Like AprA, rDPPIV can induce chemorepulsion of D. discoideum cells

In addition to its ability to inhibit proliferation, AprA causes chemorepulsion of *Dictyostelium* cells [17]. Like bac-rAprA, my colleague found that rDPPIV also induced chemorepulsion of *D. discoideum* cells (Figure 27). These data indicate further functional similarities between AprA and DPPIV.

Discussion

The *Dictyostelium discoideum* protein AprA and the human protein DPPIV are predicted to share structural similarity, but lack any significant sequence similarity. Here we show that AprA and DPPIV also have functional similarity. AprA appears to be responsible for some but not all of the DPPIV-like enzymatic activity in *D. discoideum* conditioned media. The residual activity in *aprA*$^{-}$ CM may be due to nonspecific proteases, since a variety of proteases are secreted by *D. discoideum* cells [177, 178]. Both bac-rAprA and 293-rAprA have DPPIV-like enzymatic activity, although the 293-rAprA V_{max} was higher than that of bac-rAprA, indicating that glycosylation potentiates the enzymatic activity of rAprA. This is partially consistent with observations that glycosylation of DPPIV is required for its enzymatic activity [172]. Recombinant DPPIV has a K_m of 170 μM and a V_{max} of 8 μM/(hr*μg), using the same substrate we used [179], indicating that the K_m and V_{max} of 293-rAprA and DPPIV are quite similar. In addition to

having a DPPIV-like protease activity, like DPPIV bac-rAprA binds fibronectin and weakly to collagen. Conversely, like AprA, DPPIV both inhibits *D. discoideum* cell proliferation and induces chemorepulsion of *D. discoideum* cells. Together, these observations indicate that AprA has some functional properties similar to those of DPPIV, and *vice versa*.

Despite having DPPIV-like protease activity, neither bac-rAprA nor 293-rAprA could cause chemorepulsion of human neutrophils. We previously observed that DPPIV protease inhibitors can block the chemorepellent activity of DPPIV on neutrophils [163]. Together, these observations suggest that either the neutrophil chemorepellent domain site of DPPIV is near its protease active site, but is not part of it, that the chemorepellent active site is not near the protease active site, and is disturbed by the protease inhibitor as an allosteric alteration, or that there is a difference in the recognition sites of the AprA and DPPIV proteases that is not revealed by the H-Gly-Pro-pNA p-tosylate substrate. Alternatively, DPPIV protease activity could be necessary, but not sufficient, for neutrophil chemorepulsion, with additional protein functions required that are not conserved with AprA.

Bac-rAprA inhibits the proliferation of, and induces chemorepulsion of, *D. discoideum*. Despite having a higher V_{max} than bac-rAprA, the 293-rAprA was unable to do either of these things to *D. discoideum*. These observations indicate that the effects of AprA on *D. discoideum* cells does not involve its DPPIV-like enzymatic activity, or that

as with AprA and DPPIV, there is a difference in the recognition sites of the bac-rAprA and 293-rAprA proteases that is caused by the difference in glycosylation, and that this difference is not revealed by the H-Gly-Pro-pNA p-tosylate substrate. Alternatively, the glycosylation of 293-rAprA may prevent binding of 293-rAprA to other proteins, 293-rAprA-induced chemorepulsion, and inhibition of proliferation. *D. discoideum* produces both *N*- and *O*-linked glycosylations [180]. As such, we expected that a glycosylated rAprA (293-rAprA) may function more like DPPIV since DPPIV activity is thought to be dependent on its glycosylation [172].

Throughout its developmental life cycle, *D. discoideum* is dependent on cell-cell adhesion proteins for fruiting body formation and cell fate determination [77]. Indeed, *D. discoideum* contains proteins with EGF/Laminin repeat domains and domains for cell adhesion/recognition, such as fibronectin and growth factor receptor domains [77]. An additional difference between the two forms of rAprA is their ability to bind fibronectin. The 293-rAprA, which has higher enzymatic activity, shows no detectable binding. This indicates that the binding of AprA to fibronectin is not dependent on its enzymatic activity. Taken together, our results indicate that AprA and DPPIV have remarkable similarities in their functional properties despite having little sequence similarity, and suggest that the similarities in functional activities do not depend on their similar protease activities. This then suggests the possibility that there is some domain of DPPIV that resembles the receptor-binding site of AprA, and that there may be

additional protein regions present on DPPIV but not on AprA that are required to activate the DPPIV receptor.

Figures

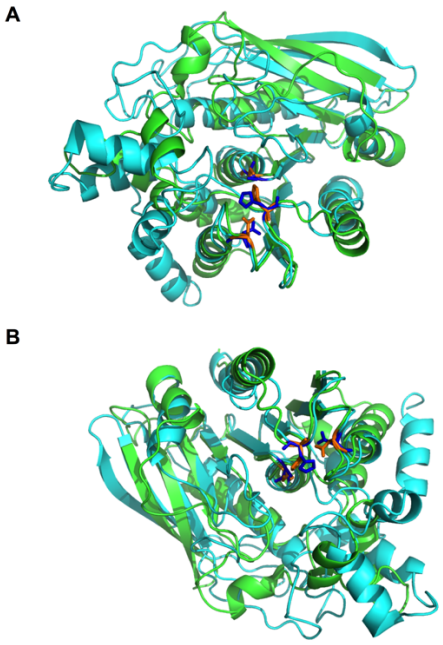

Figure 22. AprA and DPPIV have similar structures.
A and B) The predicted structure of AprA, shown in cyan, is superimposed with the α/β hydrolase domain of DPPIV (Protein Data Bank ID 1J2E), shown in green. The catalytic triad of DPPIV (Asp708, His740, and Ser630) is orange while the predicted catalytic triad of AprA (Asp288, His319, and Ser195) is blue. The predicted structure of AprA did not overlap with the β-propeller domain of DPPIV. Therefore, the β-propeller domain was removed for simplicity of the image.

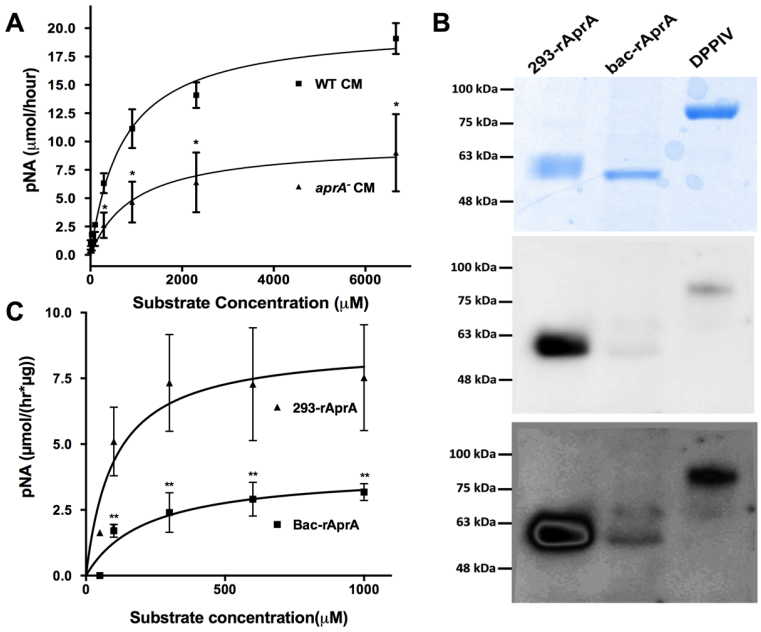

Figure 23. AprA has DPPIV-like enzymatic activity.
A) Wild-type or *aprA*¯ conditioned media were incubated with various concentrations of H-Gly-Pro-pNA p-tosylate and the formation of the pNA digestion product was measured. B) 293-rAprA, Bac-rAprA, and rDPPIV were electrophoresed on SDS-polyacrylamide gels. The upper panel shows Coomassie blue staining of a gel; the middle and lower panel shows a corresponding Western blot stained with biotinylated *Lens culinaris* agglutinin. C) 293-rAprA and Bac-RAprA were incubated with various concentrations of H-Gly-Pro-pNA p-tosylate as in panel A. Values in A and C are mean ± SEM, n=3 (n=7 for Bac-rAprA in B). * indicates $p < 0.05$, ** $p < 0.01$ (t test).

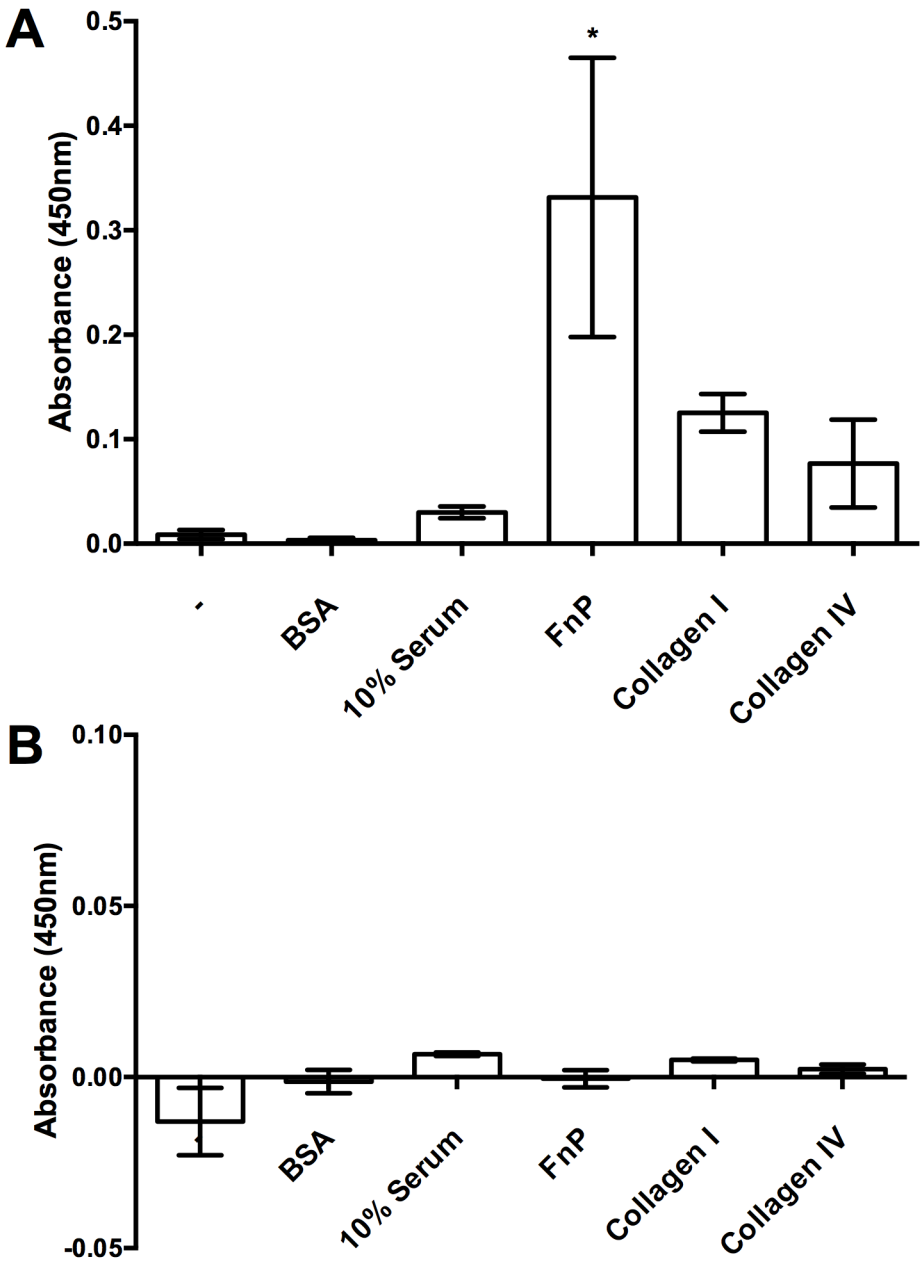

Figure 24. rAprA binds some of the binding partners of DPPIV.
Plates were coated with nothing (-), bovine serum albumin (BSA), serum, plasma fibronectin (FnP), collagen I, or collagen IV. After incubation with A) Bac-rAprA or B) 293-rAprA, and then washing, affinity-purified anti-AprA antibodies were used to detect bound rAprA. Values are mean ± SEM, n=3. * indicates $p < 0.05$ compared to the (-) control (one-way ANOVA, Dunnett's test).

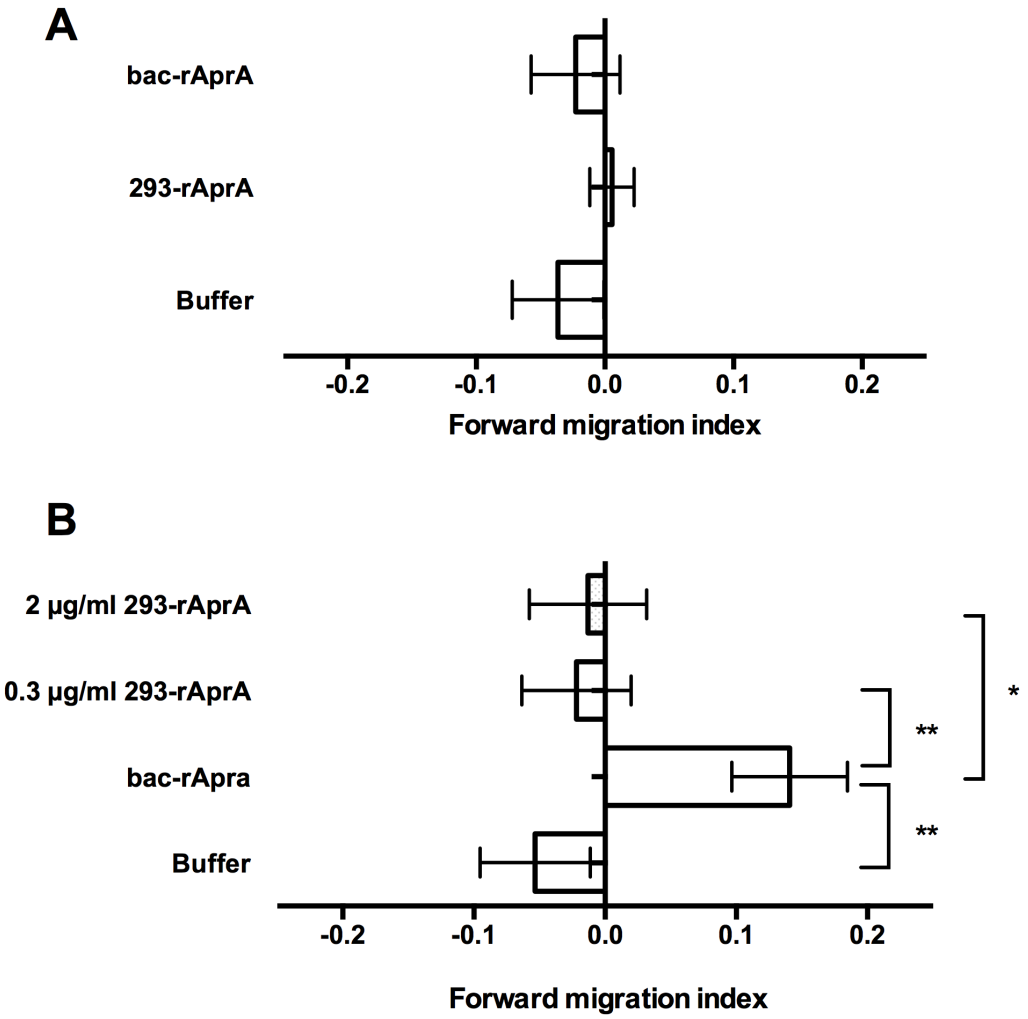

Figure 25. AprA does not induce chemorepulsion of neutrophils.
A) 1.6 µg/ml of rAprA was added to one side of an Insall chamber, and the movement of neutrophils towards or away from the AprA was measured. B) 0.3 µg/ml of bac-rAprA or the indicated concentration of 293-rAprA was added to one side of an Insall chamber, and the movement of *D. discoideum* cells was measured. Positive values indicate that cells move away from rAprA. Values are mean ± SEM, n=3. * indicates $p < 0.05$, ** $p < 0.01$ (t test).

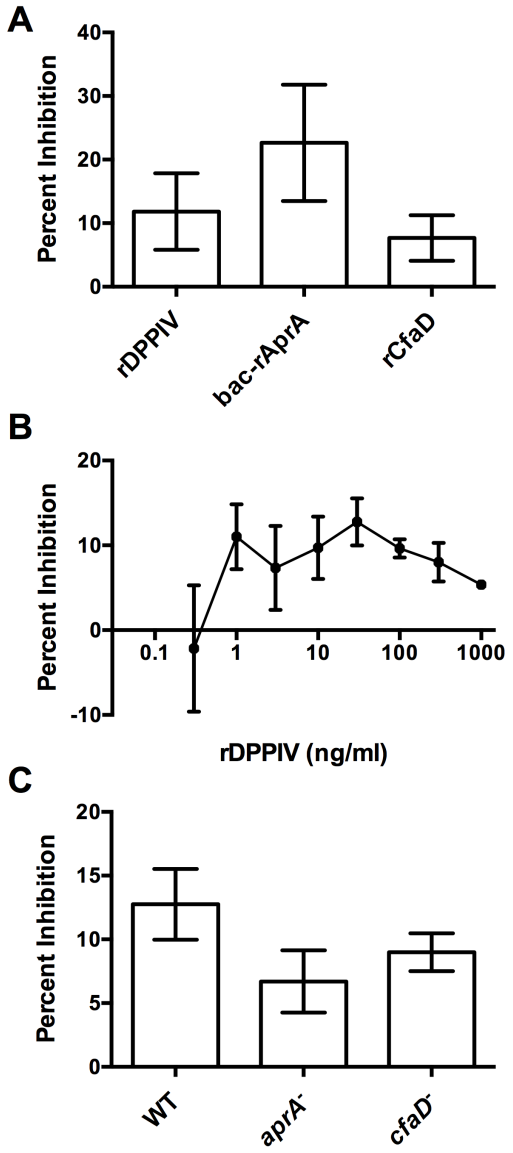

Figure 26. rDPPIV inhibits the proliferation of *D. discoideum* cells.
Buffer, rDPPIV, rAprA, or rCfaD were added to wild-type *D. discoideum* cells and the cell density was measured 18 hours later. The inhibition of proliferation was then measured in comparison to the proliferation of the buffer control cells. All 3 proteins significantly inhibited proliferation ($p < 0.05$, t tests). B) The indicated concentrations of rDPPIV were added to *D. discoideum* cells and the proliferation inhibition was assayed as in A. rDPPIV concentrations from 1 to 1000 ng/ ml significantly inhibited proliferation ($p < 0.05$, t tests). C) 300 ng/ml rDPPIV was added to wild-type, *aprA*$^{-}$, and *cfaD*$^{-}$ cells and proliferation inhibition was measures as in A. rDPPIV significantly inhibited the proliferation of all 3 cell lines ($p < 0.05$, t tests). Values are mean ± SEM, n=3.

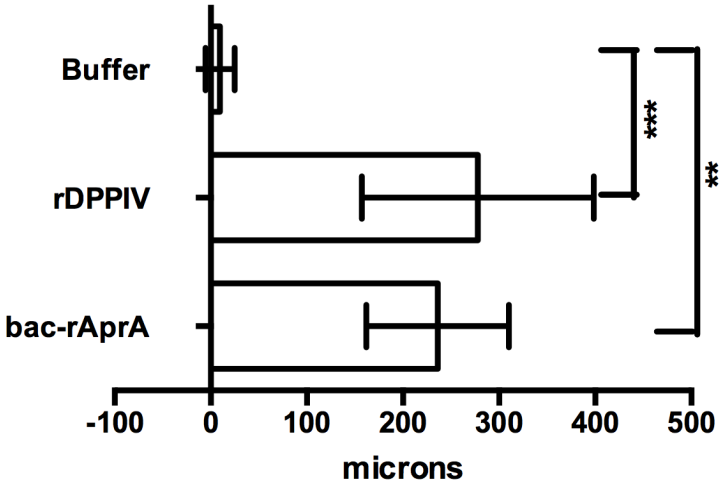

Figure 27. rDPPIV induces chemorepulsion of D. discoideum cells.
2000 ng/ml of rDPPIV or bac-rAprA was added to one side of an Insall chamber. The movement of D. discoideum cells was observed by video-microscopy and displacement on the x-axis was plotted in microns. Positive values indicate that cells moved away from rDPPIV or rAprA. Values are mean ± SEM, n=3. ** indicates $p < 0.01$, *** $p < 0.001$ (t test).

APPENDIX B

EXTRACELLULAR GLUCOSE LEVEL MEDIATES *DICTYOSTELIUM DISCOIDEUM GRLD*$^{-}$ SENSING POLYPHOSPHATE

Our lab found that *Dictyostelium* cells lacking GrlD are insensitive to polyphosphate inhibition of proliferation in 25% HL5, but not in 100% HL5 [39]. The glucose concentration in 25% HL5 (~3.4 g/L) is ¼ of that in 100% HL5 (~13.5 g/L). To test if the glucose concentration mediates cells sensing polyphosphate, *grlD*$^{-}$ cells were tested for proliferation with 0 or 150 μM polyphosphate in HL5 with 3.4 g/L glucose and 13.5 g/L glucose, and 25% HL5 with 3.4 g/L glucose and 13.5 g/L glucose. This proliferation inhibition assay was done following the method in Chapter 4.

I found that *grlD*$^{-}$ cells were insensitive to 150 μM polyphosphate in both 25% and 100% HL5 with 3.4 g/L glucose, and *grlD*$^{-}$ cells showed similar sensitivity to polyphosphate in 25% and 100% HL5 with 13.5 g/L glucose (Figure 28). These data indicate that the glucose concentration of the medium regulates the sensitivity of *grlD*$^{-}$ cells to polyphosphate inhibition of proliferation.

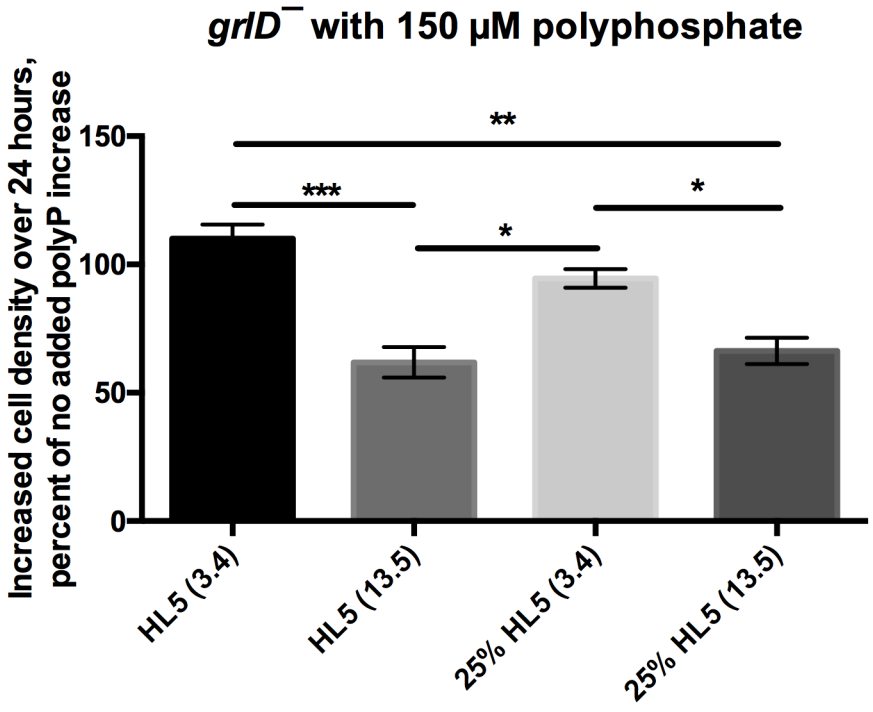

Figure 28. Glucose affect *grlD*$^{-}$ cells' sensitivity to polyphosphate.
grlD^{-} cells were tested for proliferation with 0 or 150 µM polyphosphate for 24 hours. The increase in cell density over 24 hours was normalized to no added polyphosphate for the indicated medium. All values are mean ± SEM, n ≥ 3 independent experiments. * indicates $p < 0.05$, **, $p < 0.01$, ***, $p < 0.001$, compared to no polyphosphate added (t-test).

APPENDIX C

EXTRACELLULAR MG^{2+} ATTENUATES POLYPHOSPHATE EFFECT ON *DICTYOSTELIUM DISCOIDEUM* CELLS

Dictyostelium rtoA^{-} (RtoA, required for proper fusion of endocytic vesicles [181]) cells were tested for proliferation with 0, 125 or 150 μM polyphosphate in 25% HL5 (in PBM) and 100% HL5, following the method of proliferation inhibition assay in Chapter 4. I found that polyphosphate inhibited the proliferation of *rtoA*$^{-}$ cells in 25% HL5, and the inhibition potency was not significantly different from polyphosphate inhibiting Ax2 cells. However, polyphosphate caused a significant cell death of *rtoA*$^{-}$ cells in 100% HL5, not in 25% HL5 (Figure 29). As polyphosphate was reported to be able to bind Mg^{2+} and 25% HL5 diluted in PBM has additional 750 μM Mg^{2+}, I tested if the different effect of polyphosphate on *rtoA*$^{-}$ cells between 25% and 100% HL5 was caused by the different amount of Mg^{2+} in the medium. Ax2 and *rtoA*$^{-}$ cells were incubated with 0, 150 or 300 μM polyphosphate in HL5 or HL5 plus 750 μM $MgCl_2$ for 24 hours. In HL5, 150 or 300 μM polyphosphate strongly inhibited the proliferation of Ax2 cells and caused a significant cell death of *rtoA*$^{-}$ cells. Adding 750 μM $MgCl_2$ to HL5 attenuated the polyphosphate effect on both Ax2 and *rtoA*$^{-}$ cells (Figure 30).

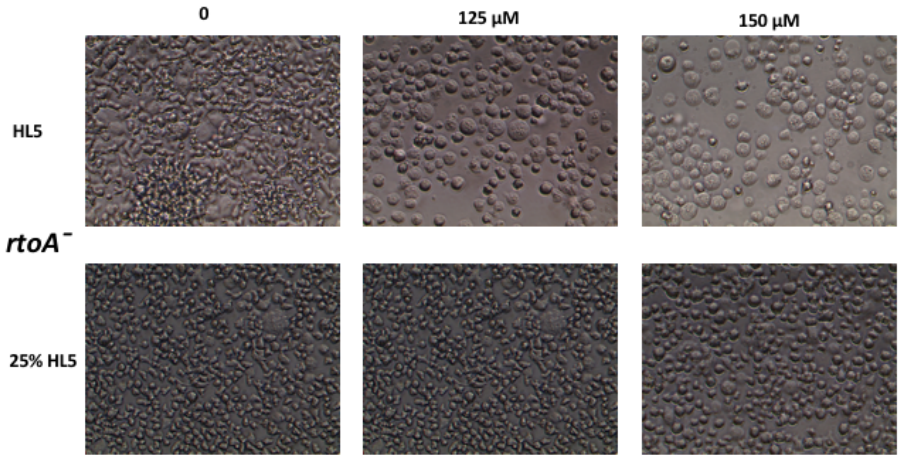

Figure 29. Polyphosphate caused cell death of rtoA⁻ cells in HL5 but not in 25% HL5.
rtoA⁻ cells were cultured with 0, 125 or 150 µM polyphosphate in HL5 or 25% HL5 for 24 hours. Images were taken at 24 hours with a 20x objective.

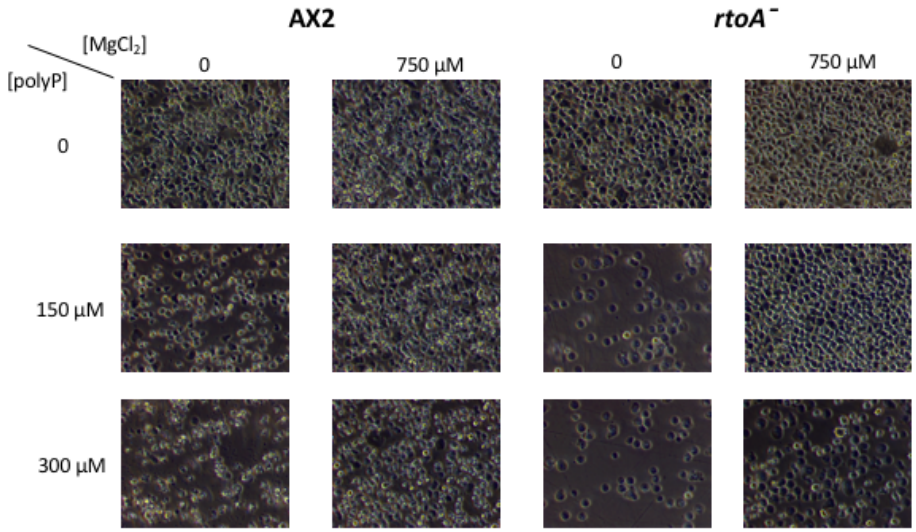

Figure 30. $MgCl_2$ attenuates polyphosphate effect on *Dictyostelium* cells.
Ax2 and rtoA⁻ cells were cultured with 0, 150 or 300 µM polyphosphate in HL5 with 0 or 750 µM $MgCl_2$ for 24 hours. Images were taken at 24 hours with a 20x objective.

APPENDIX D

POLYPHOSPHATE INHIBITS THE PROLIFERATION OF *DICTYOSTELIUM DISCOIDEUM* FEEDING ON HEAT-KILLED *E. COLI*

Polyphosphate inhibits the proliferation of *Dictyostelium discoideum* feeding on heat-killed *E. coli* in PBM

As the nutrient level affect polyphosphate inhibition of proliferation, I tested if polyphosphate could inhibit the proliferation of *Dictyostelium* cells with heat-killed *E. coli* in PBM as a food source. The proliferation inhibition assay was done following the method in Chapter 4. I found that polyphosphate could inhibit the proliferation of Ax2 cells with heat-killed *E. coli* in PBM with a concentration of 225 μM or higher (Figure 31). Compared to cells in HL5 or 25% HL5, cells with heat-killed *E. coli* in PBM were less sensitive to polyphosphate (Figure 31).

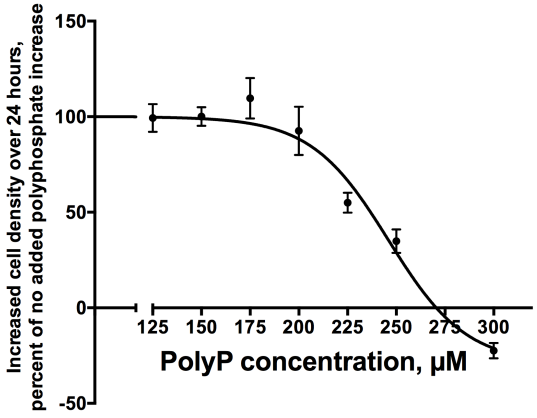

Figure 31. Polyphosphate is able to inhibit the proliferation of Ax2 cells with heat-killed *E. coli* in PBM.
Ax2 cells feeding with heat-killed bacteria were cultured with 0, 125, 150, 175, 200, 225, 250 or 300 μM polyphosphate for 24 hours. The increase in cell density over 24

hours was normalized to no added polyphosphate. All values are mean ± SEM, n ≥ 3 independent experiments.

Polyphosphate inhibits the proliferation of *Dictyostelium discoideum* feeding on heat-killed *e. coli* in KK2 buffer

As PBM contains 10 mM Mg^{2+} and I have found that Mg^{2+} in the medium or buffer would affect the polyphosphate effect on *Dictyostelium* cells, I tested the polyphosphate proliferation inhibition activity on *Dictyostelium* cells in KK2 buffer (17 mM KH_2PO_4 and 3 mM K_2HPO_4 in ultrapure water, pH 6.1). Ax2 cells at 1 x 10^4 cells/ml were cultured with polyphosphate in KK2 buffer for 24 hours, feeding on heat-killed *E. coli*. In this condition, as low as 0.6 μM polyphosphate could inhibit the proliferation of Ax2 cells and 2 μM polyphosphate caused a decreased cell density after 24 hours (Figure 32). Supplementing 10 μM $CaCl_2$ or $MgCl_2$ to KK2 buffer strongly attenuated polyphosphate inhibition of proliferation (Figure 32). I then tested the effect of various salts (10 μM) on polyphosphate effect on *Dictyostelium* cells. Compared to cells in KK2 made with ultrapure water (KK2), cells in KK2 made with tap water or KK2 supplemented with 5 μM $Al_2(SO_4)_3$ or 10 μM $CuSO_4$ showed reduced sensitivity to polyphosphate (Figure 33). This suggest that the complex salts mix in tap water, Al^{3+}, or Cu^{2+} could attenuate the polyphosphate effect. The effect of Na_2SO_4 on polyphosphate needs to be tested to determine if SO_4^{2+} affect polyphosphate activity. Without polyphosphate, cells in KK2 supplemented with 10 μM $BaCl_2$, $CrCl_3$, or $MnCl_2$ proliferated faster than cells in KK2 (Figure 33), indicating that these ions potentiate

Dictyostelium cell proliferation. Cells in KK2 supplemented with 10µM $CoCl_2$, $NiCl_2$ or SrCl died after 24 hours (Figure 33), indicating that 10 µM of these ions are toxic to *Dictyostelium* cells.

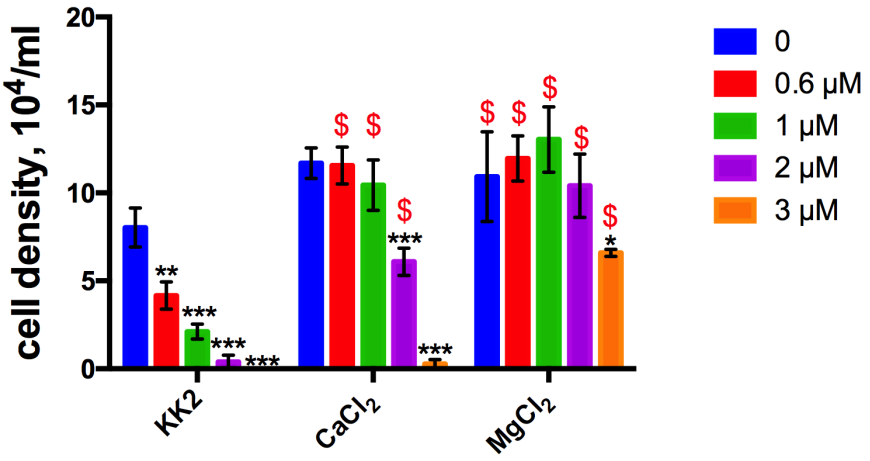

Figure 32. Low concentration of polyphosphate inhibits proliferation of Ax2 cells with heat-killed *E. coli* in KK2 buffer.
Ax2 cells feeding with heat-killed bacteria were cultured with 0, 0.6, 1, 2 or 3 µM polyphosphate for 24 hours in KK2 buffer or KK2 buffer with 10 µM $CaCl_2$ or $MgCl_2$. All values are mean ± SEM, n ≥ 3 independent experiments. * indicates $p < 0.05$, **, $p < 0.01$, ***, $p < 0.001$, compared to no polyphosphate added for each condition (t-test). $, $p < 0.05$, compared to no additional salt added for each polyphosphate concentration (one-way ANOVA, multiple comparisons with Dunnett's test within the panel).

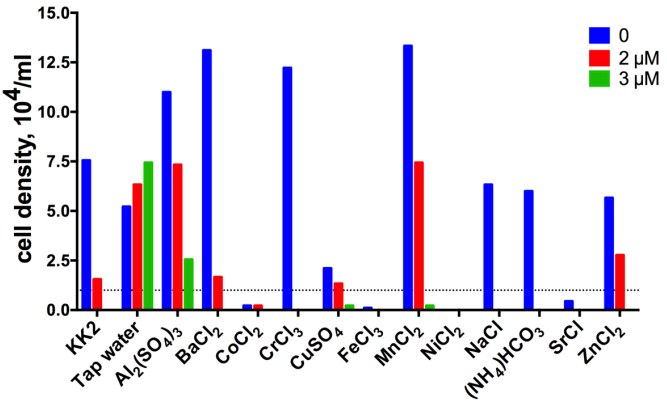

Figure 33. Ions effect on polyphosphate activity.
Ax2 cells feeding with heat-killed bacteria were cultured with 0 2 or 3 µM polyphosphate for 24 hours in KK2 buffer made with ultrapure water (KK2), KK2 buffer made with tap water (tap water) or KK2 supplemented with 10 µM of indicated salt (5 µM of $Al_2(SO_4)_3$). N = 1.

APPENDIX E

AN IP3 RECEPTOR ANTAGONIST DOES NOT AFFECT THE POLYPHOSPHATE INHIBITION OF PROLIFERATION, BUT AFFECTS POLYPHOSPHATE INDUCED AGGREGATION

2-Aminoethyl diphenylborinate (2-APB) is an IP3 receptor antagonist and blocks IP3 activated calcium release [182]. As I found that polyphosphate might inhibit *Dictyostelium* proliferation through IP3 - cytosolic Ca^{2+} pathway, I tested if the IP3 receptor antagonist 2-APB could affect the polyphosphate inhibition of proliferation in *Dictyostelium*.

I did not observe any effect of 2-APB (0 -25 μM) on the proliferation of *D. discoideum* with or without polyphosphate in 25% HL5 (Figure 34). Cells were killed with 30 μM and above concentrations of 2-APB while 75 μM or above concentrations of 2-APB were used to completely block IP3 receptor mediated activity in other organisms [182, 183]. Though the proliferation was not affected with 2-APB, the aggregation of *D. discoideum* cells was modulated with 2-APB (Figure 35). Polyphosphate promotes cell aggregation at low nutrient condition (25% HL5) [36]. Without 2-APB, cells with 125 μM polyphosphate showed aggregation after 24 hours in 25% HL5 (aggregated colonies observed), while cells without polyphosphate remained in a unicellular form (Figure 35). Without additional polyphosphate, cells with 5 μM 2-APB showed slightly increased aggregation, and cells with 10 μM 2-APB showed significantly promoted aggregation,

and cells with higher concentrations of 2-APB (25 µM as a representative) remained unicellular (Figure 35). With 125 µM polyphosphate, cells with 5 µM 2-APB showed less aggregation than no 2-APB added, and with 10 µM or higher concentrations of 2-APB the polyphosphate potentiation of aggregation was blocked (Figure 35).

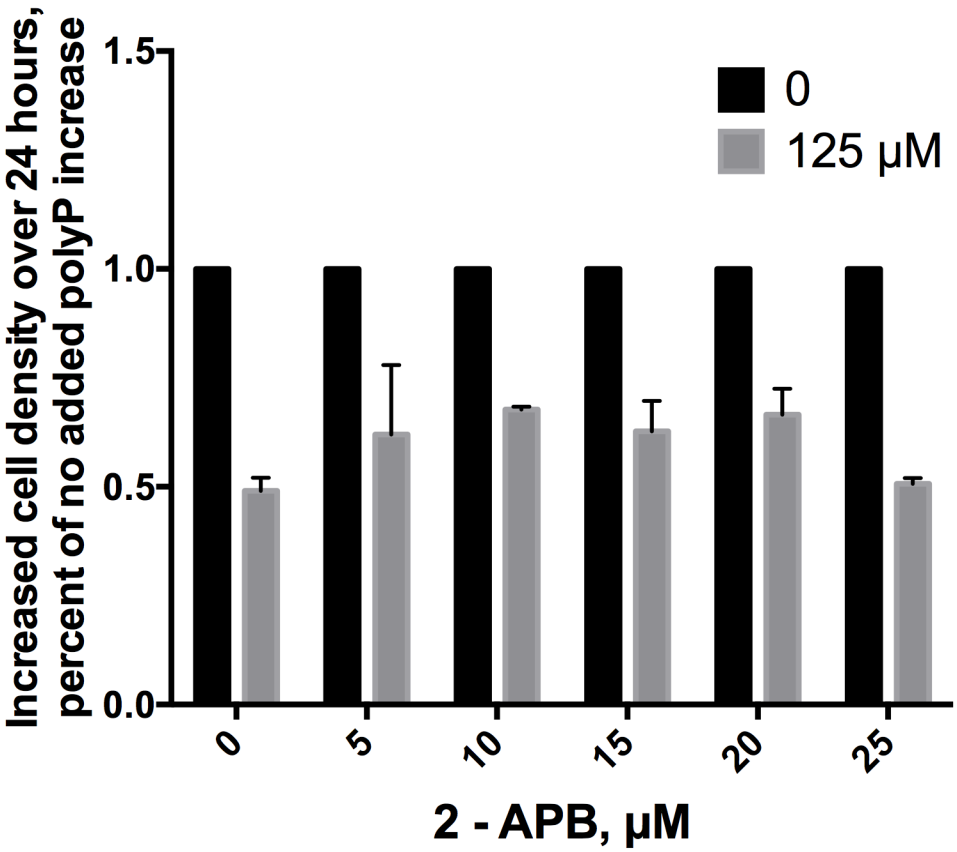

Figure 34. The IP3 receptor antagonist 2-Aminoethyl diphenylborinate does not affect polyphosphate inhibition of proliferation.
Ax2 cells were culture with 0 or 125 µM polyphosphate in 25% HL5 for 24 hours. Indicated amount of 2 – APB was added. The increase in cell density over 24 hours was normalized to no added polyphosphate for the indicated medium. All values are mean ± SEM, n ⩾ 3 independent experiments.

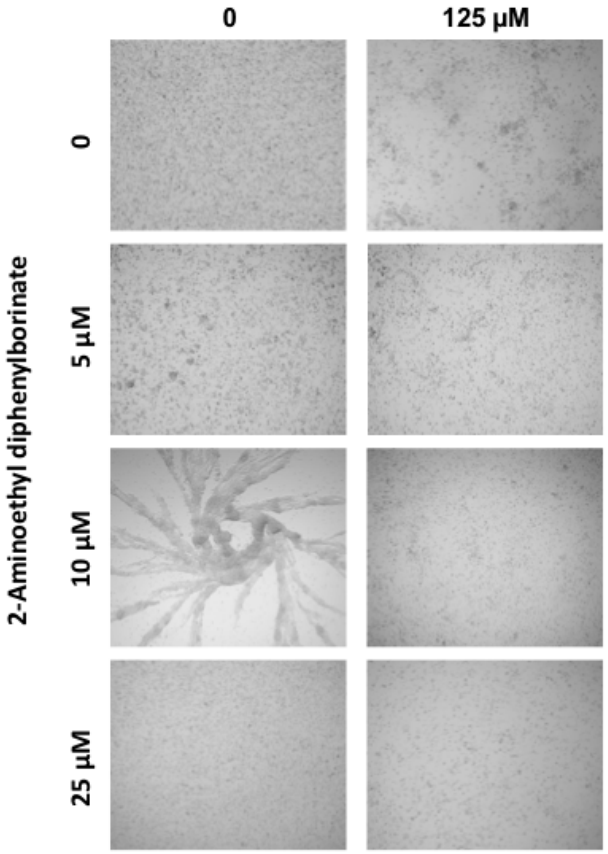

Figure 35. The IP3 receptor antagonist 2-Aminoethyl diphenylborinate affect Dictyostelium cell aggregation.
Ax2 cells starting at 1.5 x 10^6 cells/ml were cultured with 0 or 125 µM polyphosphate in 25% HL5 for 24 hours. Indicated amount of 2 – APB was added. Images were taken at 24 hour with a 4x objective.

APPENDIX F

POLYPHOSPHATE INHIBITS 2-NBDG UPTAKE OF *DICTYOSTELIUM DISCOIDEUM*

Lab colleagues have found that polyphosphate affects *Dictyostelium discoideum* phagocytosis and pinocytosis (data not published). Here I show that polyphosphate inhibits uptake of the fluorescent glucose derivative, 2-NBDG by *Dictyostelium* cells and this requires the IP3 receptor IplA. 2-NBDG is widely used for monitoring glucose uptake into living cells [184, 185]. Ax2 cells incubated with 150 μM polyphosphate for 30, 60, 90 or 120 minutes showed less uptake of 2-NBDG compared to cells with no polyphosphate (Figure 36). *iplA*$^{-}$ cells incubated with 150 μM polyphosphate for 60 minutes showed a similar 2-NBDG uptake level compared to cells with no polyphosphate (Figure 36). *iplA*$^{-}$ cells incubated with 150 μM polyphosphate for 120 minutes showed a reduced uptake of 2-NBDG compared to cells with no polyphosphate, but the reduction was less than that of Ax2 cells (Figure 36).

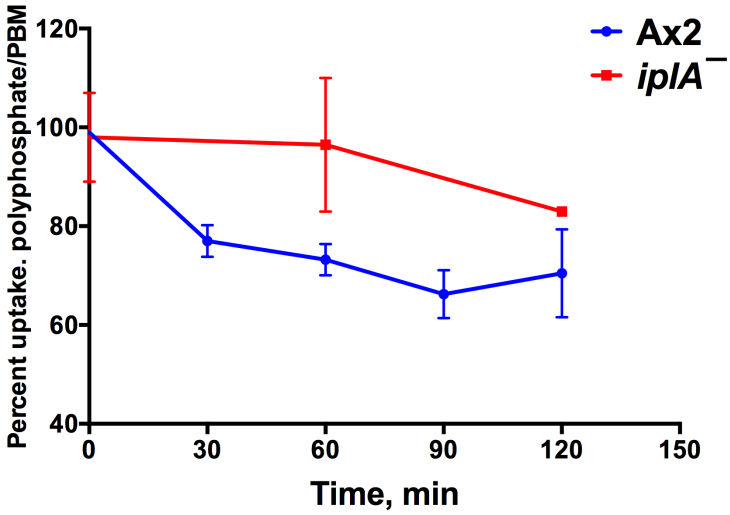

Figure 36. Polyphosphate inhibits 2-NBDG uptake of *Dictyostelium discoideum*. Indicated strains were cultured with 150 µM polyphosphate for indicated time periods and were then washed and resuspended in HL5 without glucose. Cells were then incubated with 20 µM 2-NBDG in HL5 without glucose for 30 minutes. The uptake of 2-NBDG were analyzed by flow-cytometry. The ratio of the Median RFU of 150 µM polyphosphate to no polyphosphate added was calculated. Value are mean ± SEM, n = 2 (n = 1 for *iplA*¯ at 120 min).

APPENDIX G

POLYPHOSPHATE BINDS TO LEUKEMIA K562 CELLS

Our lab has reported that polyphosphate inhibits the proliferation of K562 cells [36]. Here I show that polyphosphate binds to K562 cells.

K562 cells were tested for binding to biotinylated polyphosphate. The results showed that biotinylated polyphosphate binds to K562 cells and the concentration of polyphosphate for maximal binding is ~112.5 μM (Figure 37A). The binding activity appeared to decrease when the polyphosphate concentration went higher than 112.5 μM (Figure 37A). The binding of 100 μM polyphosphate appeared to equilibrate within 10 minutes (Figure 37B).

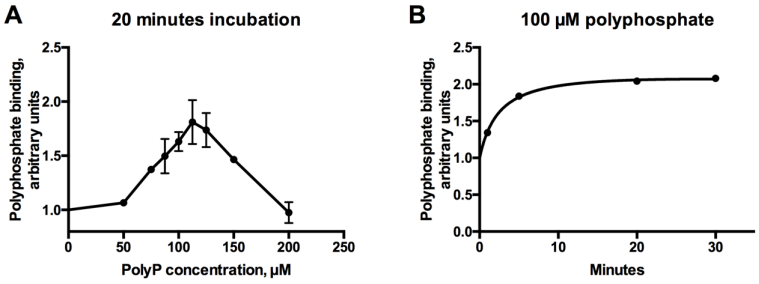

Figure 37. Polyphosphate binds to K562 cells.
A 0.1 – 0.25 x10^6 /200 μl K562 cells were incubated with 0, 50, 75, 100, 112.5, 125, 150 and 200 μM of biotinylated polyphosphate and a streptavidin-conjugated fluorophore. The cells were washed, and the fluorescence was measured using a flow cytometer. Values are mean ± SEM, n = 3 independent experiments. **B** K562 cells were incubated with 100 μM biotinylated polyphosphate for 0, 2.5, 7.5, 20 and 30 minutes, and binding was measured as **A,** n = 1.